Contents

▶ Chapter 6

Cloud Microphysics

Raindrops and snowflakes are among the smallest meteorological entities observable without special equipment. Yet from the perspective of cloud microphysics, the particles commonly encountered in precipitation are quite remarkable precisely because of their *large* sizes. To form raindrops, cloud particles have to increase in mass a million times or more, and these same cloud particles are nucleated by aerosol as small as 0.01 μm. To account for growth through such a wide range of sizes in time periods as short as 10 min or so for some convective clouds, it is necessary to consider a number of physical processes. Scientific investigations of these processes is the domain of *cloud microphysics* studies, which is the main subject of this chapter.

We begin with a discussion of the nucleation of cloud droplets from water vapor and the particles in the air that are involved in this nucleation (Section 6.1). We then consider the microstructures of warm clouds (Sections 6.2 and 6.3) and the mechanisms by which cloud droplets grow to form raindrops (Section 6.4). In Section 6.5 we turn to ice particles in clouds and describe the various ways in which ice particles form and grow into solid precipitation particles.

The artificial modification of clouds, and attempts to deliberately modify precipitation, are discussed briefly in Section 6.6.

Cloud microphysical processes are thought to be responsible for the electrification of thunderstorms. This subject is discussed in Section 6.7, together with lightning and thunder.

The final section of this chapter is concerned with chemical processes within and around clouds, which play important roles in atmospheric chemistry, including the formation of acid rain.

6.1 6.1 Nucleation of Water Vapor Condensation

Clouds form when air becomes *supersaturated*[1] with respect to liquid water (or in some cases with respect to ice). The most common means by which supersaturation is produced in the atmosphere is through the ascent of air parcels, which results in the expansion of the air and adiabatic cooling[2] (see Sections 3.4 and 3.5). Under these conditions, water vapor condenses onto some of the particles in the air to form a cloud of small water droplets or ice particles.[4] In this section we are concerned with the formation of water droplets from the condensation of water vapor.

6.1.1 Theory

We consider first the hypothetical problem (as far as the Earth's atmosphere is concerned) of the formation of a pure water droplet by condensation from a supersaturated vapor without the aid of particles in the air (i.e., in perfectly clean air). In this process, which is referred to as *homogeneous nucleation* of condensation, the first stage is the chance collisions of a number of water molecules

[1] If the water vapor pressure in the air is e, the supersaturation (in percent) with respect to liquid water is $(e/e_s - 1)100$, where e_s is the saturation vapor pressure over a plane surface of liquid water at the temperature of the air. A supersaturation with respect to ice may be defined in an analogous way. When the term supersaturation is used without qualification, it refers to supersaturation with respect to liquid water.

[2] The first person to suggest that clouds form by the adiabatic cooling of moist air appears to have been the scientist and poet Erasmus Darwin[3] in 1788.

[3] **Erasmus Darwin** (1731–1802) English freethinker and radical. Anticipated the theory of evolution, expounded by his famous grandson, by suggesting that species modify themselves by adapting to their environment.

[4] It was widely accepted well into the second half of the 19th century that clouds are composed of numerous small bubbles of water! How else can clouds float? Although John Dalton had suggested in 1793 that clouds may consist of water drops that are continually descending relative to the air, it was not until 1850 that James Espy[5] clearly recognized the role of upward-moving air currents in suspending cloud particles.

[5] **James Pollard Espy** (1785–1860) Born in Pennsylvania. Studied law; became a classics teacher at the Franklin Institute. Impressed by the meteorological writings of John Dalton, he gave up teaching to devote his time to meteorology. First to recognize the importance of latent heat release in sustaining cloud and storm circulations. Espy made the first estimates of the dry and saturated adiabatic lapse rates based on experimental data.

in the vapor phase to form small embryonic water droplets that are large enough to remain intact.

Let us suppose that a small embryonic water droplet of volume V and surface area A forms from pure supersaturated water vapor at constant temperature and pressure. If μ_l and μ_v are the Gibbs[6] free energies[7] per molecule in the liquid and the vapor phases, respectively, and n is the number of water molecules per unit volume of liquid, the decrease in the Gibbs free energy of the system due to the condensation is $nV(\mu_v - \mu_l)$. Work is done in creating the surface area of the droplet. This work may be written as $A\sigma$, where σ is the work required to create a unit area of vapor-liquid interface (called the *interfacial energy* between the vapor and the liquid, or the *surface energy* of the liquid). The student is invited to show in Exercise 6.9 that the surface energy of a liquid has the same numerical value as its *surface tension*. Let us write

$$\Delta E = A\sigma - nV(\mu_v - \mu_l) \tag{6.1}$$

then ΔE is the net increase in the energy of the system due to the formation of the droplet. It can be shown that[8]

$$\mu_v - \mu_l = kT \ln \frac{e}{e_s} \tag{6.2}$$

where e and T are the vapor pressure and temperature of the system, and e_s the saturation vapor pressure over a plane surface of water at temperature T. Therefore,

$$\Delta E = A\sigma - nVkT \ln \frac{e}{e_s} \tag{6.3}$$

For a droplet of radius R, (6.3) becomes

$$\Delta E = 4\pi R^2\sigma - \frac{4}{3}\pi R^3 nkT \ln \frac{e}{e_s} \tag{6.4}$$

[6] **Josiah Willard Gibbs** (1839–1903) Received his doctorate in engineering from Yale in 1863 for a thesis on gear design. From 1866 to 1869 Gibbs studied mathematics and physics in Europe. Appointed Professor of Mathematical Physics (without salary) at Yale. Subsequently Gibbs used the 1st and 2nd Laws of Thermodynamics to deduce the conditions for equilibrium of thermodynamic systems. Also laid the foundations of statistical mechanics and vector analysis.

[7] See Chapter 2 in "Basic Physical Chemistry for the Atmospheric Sciences" by P. V. Hobbs, Camb. Univ. Press, 2000, for a discussion of the Gibbs free energy. For the present purpose, the Gibbs free energy can be considered, very loosely, as the microscopic energy of the system.

[8] See Chapter 2 in "Basic Physical Chemistry for the Atmospheric Sciences" *loc. cit.*

Under subsaturated conditions, $e < e_s$. In this case, $\ln(e/e_s)$ is negative and ΔE is always positive and increases with increasing R (green curve in Fig. 6.1). In other words, the larger the embryonic droplet that forms in a subsaturated vapor the greater is the increase in the energy, ΔE, of the system. Since a system approaches an equilibrium state by reducing its energy, the formation of droplets is clearly not favored under subsaturated conditions. Even so, due to random collisions of water molecules, very small embryonic droplets continually form (and evaporate) in a subsaturated vapor, but they do not grow large enough to become visible as a cloud of droplets.

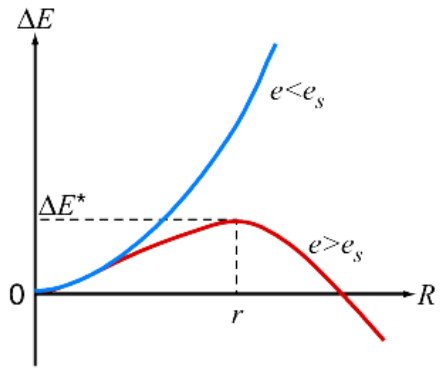

Figure 6.1 Increase ΔE in the energy of a system due to the formation of a water droplet of radius R from water vapor with pressure e; e_s is the saturation vapor pressure with respect to a plane surface of water at the temperature of the system.

Under supersaturated conditions, $e > e_s$, and $\ln(e/e_s)$ is positive. In this case, ΔE in (6.4) can be either positive or negative depending upon the value of R. The variation of ΔE with R for $e > e_s$ is also shown in Fig. 6.1 (red curve), where it can be seen that ΔE initially increases with increasing R, reaches a maximum value at $R = r$, and then decreases with increasing R. Hence, under supersaturated conditions, embryonic droplets with $R < r$ tend to evaporate, since by so doing they decrease ΔE. However, droplets that manage to grow by chance collisions to a radius that just exceeds r will continue to grow spontaneously by condensation from the vapor phase, since this will produce a decrease in ΔE. At $R = r$, a droplet can grow or evaporate infinitesimally without any change in ΔE. We can obtain an expression for r in terms of e by setting $\partial(\Delta E)/\partial R = 0$ at $R = r$.

Hence, from (6.4),

$$r = \frac{2\sigma}{nkT \ln \dfrac{e}{e_s}} \tag{6.5}$$

Equation (6.5) is referred to as *Kelvin's equation*, after Lord Kelvin who first derived it.

We can use (6.5) in two ways. It can be used to calculate the radius r of a droplet that is in (unstable) equilibrium[9] with a given water vapor pressure e. Alternatively, it can be used to determine the saturation vapor pressure e over a droplet of specified radius r. It should be noted that the relative humidity at which a droplet of radius r is in (unstable) equilibrium is $100e/e_s$, where e/e_s is given by (6.5). The variation of this relative humidity with droplet radius is shown in Fig. 6.2. It can be seen from Fig. 6.2 that a pure water droplet of radius 0.01 μm requires a relative humidity of 112.5% (i.e., a supersaturation of 12.5%) to be in (unstable) equilibrium with its environment, while a droplet of radius 1 μm requires a relative humidity of only 100.12% (i.e., a supersaturation of 0.12%).

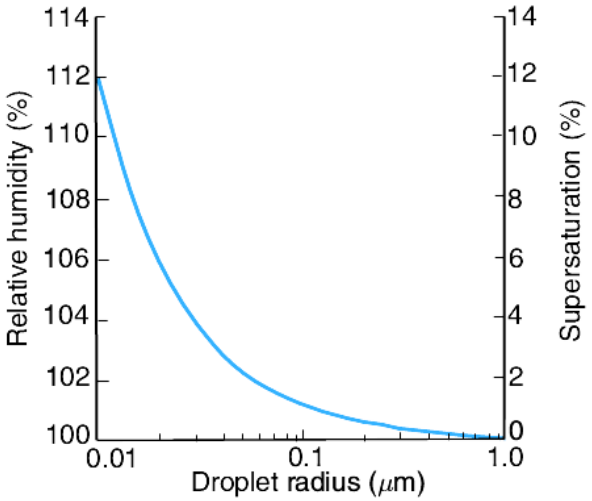

Figure 6.2 The relative humidity and supersaturation (both with respect to a plane surface of water) at which pure water droplets are in (unstable) equilibrium at 5°C.

[9]The equilibrium is unstable in the sense that if the droplet begins to grow by condensation it will continue to do so, and if the droplet begins to evaporate it will continue to evaporate (compare with Fig. B3.4b).

Begin Note CHANGE ALL "PROBLEM" TAGS TO PRINT THE WORD "EXERCISE" INSTEAD OF "PROBLEM" End Note

PROBLEM 6.1 (a) Show that the height of the critical energy barrier ΔE^* in Fig. 6.1 is given by

$$\Delta E^* = \frac{16\pi\sigma^3}{3\left(nkT\ln\dfrac{e}{e_s}\right)^2}$$

(b) Determine the fractional changes in ΔE^* and r if the surface tension, σ, is decreased by 10% by adding sodium laurel sulfate (a common ingredient in soap) to pure water. Neglect the effect of the sodium laurel sulfate on n and e. (c) What effect would the addition of the sodium laurel sulfate have on the homogeneous nucleation of droplets? ◄

SOLUTION ► (a) With reference to Fig. 6.1, $\Delta E = \Delta E^*$ when $R = r$. Therefore, from (6.4),

$$\Delta E^* = 4\pi r^2\sigma - \frac{4}{3}\pi r^3 nkT\ln\frac{e}{e_s}$$

Using (6.5)

$$\Delta E^* = 4\pi r^2\sigma - \frac{4}{3}\pi r^2(2\sigma)$$

or

$$\Delta E^* = \frac{4}{3}\pi r^2\sigma$$

Substituting for r from (6.5) into this last expression

$$\Delta E^* = \frac{16\pi\sigma^3}{3\left(nkT\ln\dfrac{e}{e_s}\right)^2}$$

(b) Differentiating the last equation with respect to σ

$$\frac{d(\Delta E^*)}{d\sigma} = \frac{16\pi\sigma^2}{\left(nkT\ln\dfrac{e}{e_s}\right)^2}$$

or

$$\frac{d(\Delta E^*)}{\Delta E^*} = 3\frac{d\sigma}{\sigma}$$

If the surface tension of the droplet is decreased by 10%, that is, if $d\sigma/\sigma = -0.1$, then $d(\Delta E^*)/\Delta E^* = -0.3$ and the critical energy barrier ΔE^* will be decreased by 30%. From (6.5), $dr/r = d\sigma/\sigma$. Therefore, if σ is decreased by 10%, r will also be decreased by 10%.

(c) As shown in Fig. 6.1, r is the critical radius that an embryonic droplet must attain, due to the chance collision of water molecules, if it is to continue to grow spontaneously by condensation. Therefore, for a specified supersaturation of the ambient air, if r is decreased (which it is by the addition of the sodium laurel sulfate) the homogeneous nucleation of droplets will be achieved more readily. ◄

Since the supersaturations that develop in natural clouds due to the adiabatic ascent of air rarely exceed a few percent (see Section 6.4.1), it follows from the preceding discussion that even if embryonic droplets of pure water as large as 0.01 μm in radius formed by the chance collision of water molecules they would be well below the critical radius required for survival in air that is just a few percent supersaturated. Consequently, droplets do not form in natural clouds by the homogeneous nucleation of pure water. Instead they form on atmospheric aerosol[10] by what is known as *heterogeneous nucleation*[12].

As we have seen in Section 5.4.5, the atmosphere contains many particles that range in size from submicrometer to several tens of micrometers. Those particles that are *wettable*[13] can serve as centers upon which water vapor condenses. Moreover, droplets can form and grow on these particles at much lower supersaturations than those required for homogeneous nucleation. For example, if sufficient water condenses onto a completely wettable particle 0.3 μm in radius to form a thin film of water over the surface of the particle, we see from Fig. 6.2 that the water film will be in (unstable) equilibrium with air that has a supersaturation of 0.4%. If the supersaturation were slightly greater than 0.4%, water would condense onto the film of water and the droplet would increase in size.

Some of the particles in air are soluble in water. Consequently, they dissolve, wholly or in part, when water condenses onto them, so that a solution (rather than a pure water) droplet is formed. Let us now consider the behavior of such a droplet.

The saturation vapor pressure of water adjacent to a solution droplet (that is, a water droplet containing some dissolved material, such as sodium chloride or ammonium sulfate) is less than that

[10] That aerosol play a role in the condensation of water was first clearly demonstrated by Coulier[11] in 1875. His results were rediscovered independently by Aitken in 1881 (see Section 5.4.5).

[11] **Paul Coulier** (1824–1890) French physician and chemist. Carried out research on hygiene, nutrition, and the ventilation of buildings.

[12] Cloud physicists use the terms homogeneous and heterogeneous differently than chemists. In chemistry, a homogeneous system is one in which all the species are in the same phase (solid, liquid or gas), and a heterogeneous system is one in which species are present in more than one phase. In cloud physics, a homogeneous system is one involving just one species (in one or more phases), and a heterogeneous system is one in which there is more than one species. In this chapter these two terms are used in the cloud physicist's sense.

[13] A surface is said to be perfectly wettable (hydrophilic) if it allows water to spread out on it as a horizontal film (detergents are used for this purpose). A surface is completely unwettable (hydrophobic) if water forms spherical drops on its surface (cars are waxed to make them hydrophobic).

adjacent to a pure water droplet of the same size. The fractional reduction in the water vapor pressure is given by *Raoult's*[14] *law*

$$\frac{e'}{e} = f \tag{6.6}$$

where e' is the saturation vapor pressure of water adjacent to a solution droplet containing a mole fraction f of pure water, and e is the saturation vapor pressure of water adjacent to a pure water droplet of the same size and at the same temperature. The *mole fraction of pure water* is defined as the number of moles of pure water in the solution divided by the total number of moles (pure water plus dissolved material) in the solution.

Consider a solution droplet of radius r that contains a mass m (in kg) of a dissolved material of molecular weight M_s. If each molecule of the material dissociates into i ions in water, the effective number of moles of the material in the droplet is $i\,(1000\ m)\,/M_s$. If the density of the solution is ρ' and the molecular weight of water M_w, the number of moles of pure water in the droplet is $1000\ (\frac{4}{3}\pi r^3\,\rho' - m)/M_w$. Therefore, the mole fraction of water in the droplet is

$$f = \frac{(\frac{4}{3}\pi r^3\,\rho' - m)/M_w}{\left[(\frac{4}{3}\pi r^3\,\rho' - m)/M_w\right] + im/M_s} = \left[1 + \frac{imM_w}{M_s(\frac{4}{3}\pi r^3\,\rho' - m)}\right]^{-1} \tag{6.7}$$

Combining (6.5)–(6.7) (but replacing σ and n by σ' and n' to indicate the surface energy and number concentration of water molecules, respectively, for the solution) we obtain the following expression for the saturation vapor pressure e' adjacent to a solution droplet of radius r

$$\frac{e'}{e_s} = \left[\exp\frac{2\sigma'}{n'kTr}\right]\left[1 + \frac{imM_w}{M_s(\frac{4}{3}\pi r^3\,\rho' - m)}\right]^{-1} \tag{6.8}$$

Equation (6.8) may be used to calculate the saturation vapor pressure e' [or relative humidity $100e'/e_s$, or supersaturation $\left(\frac{e'}{e_s} - 1\right)100$] adjacent to a solution droplet with a specified radius

[14] **François Marie Raoult** (1830–1901) Leading French experimental physical chemist of the nineteenth century. Professor of chemistry at Grenoble. His labors were met with ample, though tardy recognition (Commander of de la Legion of d' Honneur; Davy medallist of the Royal Society, etc.).

r. If we plot the variation of the relative humidity (or supersaturation) adjacent to a solution droplet as a function of its radius, we obtain what is referred to as a *Köhler*[15] *curve*. Several such curves, derived from (6.8), are shown in Fig. 6.3. Below a certain droplet radius, the vapor pressure adjacent to a solution droplet is less than that which is in equilibrium with a plane surface of pure water at the same temperature. As the droplet increases in size, the solution becomes weaker, the Kelvin curvature effect becomes the dominant influence, and eventually the relative humidity of the air adjacent to the droplet becomes essentially the same as that adjacent to a pure water droplet of the same size.

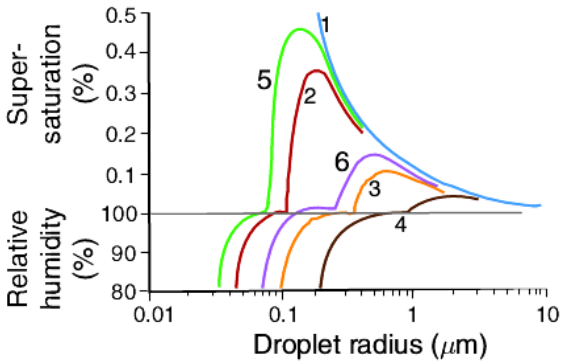

Figure 6.3 Variations of the relative humidity and supersaturation adjacent to droplets of (l) pure water (blue), and adjacent to solution droplets containing the following fixed masses of salt: (2) 10^{-19} kg of NaCl (red), (3) 10^{-18} kg of NaCl (orange), (4) 10^{-17} kg of NaCl (brown), (5) 10^{-19} kg of $(NH_4)_2SO_4$ (green), and (6) 10^{-18} kg of $(NH_4)_2SO_4$ (violet). Note the discontinuity in the ordinate at 100% relative humidity. [Adapted from S. I. Rasool, ed., "Chemistry of the Lower Atmosphere," Plenum Press, New York (1973), p. 16.]

To illustrate further the interpretation of the Köhler curves we reproduce in Fig. 6.4 the Köhler curves for solution droplets containing 10^{-19} kg of NaCl (the red curve from Fig. 6.3) and 10^{-19} kg of $(NH_4)_2SO_4$ (the green curve from Fig. 6.3). Suppose that a particle of NaCl with mass 10^{-19} kg were placed in air with a water supersaturation of 0.4% (indicated by the dashed line in Fig. 6.4). Condensation would occur on this particle to form a solution

[15] **Hilding Köhler**, (1888–1982) Swedish meteorologist. Former Chair of the Meteorology Department, and Director of the Meteorological Observatory, University of Uppsala.

droplet, and the droplet would grow along the red curve in Fig. 6.4. As it does so, the supersaturation adjacent to the surface of this solution droplet will initially increase, but even at the peak in its Köhler curve the supersaturation adjacent to the droplet is less than the ambient supersaturation. Consequently, the droplet will grow over the peak in its Köhler curve and down the right-hand side of this curve to form a fog or cloud droplet. A droplet that has passed over the peak in its Köhler curve and continues to grow is said to be *activated*.

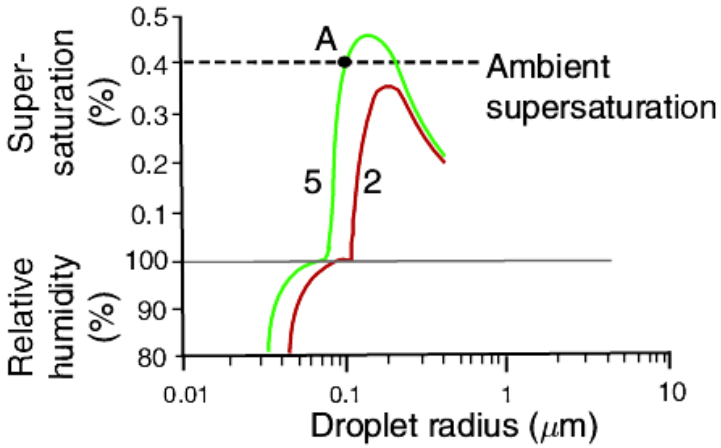

Figure 6.4. Köhler curves 2 and 5 from Fig. 6.3. Curve 2 (red) is for a solution droplet containing 10^{-19} kg of NaCl, and curve 5 (green) is for a solution droplet containing 10^{-19} kg of $(NH_4)_2SO_4$. The dashed line is an assumed ambient supersaturation discussed in the text.

Now consider a particle of $(NH_4)_2SO_4$ with mass 10^{-19} kg that is placed in the same ambient supersaturation of 0.4%. In this case, condensation will occur on the particle and it will grow as a solution droplet along its Köhler curve (the green curve in Fig. 6.4) until it reaches point A. At point A the supersaturation adjacent to the droplet is equal to the ambient supersaturation. If the droplet at A should grow slightly, the supersaturation adjacent to it would increase above the ambient supersaturation, and therefore the droplet would evaporate back to point A. If the droplet at A should evaporate slightly, the supersaturation adjacent to it would decrease below the ambient supersaturation, and the droplet would grow by condensation back to A in Fig. 6.4. Hence, in this case, the solution droplet at A is in stable equilibrium with the ambient supersaturation. If

the ambient supersaturation were to change a little, the location of A in Fig. 6.4 would shift and the equilibrium size of the droplet would change accordingly. Droplets in this state are said to be *unactivated* or *haze droplets*. Haze droplets in the atmosphere can considerably reduce visibility by scattering light.

6.1.2 Cloud Condensation Nuclei

In Section 5.4 we discussed atmospheric aerosol. A small sub-set of the atmospheric aerosol serves as particles upon which water vapor condenses to form droplets that are activated and grow by condensation to form cloud droplets at the supersaturations achieved in clouds ($\sim$0.1–1%). These particles are called *cloud condensation nuclei* (CCN). It follows from the discussion in Section 6.1.1 that the larger the size of a particle, the more readily it is wetted by water, and the greater its solubility, the lower will be the supersaturation at which the particle can serve as a CCN. For example, to serve as a CCN at 1% supersaturation, completely wettable but water insoluble particles need to be at least $\sim$0.1 μm in radius, whereas soluble particles can serve as CCN at 1% supersaturation even if they are as small as $\sim$0.01 μm in radius. Most CCN consist of a mixture of soluble and insoluble components (called *mixed nuclei*).

The concentrations of CCN active at various supersaturations can be measured with a *thermal diffusion chamber*. This device consists of a flat chamber in which the upper and lower horizontal plates are kept wet and maintained at different temperatures, the lower plate being several degrees colder than the upper plate. By varying the temperature difference between the plates, it is possible to produce maximum supersaturations in the chamber that range from a few tenths of 1% to a few percent (see Exercise 6.14), which are similar to the supersaturations that activate droplets in clouds. Small water droplets form on those particles that act as CCN at the peak supersaturation in the chamber. The concentration of these droplets can be determined by photographing a known volume of the cloud and counting the number of droplets visible in the photograph, or by measuring the intensity of light scattered from the droplets. By repeating the above procedure with different temperature gradients in the chamber, the concentrations of CCN in the air at several supersaturations (called the *CCN supersaturation spectrum*) can be determined.

World-wide measurements of CCN concentrations have not revealed any systematic latitudinal or seasonal variations. However, near the Earth's surface continental air masses generally contain larger concentrations of CCN than marine air masses (Fig. 6.5). For example, the concentration of CCN in the continental air mass over the Azores, depicted in Fig. 6.5, is about $\sim$300 cm^{-3} at 1% supersaturation, while in the marine air mass over Florida it is $\sim$100 cm^{-3}, and in clean Arctic air it is only $\sim$30 cm^{-3}. The ratio of CCN (at 1% supersaturation) to the total number of particles in the air (CN) is $\sim$0.2-0.6 in marine air; in continental air this ratio is generally less than $\sim$0.01 but can rise to $\sim$0.1. The very low ratio of CCN to CN in continental air is attributable to the large number of very small particles, which are not activated at low supersaturations. Concentrations of CCN over land decline by about a factor of five between the planetary boundary layer and the free troposphere. Over the same height interval, concentrations of CCN over the ocean remain fairly constant, or may even increase with height reaching a maximum concentration just above the mean cloud height. Ground-based measurements indicate that there is a diurnal variation in CCN concentrations, with a minimum at about 6 a.m. and a maximum at about 6 p.m.

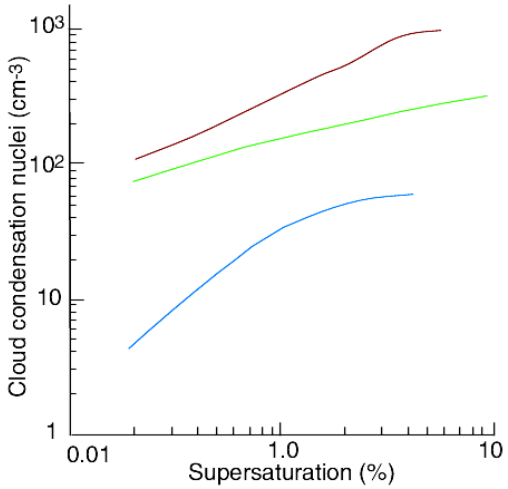

Figure 6.5. Cloud condensation nucleus spectra in the boundary layer from measurements near the Azores in a polluted continental air mass (brown line), in Florida in a marine air mass (green line), and in clean air in the Arctic (blue line). [Data from J. Geophys. Res., 107(D19), INX2 21 (2002).]

The observations described above provide clues as to the origins of CCN. First of all it appears that the land acts as a source of CCN, because the concentrations of CCN are higher over land and decrease with altitude. Some of the soil particles and dusts that enter the atmosphere probably serve as CCN, but they do not appear to be a dominant source. The rate of production of CCN from burning vegetable matter is on the order of $10^{12} - 10^{15}$ per kg of material consumed. Thus, forest fires are a source of CCN. About 80% of the particles emitted by idling diesel engines are CCN at 1% supersaturation. About 70% of the particles emitted by the 1991 Kuwait oil fires were CCN at 1% supersaturation. Although sea-salt particles enter the air over the oceans by the mechanisms discussed in Section 5.4.1, they do not appear to be a dominant source of CCN, even over the oceans.

There appears to be a widespread and probably a fairly uniform source of CCN over both the oceans and the land, the nature of which has not been definitely established. A likely candidate is gas-to-particle conversion, which can produce particles up to a few tenths of a micrometer in diameter that can act as CCN if they are soluble or wettable. Gas-to-particle conversion mechanisms that require solar radiation might be responsible for the observed peak in CCN concentrations at ∼6 p.m. Many CCN consist of sulfates. Over the oceans, organic sulfur from the ocean (in the form of the gases dimethylsulfide (DMS) and methane sulfonic acid (MSA)) provide a source of CCN, with the DMS and MSA being converted to sulfate in the atmosphere. Evaporating clouds also release sulfate particles (see Section 6.8.9).

6.2 6.2 Microstructures of Warm Clouds

Clouds that lie completely below the 0°C isotherm, referred to as *warm clouds*, contain only water droplets. Therefore, in describing the microstructure of warm clouds we are interested in the amount of liquid water per unit volume of air (called the *liquid water content* (LWC), usually expressed in grams per cubic meter[16]), the total number of water droplets per unit volume of air (called the *cloud droplet concentration*, usually expressed as a number per cubic centimeter), and the size distribution of cloud droplets (called

[16] Since the densily of air is approximately 1 kg m^{-3}, a LWC of 1 g m^{-3} expressed as a mixing ratio is approximately the same as 1 g kg^{-3}.

the *droplet size spectrum*, usually displayed as a histogram of the number of droplets per cubic centimeter in various droplet size intervals). These three parameters are not independent; for example, if the droplet spectrum is known the droplet concentration and LWC can be derived.

In principle, the most direct way of determining the microstructure of a warm cloud is to collect all the droplets in a measured volume of the cloud and then to size and count them under a microscope. In the early days of cloud measurements, oil-coated slides were exposed from an aircraft to cloudy air along a measured path length. Droplets that collided with a slide, and became completely immersed in the oil, were preserved for subsequent analysis. An alternative method was to obtain replicas of the droplets by coating a slide with magnesium oxide powder (obtained by burning a magnesium ribbon near the slide). When water droplets collide with these slides they leave clear imprints, the sizes of which can be related to the actual sizes of the droplets. Direct impaction methods, of the type described above, bias against smaller droplets, which tend to follow the streamlines around the slide and thereby avoid capture. Consequently, corrections have to be made, based on theoretical calculations of droplet trajectories around the slide.

Automatic techniques are now available for sizing cloud droplets from an aircraft without collecting the droplets (e.g., by measuring the angular distribution of light scattered from individual cloud drops). These techniques are free from the collection problems described above, and they permit a cloud to be sampled continuously so that variations in cloud microstructures in space and time can be investigated more readily.

Several techniques are available for measuring the LWC of clouds from an aircraft. A common instrument is a device in which an electrically-heated wire is exposed to the airstream. When cloud droplets impinge on the wire they are evaporated and therefore tend to cool and lower the electrical resistance of the wire. The resistance of the wire is used in an electrical feedback loop to maintain the temperature of the wire constant. The power required to do this can be calibrated to give the LWC. Another more recently developed instrument uses light scattering from an ensemble of drops to derive LWC.

The optical thickness (τ_c) and effective particle radius (r_e) of a liquid water or an ice cloud can be derived from satellites or

airborne solar spectral reflectance measurements. Such retrievals exploit the spectral variation of bulk water absorption (liquid or ice) in atmospheric window regions. Condensed water is essentially transparent in the visible and near-infrared portions of the spectrum (e.g., 0.4-1.0 μm) and therefore cloud reflectance is dependent only on τ_c and the particle phase function (or the asymmetry parameter, g, a cosine weighting of the phase function that is pertinent to multiple scattering problems). However, water is weakly absorbing in the shortwave and midwave infrared windows (1.6, 2.1, and 3.7 μm bands) with an order of magnitude increase in absorption in each longer wavelength window. Therefore, in these spectral bands, cloud reflectance is also dependent on particle absorption, which is described by the single scattering albedo (ω_o). Specifically, r_e is the relevant radiative measure of the size distribution and is approximately linearly related to ω_o for weak absorption. Therefore, a reflectance measurement in an absorbing band contains information about r_e. Retrieval algorithms use a radiative transfer model to predict the reflectance in transparent and absorbing sensor bands as a function of τ_c and r_e including specifications of relevant non-cloud parameters (e.g., absorbing atmospheric gases, surface boundary conditions, etc.). The unknown cloud optical parameters τ_c and r_e are then adjusted until the differences between predicted and observed reflectances are minimized. The liquid water path, LWP (i.e., the mass of cloud liquid water in a vertical column with a cross-sectional area of 1 m^2), is approximately proportional to the product of τ_c and r_e (see Exercise 6.16) and is often reported as part of the retrieval output.

Shown in Fig. 6.6 are measurements of the vertical velocity of the air, the LWC, and droplet size spectra in a small cumulus cloud. The cloud itself is primarily a region of updrafts, with downdrafts just outside its boundary. Regions of higher LWC correspond quite closely to regions of stronger updrafts which are, of course, the driving force for the formation of clouds (see Section 3.5). It can be seen from the LWC measurements that the cloud was very inhomogeneous, containing pockets of relatively high LWC interspersed with regions of virtually no liquid water (like Swiss cheese). The droplet spectrum measurements depicted in Fig. 6.6c show droplets ranging from a few micrometers up to about 17 μm in radius.

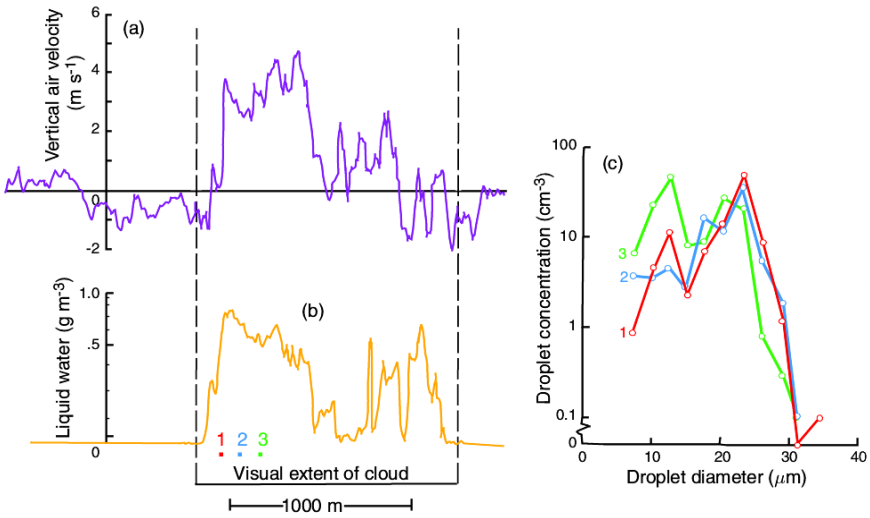

Figure 6.6. (a) Vertical air velocity (with positive values indicating updrafts and negative values downdrafts), (b) liquid water content, and (c) droplet size spectra at points 1, 2, and 3 in (b), measured from an aircraft as it flew in a horizontal track across the width and about half-way between the cloud base and cloud top in a small, warm, non-raining cumulus cloud. The cloud was about 2 km deep. [Adapted from J. Atmos. Sci., 26, 1049 (1969).]

Cloud LWC typically increases with height above cloud base, reaches a maximum somewhere in the upper half of a cloud, and then decreases toward cloud top.

To demonstrate the profound effects that CCN can have on the concentrations and size distributions of cloud droplets, we show in Fig. 6.7 measurements in cumulus clouds in marine and continental air masses. Most of the marine clouds have droplet concentrations less than 100 cm^{-3}, and none has a droplet concentration greater than 200 cm^{-3} (Fig. 6.7a). By contrast, some of the continental cumulus clouds have droplet concentrations in excess of 900 cm^{-3}, and most have concentrations of a few hundred per cubic centimeter (Fig. 6.7c). These differences reflect the much higher concentrations of CCN present in continental air (see Section 6.1.2 and Fig. 6.5). Since the LWC of marine cumulus clouds do not differ significantly from those of continental cumulus, the higher droplet concentrations inthecontinentalcumulusmustresultinsmalleraverage droplet sizes in continental clouds than in marine clouds. By comparing the results

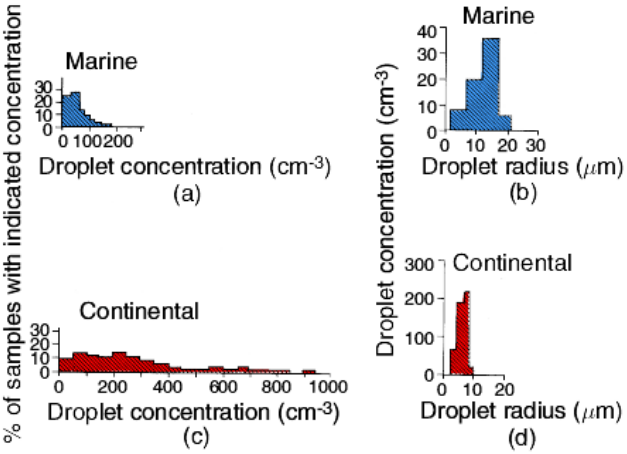

Figuare 6.7. (a) Percentage of marine cumulus clouds with indicated droplet concentrations. (b) Droplet size distributions in a marine cumulus cloud. (c) Percentage of continental cumulus clouds with indicated droplet concentrations. (d) Droplet size distributions in a continental cumulus cloud. Note change in ordinate from (b). [Adapted from Tellus 10, 258 (1958).]

shown in Fig. 6.7b and 6.7d, it can be seen that not only is the droplet size spectrum for the continental cumulus cloud much narrower than that for the marine cumulus cloud, but the average droplet radius is significantly smaller. To describe this distinction in another way, droplets with a radius of about 20 μm exist in concentrations of a few per cubic centimeter in the marine clouds, whereas, in continental clouds the radius has to be lowered to 10 μm before there are droplets in concentrations of a few per cubic centimeter. The generally smaller droplets in continental clouds result in the boundaries of these clouds being well defined, because the droplets evaporate quickly in the non-saturated ambient air. The absence of droplets much beyond the main boundary of continental cumulus clouds gives them a "harder" appearance than maritime clouds.[17] We will see in Section 6.4.2 that the larger droplets in marine clouds lead to the release of precipitation in shallower clouds, and with smaller updrafts, than in continental clouds.

Shown in Fig. 6.8 are retrievals from satellite measurements of cloud optical thickness (τ_c) and cloud droplet effective radius (r_e) for low-level water clouds over the globe. It can be seen that the r_e

[17] The formation of ice particles in clouds also affects their appearance (see Section 6.5.3).

values are generally smaller over the land than over the oceans, in agreement with the above discussion.

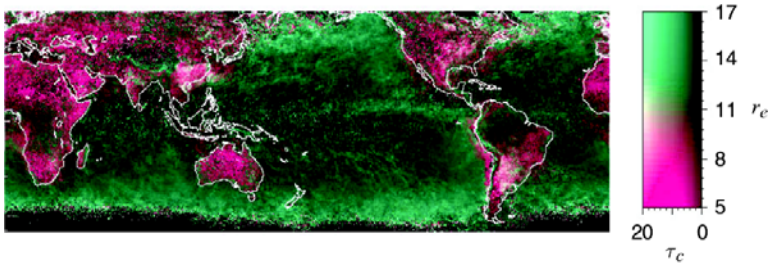

Figure 6.8. Retrievals from a satellite of cloud optical thickness (τ_c) and cloud particle effective radius (r_e in μm) for low-level water clouds. [From Geophys. Res. Lett., 28, 1171 (2001).]

begin box **BOX 6.1: SHIP TRACKS IN CLOUDS**

The effects of CCN on increasing the number concentration of cloud droplets is demonstrated dramatically by a feature known as *ship tracks*, which is illustrated in Fig. 6.9. As we have seen, under natural conditions marine air contains relatively few CCN, which is reflected in the low concentrations of small droplets in marine clouds. Ships emit large numbers of CCN ($\sim 10^{15}$ s^{-1} at 0.2% supersaturation), and when these particles are carried up into the bases of marine stratus clouds they increase the number concentration and decrease the average size of the cloud droplets. The greater concentrations of droplets in these regions cause more sunlight to be reflected back to space, so they appear as white lines in the cloud when viewed from a satellite.

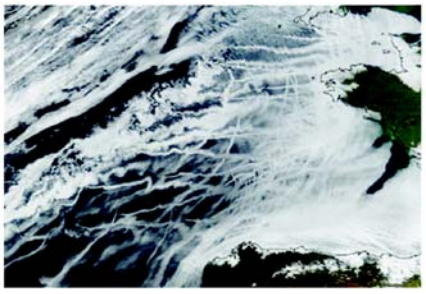

Figure 6.9. Ship tracks (white lines) in marine stratus clouds over the Atlantic Ocean as viewed from the NASA Aqua satellite on January 27, 2003. Brittany and the southwest coast of England can be seen on the upper right side of the image. end box

6.3 6.3 Cloud Liquid Water Content and Entrainment

In Exercise 3.10 we explained how the skew $T - \ln p$ chart can be used to determine the quantity of liquid water that is condensed when a parcel of air is lifted above its lifting condensation level (LCL). Since the skew $T - \ln p$ chart is based on adiabatic assumptions for air parcels (see Section 3.4.1), the LWC derived in this manner is called the *adiabatic liquid water content*.

Shown in Figs. 6.10 and 6.11 are measurements of LWC in cumulus clouds. The measured LWC are well below the adiabatic LWC, because unsaturated ambient air is *entrained* into cumulus clouds. Consequently, some of the cloud water evaporates to saturate the entrained parcels of air, thereby reducing the cloud LWC.

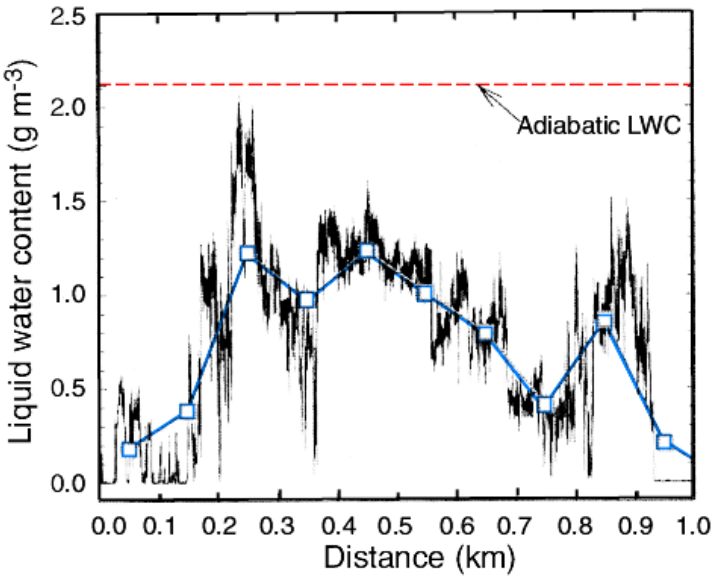

Figure 6.10. High resolution liquid water content (LWC) measurements (black line) derived from a horizontal pass through a small cumulus cloud. Note that a small portion of the cumulus cloud had nearly an adiabatic LWC. This feature disappears when the data are smoothed (blue line) to mimic the much lower sampling rates that were prevalent in older measurements. [Adapted from Proc. 13th Intern. Conf. on Clouds and Precipitation, Reno, NV, p. 105 (2000).]

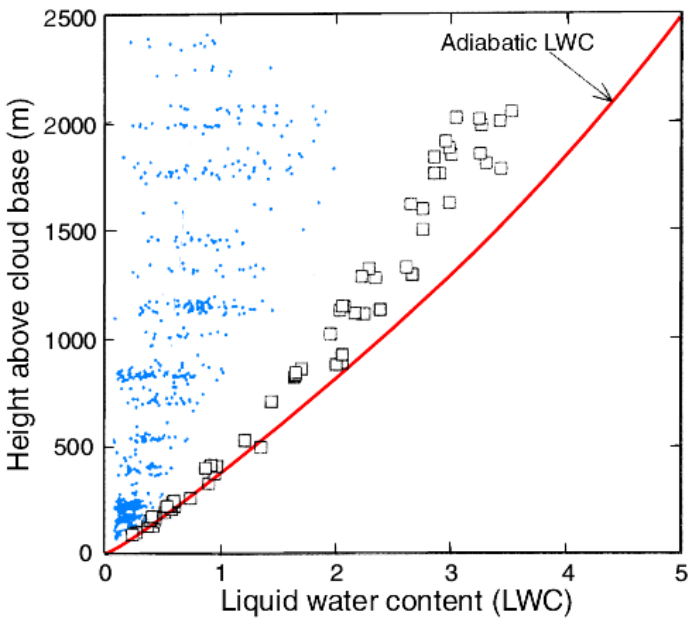

Figure 6.11. The blue dots are average liquid water contents (LWC) measured in traverses of 802 cumulus clouds. The squares are the largest measured LWC. Note that no adiabatic LWC was measured beyond ∼900 m above cloud base. Cloud base temperatures varied little for all flights, which permitted this summary to be constructed with cloud base normalized to a height of 0 m. [Adapted from Proc. 13th Intern. Conf. on Clouds and Precipitation, Reno, NV, p. 105 (2000).]

Measurements in and around small cumulus clouds suggest that entrainment occurs primarily at their tops, as shown schematically in Fig. 6.12. Some field measurements have suggested the presence of adiabatic cores deep within cumulus clouds, where the cloud water is undiluted by entrainment. However, more recent measurements, utilizing very fast response instruments that can reveal the fine structures of clouds (Figs. 6.10 and 6.11), indicate that adiabatic cores, if they exist at all, must be quite rare.

Air entrained at the top of a cloud is distributed to lower levels as follows. When cloud water is evaporated to saturate an entrained parcel of air, the parcel is cooled. If sufficient evaporation occurs before the parcel loses its identity by mixing, the parcel will sink, mixing with more cloudy air as it does so. The sinking parcel will descend until it runs out of negative buoyancy or loses its identity.

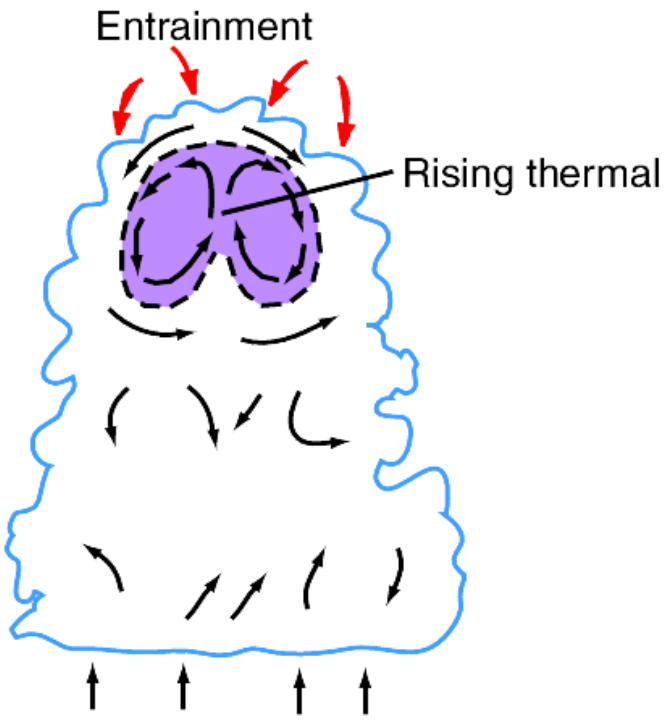

Figure 6.12. Schematic of entrainment of ambient air into a small cumulus cloud. The thermal (shaded violet region) has ascended from cloud base. [Adapted from J. Atmos. Sci., 45, 394 (1988).]

Such parcels can descend several kilometers in a cloud, even in the presence of substantial updrafts, in which case they are referred to as *penetrative downdrafts*. This process is responsible in part for the "Swiss cheese" distribution of LWC in cumulus clouds (see Fig. 6.6). Patchiness in the distribution of LWC in a cloud will tend to broaden the droplet size distribution, since droplets will evaporate partially or completely in downdrafts and grow again when they enter updrafts.

Over large areas of the oceans stratocumulus clouds often form just below a strong temperature inversion at a height of ∼0.5–1.5 km, which marks the top of the marine boundary layer. The tops of the stratocumulus clouds are cooled by longwave radiation to space, and their bases are warmed by longwave radiation from the surface. This differential heating drives shallow convection, in which cold cloudy air sinks and droplets within it tend to evaporate, while the warm

cloudy air rises and the droplets within it tend to grow. These motions are responsible in part for the cellular appearance of stratocumulus clouds (Fig. 6.13).

Figure 6.13. Looking down on stratocumulus clouds over the Bristol Channel, England. (Photo: R. Wood.)

Entrainment of warm, dry air from the free troposphere into the cool, moist boundary layer air below plays an important role in the marine stratocumulus-topped boundary layer. The rate at which this entrainment occurs increases with the vigor of the boundary layer turbulence, but it is hindered by the stability associated with the temperature inversion. Figure 6.14, based on model simulations, indicates how a parcel of air from the free troposphere might become engulfed into the stratocumulus-topped boundary layer. As in the case of cumulus clouds, following such engulfment, cooling of entrained air parcels by the evaporation of cloud water will tend to drive the parcel downward. Under extreme conditions, such downdrafts might lead to the breakup of a stratocumulus cloud layer.

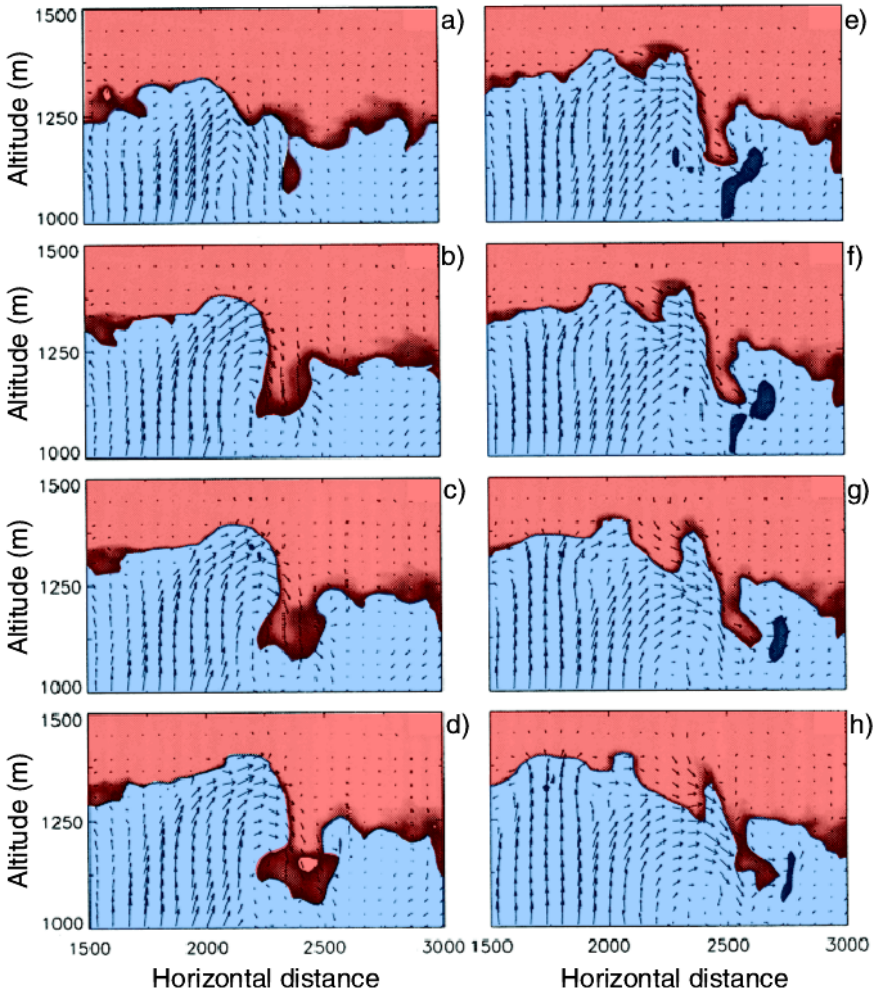

Figure 6.14. Model simulations showing the entrainment of air (darker orange) from the free troposphere (lighter orange) into the boundary layer (blue) over a period of ∼6 min. Arrows show fluid motions. [Adapted from Sullivan et al. (J. Atmos. Sci., 55, 3042 (1998).]

PROBLEM 6.2 Derive an expression for the fractional change $d\theta'/\theta'$ in the potential temperature θ' of a parcel of cloudy air produced by a fractional change in the mass m of the parcel due to the entrainment of mass dm of unsaturated ambient air. ◄

SOLUTION ► Let the parcel of cloudy air have temperature T', pressure p' and volume V', and the ambient air have temperature T and mixing ratio w. The heat dQ_1, needed to warm the entrained air of mass dm is

$$dQ_1 = c_p \left(T' - T\right)\ dm \tag{6.9}$$

where c_p is the specific heat at constant pressure of the entrained air. To evaporate just enough cloud liquid water to saturate the entrained air requires heat

$$dQ_2 = L_v \left(w_s - w\right)\ dm \tag{6.10}$$

Suppose the entrainment occurs as the parcel of cloudy air ascends moist adiabatically and cools while its saturation mixing ratio decreases by dw_s. The heat released by the associated condensation of liquid water is

$$dQ_3 = -mL_v\ dw_s \tag{6.11}$$

(Note: Since dw_s is negative, dQ_3 given by (6.11) is positive.) Therefore, the net heat gained by the parcel of cloudy air is $dQ_3 - dQ_1 - dQ_2$.

Applying the First Law of Thermodynamics (Section 3.3) to the cloudy parcel of air, $dQ_3 - dQ_1 - dQ_2 = dU' + p'dV'$ where $dU' = mc_v dT'$ is the change in the internal energy of the cloudy air parcel. Therefore,

$$dQ_3 - dQ_1 - dQ_2 = mc_v dT' + p'dV' \tag{6.12}$$

If we ignore the difference between the temperature and virtual temperature of the cloudy air, we have from the ideal gas equation

$$p'V' = mR_d T' \tag{6.13}$$

or

$$p'dV' = mR_d dT' - V'dp' \tag{6.14}$$

Substituting (6.14) into (6.12),

$$dQ_3 - dQ_1 - dQ_2 = mc_v dT' + mR_d dT' - V'dp'$$

or, using (3.48) and (6.13),

$$dQ_3 - dQ_1 - dQ_2 = mc_p dT' - \frac{mR_d T'}{p'} dp' \tag{6.15}$$

From (6.9), (6.10), (6.11) and (6.15)

$$-\frac{L_v}{c_p T'} dw_s - \frac{dm}{m}\left[\frac{T' - T}{T'} + \frac{L_v}{c_p T'}\left(w_s - w\right)\right] = \frac{dT'}{T'} - \frac{R_d}{c_p}\frac{dp'}{p'} \tag{6.16}$$

Applying (3.57) to the cloudy air

$$\ln\ \theta' = \ln\ T' + \frac{R_d}{c_p} \ln\ p_o - \frac{R_d}{c_p} \ln\ p'$$

Differentiating this last expression

$$\frac{d\theta'}{\theta'} = \frac{dT'}{T'} - \frac{R_d}{c_p}\frac{dp'}{p'} \tag{6.17}$$

From (6.16) and (6.17)

$$\frac{d\theta'}{\theta'} = -\frac{L_v}{c_p T'} dw_s - \left[\frac{T' - T}{T'} + \frac{L_v}{c_p T'}\left(w_s - w\right)\right]\frac{dm}{m} \tag{6.18}$$

◀

6.4 6.4 Growth of Cloud Droplets in Warm Clouds

In warm clouds, droplets can grow by condensation in a supersaturated environment and by colliding and coalescing with other cloud droplets. In this section we consider these two growth processes and assess the extent to which they can explain the formation of rain in warm clouds.

6.4.1 Growth by Condensation

In Section 6.1.1 we followed the growth of a droplet by condensation up to a few micrometers in size. We saw that if the supersaturation is large enough to activate a droplet, the droplet will pass over the peak in its Köhler curve (Fig. 6.4) and continue to grow. We will now consider the rate at which such a droplet grows by condensation.

Let us consider first an isolated droplet, with radius r at time t, situated in a supersaturated environment in which the water vapor density at a large distance from the droplet is $\rho_v(\infty)$ and the water vapor density adjacent to the droplet is $\rho_v(r)$. If we assume that the system is in equilibrium (i.e., there is no accumulation of water vapor in the air surrounding the drop), the rate of increase in the mass M of the droplet at time t is equal to the flux of water vapor across any spherical surface of radius x centered on the droplet. Hence, if we define the *diffusion coefficient* D of water vapor in air as the rate of mass flow of water vapor across (and normal to) a unit area in the presence of a unit gradient in water vapor density, the rate of increase in the mass of the droplet is given by

$$\frac{dM}{dt} = 4\pi x^2 D \frac{d\rho_v}{dx}$$

where ρ_v is the water vapor density at distance $x(>r)$ from the droplet. Since, under steady-state conditions, dM/dt is independent of x, the above equation can be integrated as follows

$$\frac{dM}{dt} \int_{x=r}^{x=\infty} \frac{dx}{x^2} = 4\pi D \int_{\rho_v(r)}^{\rho_v(\infty)} d\rho_v$$

or

$$\frac{dM}{dt} = 4\pi r D \left[\rho_v(\infty) - \rho_v(r)\right] \tag{6.19}$$

Substituting $M = \frac{4}{3}\pi r^3 \rho_l$, where ρ_l is the density of liquid water, into this last expression we obtain

$$\frac{dr}{dt} = \frac{D}{r\rho_l}\left[\rho_v(\infty) - \rho_v(r)\right]$$

Finally, using the ideal gas equation for the water vapor, and with some algebraic manipulation,

$$\frac{dr}{dt} = \frac{1}{r}\frac{D\rho_v(\infty)}{\rho_l e(\infty)}\left[e(\infty) - e(r)\right] \tag{6.20}$$

where $e(\infty)$ is the water vapor pressure in the ambient air well removed from the droplet and $e(r)$ is the vapor pressure adjacent to the droplet.[18]

Strictly speaking, $e(r)$ in (6.20) should be replaced by e', where e' is given by (6.8). However, for droplets in excess of 1 μm or so in radius it can be seen from Fig. 6.3 that the solute effect and the Kelvin curvature effect are not very important, so the vapor pressure $e(r)$ is approximately equal to the saturation vapor pressure e_s over a plane surface of pure water (which depends only on temperature). In this case, if $e(\infty)$ is not too different from e_s,

$$\frac{e(\infty) - e(r)}{e(\infty)} \simeq \frac{e(\infty) - e_s}{e_s} = S$$

where S is the supersaturation of the ambient air (expressed as a fraction rather than a percentage). Hence (6.20) becomes

$$r\frac{dr}{dt} = G_\ell S \tag{6.21}$$

[18] Several assumptions have been made in the derivation of (6.20). For example, we have assumed that all of the water molecules that land on the droplet remain there and that the vapor adjacent to the droplet is at the same temperature as the environment. Due to the release of latent heat of condensation, the temperature at the surface of the droplet will, in fact, be somewhat higher than the temperature of the air well away from the droplet. We have also assumed that the droplet is at rest; droplets that are failing with appreciable speeds will be ventilated, and this will affect both the temperature of the droplet and the flow of vapor to the droplet.

where

$$G_\ell = \frac{D\rho_v(\infty)}{\rho_l}$$

which has a constant value for a given environment. It can be seen from (6.21) that, for fixed values of G_ℓ and the supersaturation S, dr/dt is inversely proportional to the radius r of the droplet. Consequently droplets growing by condensation initially increase in radius very rapidly but their rate of growth diminishes with time, as shown schematically by curve (a) in Fig. 6.15.

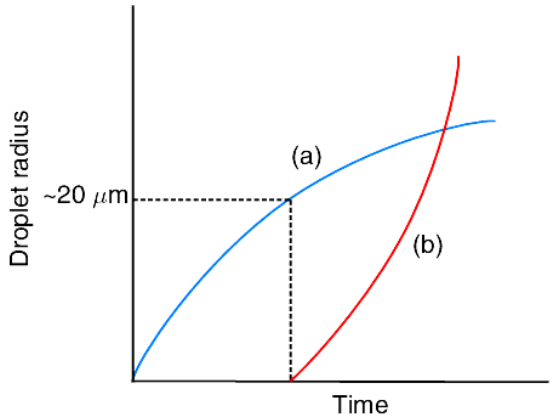

Figure 6.15. Schematic curves of droplet growth a) by condensation from the vapor phase (blue curve) and b) by collection of droplets (red curve).

In a cloud we are concerned with the growth of a large number of droplets in a rising parcel of air. As the parcel rises it expands, cools adiabatically, and eventually reaches saturation with respect to liquid water. Further uplift produces supersaturation that initially increases at a rate proportional to the updraft velocity. As the supersaturation rises CCN are activated, starting with the most efficient. When the rate at which water vapor in excess of saturation is made available by the adiabatic cooling is equal to the rate at which water vapor condenses onto the CCN and droplets, the supersaturation in the cloud reaches a maximum value. The concentration of cloud droplets is determined at this stage (which generally occurs within 100 m or so of cloud base) and is equal to the concentration of CCN activated by the peak supersaturation that has been attained. Subsequently, the growing droplets consume water vapor faster than it is made available by the cooling of the air, so the supersaturation begins to decrease. The haze droplets then begin to evaporate while

the activated droplets continue to grow by condensation. Since the rate of growth of a droplet by condensation is inversely proportional to its radius (see (6.21)), the smaller activated droplets grow faster than the larger droplets. Consequently, in this simplified model, the sizes of the droplets in the cloud become increasingly uniform with time (that is, the droplets approach a *monodispersed* distribution). This sequence of events is illustrated by the results of theoretical calculations shown in Fig. 6.16.

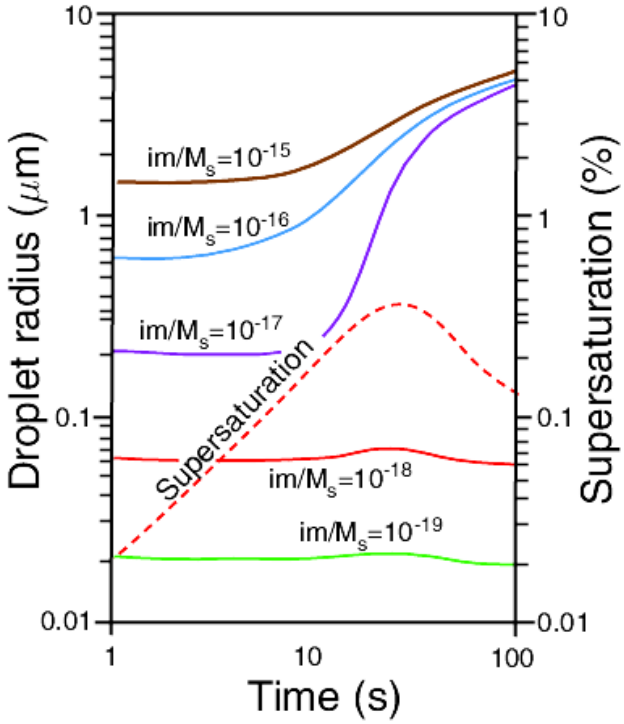

Figure 6.16. Theoretical computations of the growth of cloud condensation nuclei by condensation in a parcel of air rising with a speed of 60 cm s^{-1}. A total of 500 CCN cm^{-1} was assumed with im/M_s values [see Eq. (6.8)] as indicated. Note how the droplets that have been activated (brown, blue and purple curves) approach a monodispersed size distribution after just 100 s. The variation with time of the supersaturation of the air parcel is also shown (dashed red line). [Based on data from J. Meteor. 6, 143 (1949).]

Comparisons of cloud droplet size distributions measured a few hundred meters above the bases of non-precipitating warm cumulus clouds with droplet size distributions computed assuming growth by

condensation for about 5 min show good agreement (Fig. 6.17). Note that the droplets produced by condensation during this time period only extend up to about 10 μm in radius. Moreover, as mentioned above, the rate of increase in the radius of a droplet growing by condensation decreases with time. It is clear, therefore, as first noted by Reynolds[19] in 1877, that growth by condensation alone in warm clouds is much too slow to produce raindrops with radii of several millimeters. Yet rain does form in warm clouds. The enormous increases in size required to transform cloud droplets into raindrops is illustrated by the scaled diagram shown in Fig. 6.18. For a cloud droplet 10 μm in radius to grow to a raindrop 1 mm in radius requires an increases in volume of one millionfold! However, only about one droplet in a million (about 1 liter^{-1}) in a cloud has to grow by this amount for the cloud to rain. The mechanism responsible for the selective growth of a few droplets into raindrops in warm clouds is discussed in the next section.

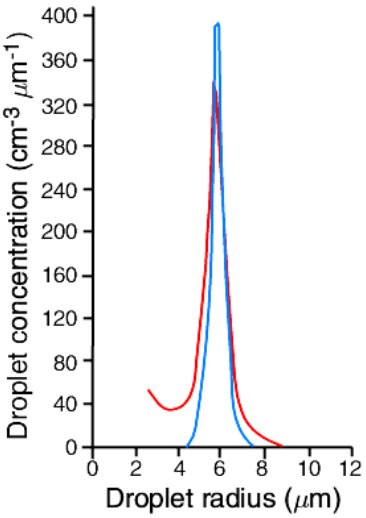

Figure 6.17. Comparison of the cloud droplet size distribution measured 244 m above the base of a warm cumulus cloud (red line) and the corresponding computed droplet size distribution assuming growth by condensation only (blue line). [Adapted from Tech. Note No. 44, Cloud Physics Lab., Univ. of Chicago.]

[19] **Osborne Reynolds** (1842–1912) Probably the outstanding English theoretical mechanical engineer of the 19th century. Carried out important work on hydrodynamics and the theory of lubrication. Studied atmospheric refraction of sound. The Reynolds number, which he introduced, is named after him.

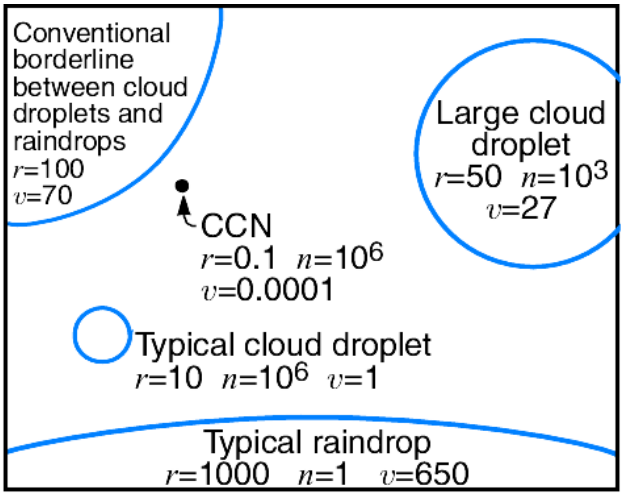

Figure 6.18. Relative sizes of cloud droplets and raindrops; r is the radius in micrometers, n the number per liter of air, and v the terminal fall speed in centimeters per second. The circumference of the circles are drawn approximately to scale, but the black dot representing a typical CCN is twenty-five times larger than it should be relative to the other circles. [Adapted from Adv. in Geophys. 5, 244 (1958).]

6.4.2 Growth by Collection

In warm clouds the growth of some droplets from the relatively small sizes achieved by condensation to the sizes of raindrops is achieved by the collision and coalescence of droplets.[20] Since the steady settling velocity of a droplet as it falls under the influence of gravity through still air (called the *terminal fall speed* of the droplet) increases with the size of the droplet (see Box 6.2), those droplets in a cloud that are somewhat larger than average will have a higher than average terminal fall speed and will collide with smaller droplets lying in their paths.

[20] As early as the 10th century a secret society of Basra ("The Brethren of Purity") suggested that rain is produced by the collision of cloud drops. In 1715 Barlow[21] also suggested that raindrops form due to larger cloud drops overtaking and colliding with smaller droplets. These ideas, however, were not investigated seriously until the first half of the 20th century.

[21] **Edward Barlow** (1639–1719) English priest. Author of "Meteorological Essays Concerning the Origin of Springs, Generation of Rain, and Production of Wind, with an Account of the Tide," John Hooke and Thomas Caldecott, London, 1715.

begin box **BOX 6.2: WAS GALILEO[22] CORRECT? TERMINAL FALL SPEEDS OF WATER DROPLETS IN AIR**

By dropping objects of different masses from the leaning tower of Pisa (so the story goes) Galileo showed that freely falling bodies with different masses fall through a given distance in the same time (i.e., they experience the same acceleration). However, this is true only if the force acting on the body due to gravity is much greater than the frictional drag on the body due to the air, and if the density of the body is much greater than the density of air. (Both of these requirements were met by the heavy, dense objects used by Galileo.)

Consider, however, the more general case of a body of density ρ' and volume V' falling through still air of density ρ. The downward force acting on the body due to gravity is $\rho' V' g$, and the (Archimedes') upward force acting on the body, due to the mass of air displaced by the body, is $\rho V'$. In addition, the air exerts a drag force F_{drag} on the body, which acts upwards. The body will attain a steady *terminal fall speed* when these three forces are in balance, that is

$$\rho' V' g = \rho V' g + F_{\text{drag}}$$

or, if the body is a sphere of radius r, when

$$\frac{4}{3}\pi r^3 g(\rho' - \rho) = F_{\text{drag}} \tag{6.22}$$

For spheres with radius ≤ 20 μm

$$F_{\text{drag}} = 6\pi\eta r v \tag{6.23}$$

where v is the terminal fall speed of the body and η the viscosity of the air. The expression for F_{drag} given by (6.23) is called the *Stokes' drag force*. From (6.22) and (6.23)

[22] **Galileo Galilei** (1564–1642) Renowned Italian scientist. Carried out fundamental investigations into the motion of falling bodies and projectiles, and the oscillation of pendulums. The thermometer had its origins in Galileo's thermoscope. Invented the microscope. Built a telescope with which he discovered the satellites of Jupiter and observed sunspots. Following the publication of his "Dialogue on the Two Chief Systems of the World," a tribunal of the Catholic Church (the Inquisition) compelled Galileo to renounce his view that the Earth revolved around the Sun (he is reputed to have muttered "It's true nevertheless") and committed him to lifelong house arrest. He died the year of Newton's birth. On 31 October 1992, 350 years after Galileo's death, Pope John Paul II admitted that errors had been made by the Church in the case of Galileo, and declared the case closed.

$$v = \frac{2}{9}\,\frac{g(\rho' - \rho)r^2}{\eta}$$

or, if $\rho' >> \rho$ (which it is for liquid and solid objects)

$$v = \frac{2}{9}\,\frac{g\rho' r^2}{\eta} \tag{6.24}$$

The terminal fall speeds of 10 and 20 μm radius water droplets in air at 1013 hPa and 20°C are 0.3 and 1.2 cm s^{-1}, respectively. The terminal fall speed of a water droplet with radius 40 μm is 4.7 cm s^{-1}, which is about 10% less than given by (6.24). Water drops of radius 100 μm, 1 mm and 4 mm have terminal fall speeds of 25.6, 403 and 883 cm s^{-1}, respectively, which are very much less than given by (6.24). This is because as a drop increases in size it becomes increasingly non-spherical and has an increasing wake. This gives rise to a drag force that is much greater than that given by (6.23). end box

Consider a single drop[23] of radius r_1 (called the *collector drop*) that is overtaking a smaller droplet of radius r_2 (Fig. 6.19). As the

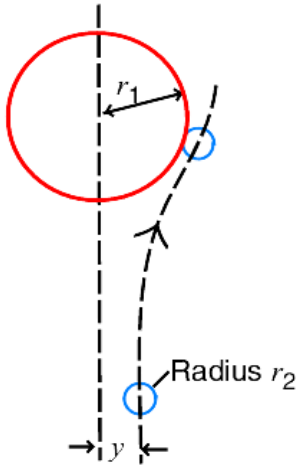

Figure 6.19. Relative motion of a small droplet (blue) with respect to a collector drop (red). y is the maximum impact parameter for a droplet of radius r_2 with a collector drop of radius r_1.

[23] In this section "drop" will refer to the larger and "droplet" to the smaller body.

collector drop approaches the droplet, the latter will tend to follow the streamlines around the collector drop and thereby might avoid capture. We define an effective collision cross section in terms of the parameter y shown in Fig. 6.19, which represents the critical distance between the center fall line of the collector drop and the center of the droplet (measured at a large distance from the collector drop) that just makes a grazing collision with the collector drop. If the center of a droplet of radius r_2 is any closer than y to the center fall line of a collector drop of radius r_1 it will collide with the collector drop; conversely, if the center of a droplet of radius r_2 is at a greater distance than y from the center fall line it will not collide with the collector drop. The effective collision cross section of the collector drop for droplets of radius r_2 is then πy^2, whereas the geometrical collision cross section is $\pi(r_1 + r_2)^2$. The *collision efficiency* E of a droplet of radius r_2 with a drop of radius r_1 is therefore defined as

$$E = \frac{y^2}{(r_1 + r_2)^2} \tag{6.25}$$

Determination of the values of the collision efficiency is a difficult mathematical problem, particularly when the drop and droplet are similar in size, in which case they strongly affect each other's motion. Computed values for E are shown in Fig. 6.20, from which it can be seen that the collision efficiency increases markedly as the size of the collector drop increases, and that the collision efficiencies for collector drops less than about 20 μm in radius are quite small. When the collector drop is much larger than the droplet, the collision efficiency is small because the droplet tends to follow closely the streamlines around the collector drop. As the size of the droplet increases, E increases because the droplet tends to move more nearly in a straight line rather than follow the streamlines around the collector drop. However, as r_2/r_1 increases from about 0.6 to 0.9, E falls off, particularly for smaller collector drops, because the terminal fall speeds of the collector drop and the droplets approach one another so the relative velocity between them is very small. Finally, however, as r_2/r_1 approaches unity, E tends to increase again because two nearly equal sized drops strongly interact to produce a closing velocity between them. Indeed, wake effects behind the collector drop can produce values of E greater than unity (Fig. 6.20).

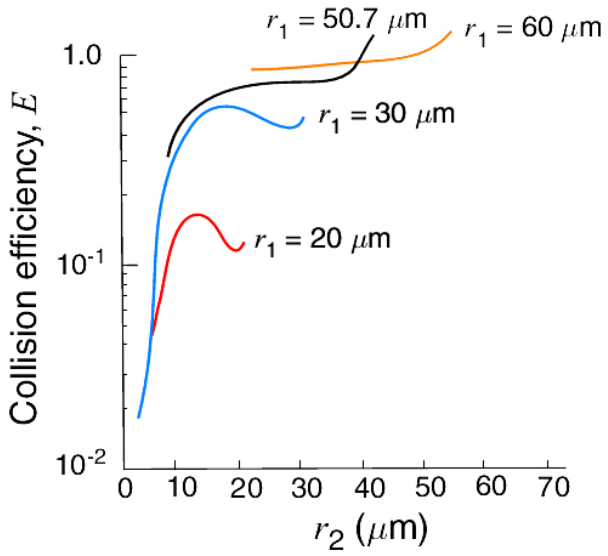

Figure 6.20. Calculated values of the collision efficiency, E, for collector drops of radius r_1 with droplets of radius r_2. [Adapted from H. R. Pruppacher and J. D. Klett, "Microphysics of Clouds and Precipitation," Kluwer Academic Pub., 1997, p. 584. Based on J. Atmos. Sci., 30, 112 (1973).]

The next issue to be considered is whether or not a droplet is captured (i.e., does coalescence occur?) when it collides with a larger drop. It is known from laboratory experiments that droplets can bounce off one another or off a plane surface of water, as demonstrated in Fig. 6.21a). This occurs when air becomes trapped between the colliding surfaces, so that they deform without actually touching.[24] In effect, the droplet rebounds on a cushion of air. If the cushion of air is squeezed out before rebound occurs, the droplet will make physical contact with the drop and coalescence will occur (Fig. 6.21b).[26] The *coalescence efficiency* E' of a droplet of radius

[24] Lenard[25] pointed out in 1904 that cloud droplets might not always coalesce when they collide, and he suggested that this could be due to a layer of air between the droplets or to electrical charges.

[25] **Phillip Lenard** (1862 –1947) Austrian physicist. Studied under Helmholtz and Hertz. Professor of physics at Heidelberg and Kiel. Won the Nobel prize in physics (1905) for work on cathode rays. One of the first to study the charging produced by the disruption of water (for example, in waterfalls).

[26] Even after two droplets have coalesced, the motions set up in their combined mass may cause subsequent breakup into several droplets (see Box 6.2 below).

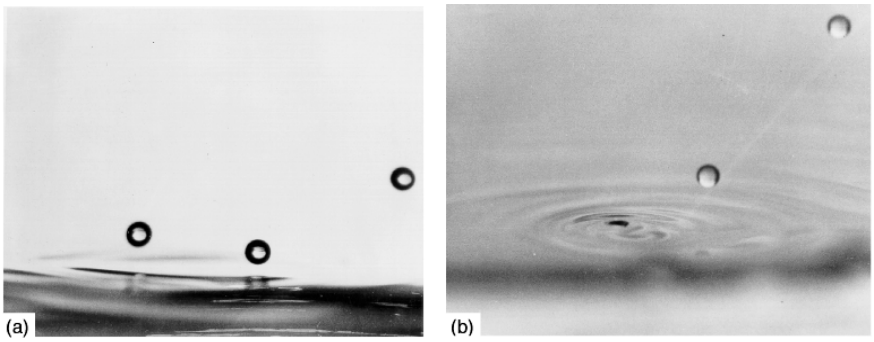

Figure 6.21. a) A stream of water droplets (entering from the right), about 100 μm in diameter, rebounding from a plane surface of water. b) When the angle between the stream of droplets and the surface of the water is increased beyond a critical value, the droplets coalesce with the water. (Photo: P. V. Hobbs.)

r_2 with a drop of radius r_1 is defined as the fraction of collisions that result in a coalescence. The *collection efficiency* E_c is equal to EE'.

The results of laboratory measurements on coalescence are shown in Fig. 6.22. The coalescence efficiency E' is large for very small droplets colliding with larger drops. E' initially decreases as the size of the droplet being collected increases relative to the collector drop but, as the droplet and drop approach each other in size, E' increases

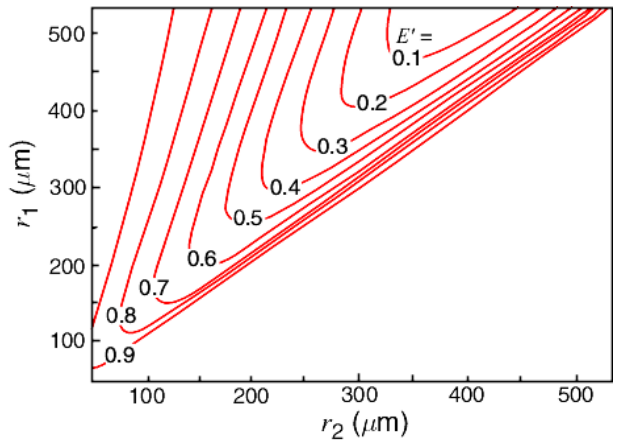

Figure 6.22. Coalescence efficiencies E' for droplets of radius r_2 with collector drops of radius r_1 based on an empirical fit to laboratory measurements. [Adapted from J. Atmos. Sci., 52, 3977 (1995).]

sharply. This behavior can be explained as follows. Whether or not coalescence occurs depends on the relative magnitude of the impact energy to the surface energy of water. This energy ratio provides a measure of the deformation of the collector drop due to the impact which, in turn, determines how much air is trapped between the drop and the droplet. The tendency for bouncing is a maximum for intermediate values of the size ratio of the droplet to the drop. At smaller and larger values of the size ratio, the impact energy is relatively smaller and less able to prevent contact and coalescence.

The presence of an electric field enhances coalescence. For example, in the experiment illustrated in Fig. 6.21a droplets that bounce at a certain angle of incidence can be made to coalesce by applying an electric field of about 10^4 V m^{-1}, which is within the range of measured values in clouds. Similarly, coalescence is aided if the impacting droplet carries an electric charge in excess of about 0.03 pC. The maximum electric charge that a water drop can carry occurs when the surface electrostatic stress equals the surface tension stress. For a droplet 5 μm in radius, the maximum charge is $\sim$0.3 pC; for a drop 0.5 mm in radius it is $\sim$300 pC. Measured charges on cloud drops are generally several orders of magnitude below the maximum possible charge.

Let us now consider a collector drop of radius r_1 that has a terminal fall speed v_1. Let us suppose that this drop is falling in still air through a cloud of equal sized droplets of radius r_2 with terminal fall speed v_2. We will assume that the droplets are uniformly distributed in space and that they are collected uniformly at the same rate by all collector drops of a given size. This so-called *continuous collection model* is illustrated in Fig. 6.23. The rate of increase in the mass M of the collector drop due to collisions is given by

$$\frac{dM}{dt} = \pi r_1^2 \left(v_1 - v_2\right) w_l E_c \tag{6.26}$$

where w_l is the LWC (in kg m^{-3}) of the cloud droplets of radius r_2. Substituting $M = \frac{4}{3}\pi r_1^3 \rho_l$ into (6.26), where ρ_l is the density of liquid water, we obtain

$$\frac{dr_1}{dt} = \frac{\left(v_1 - v_2\right) w_l E_c}{4\rho_l} \tag{6.27}$$

If $v_1 >> v_2$ and we assume that the coalescence efficiency is unity, so that $E_c = E$, (6.27) becomes

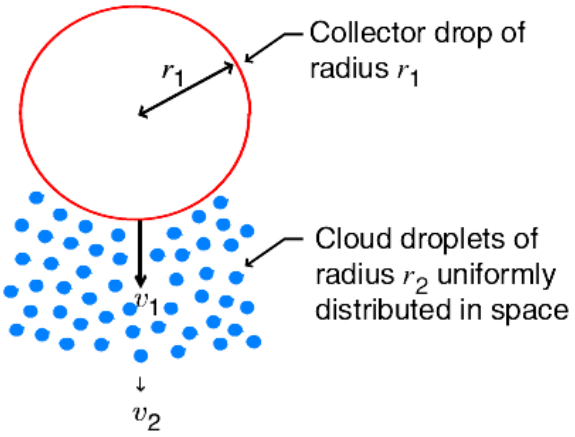

Figure 6.23. Schematic to illustrate the continuous collection model for the growth of a cloud drop by collisions and coalescence.

$$\frac{dr_1}{dt} = \frac{v_1 w_l E}{4\rho_l} \tag{6.28}$$

Since v_1 increases as r_1 increases (see Box 6.2), and E also increases with r_1 (see Fig. 6.20), it follows from (6.28) that dr_1/dt increases with increasing r_1; that is, the growth of a drop by collection is an accelerating process. This behavior is illustrated by the red curve in Fig. 6.15, which indicates negligible growth by collection until the collector drop has reached a radius of $\sim$20 μm (see Fig. 6.20). It can be seen from Fig. 6.15 that for small cloud droplets growth by condensation is initially dominant but, beyond a certain radius, growth by collection dominates and rapidly accelerates.

If there is a steady updraft velocity w in the cloud, the velocity of the collector drop with respect to the ground will be $w - v_1$ and the velocity of the cloud droplets $w - v_2$. Hence dr_1/dt will still be given by (6.28), but the motion of the collector drops is

$$\frac{dh}{dt} = w - v_1 \tag{6.29}$$

where h is the height above a fixed level (say, cloud base) at time t. Eliminating dt between (6.28) and (6.29), and assuming $v_1 >> v_2$ and $E_c = E$, we obtain

$$\frac{dr_1}{dh} = \frac{v_1 w_l E}{4\rho_l (w - v_1)}$$

or, if the radius of the collector drop at height H above cloud base is r_H and its radius at cloud base is r_0,

$$\int_0^H w_l \, dh = 4\rho_l \int_{r_0}^{r_H} \frac{(w - v_1)}{v_1 E} \, dr_1$$

Hence, if we assume that w_l is independent of h,

$$H = \frac{4\rho_l}{w_l} \left[\int_{r_0}^{r_H} \frac{w}{v_1 E} \, dr_1 - \int_{r_0}^{r_H} \frac{dr_1}{E} \right] \tag{6.30}$$

If values of E and v_1 as functions of r_1 are known, (6.30) can be used to determine the value of H corresponding to any value of r_H and *vice versa*. We can also deduce from (6.30) the general behavior of a cloud drop that grows by collection. When the drop is still quite small $w > v_1$, therefore the first integral in (6.30) dominates over the second integral; H then increases as r_H increases, that is, a drop growing by collection is initially carried upward in the cloud. Eventually, as the drop grows, v_1 becomes greater than w and the magnitude of the second integral in (6.30) becomes greater than that of the first integral. H then decreases with increasing r_H, that is, the drop begins to fall through the updraft and will eventually pass through the cloud base and may reach the ground as a raindrop. Some of the larger drops may break up as they fall through the air (see Box 6.3 below). The resulting fragments may be carried up into the cloud on updrafts, grow by collection, fall out, and perhaps break up again; such a chain reaction would serve to enhance precipitation.

PROBLEM 6.3 A drop enters the base of a cloud with a radius r_0 and, after growing with a constant collection efficiency while traveling up and down in the cloud, the drop reaches cloud base again with a radius R. Show that R is a function only of r_0 and the updraft velocity w (assumed to be constant). ◀

SOLUTION ▶ Putting $H = 0$ and $r_H = R$ into the equation before (6.30) we obtain

$$0 = 4\rho_l \int_{r_0}^{R} \frac{w - v_1}{v_1 E} \, dr_1$$

or, since E and w are assumed to be constant,

$$w \int_{r_0}^{R} \frac{dr_1}{v_1} = \int_{r_0}^{R} dr_1 = R - r_0$$

Therefore

$$R = r_0 + w \int_{r_0}^{R} \frac{dr_1}{v_1} \tag{6.31}$$

Since $\int_{r_0}^{R} dr_1/v_1$ is a function only of R and r_0, it follows from (6.31) that R is a function only of r_0 and w. ◀

Provided that a few drops are large enough to be reasonably efficient collectors (i.e., with radius $\geq$20 μm), and the cloud is deep enough and contains sufficient liquid water, the equations derived above for growth by continuous collection indicate that raindrops should grow within reasonable time periods ($\sim$1 h), see Exercise 6.23, and that deep clouds with strong updrafts should produce rain quicker than shallower clouds with weak updrafts.

We have seen in Section 6.4.1 that growth by condensation slows appreciably as a droplet approaches $\sim$20 μm in radius (Fig. 6.15). Also, growth by condensation alone in a homogeneous cloud and a uniform updraft tends to produce a monodispersed droplet size distribution (Fig. 6.17), in which the fall speeds of the droplets would be very similar and therefore collisions unlikely. Consequently, there has been considerable interest in the origins of the few ($\sim$1 liter^{-1}) large drops that become the collectors in warm clouds that go on to produce raindrops, and in the mechanisms responsible for the broad spectrum of droplet sizes measured in clouds (Figs. 6.6 and 6.7). Possible mechanisms include the rapid growth of a few droplets that originate on giant CCN, spectrum broadening due to the different histories of droplets growing in inhomogeneous clouds, the effects of turbulence in clouds on growth by condensation and on the collisions of droplets, and the stochastic growth of droplets. The latter mechanism is discussed below.

In the continuous collection model, it is assumed that the collector drop collides in a continuous and uniform fashion with smaller cloud droplets that are uniformly distributed in space. Consequently, the continuous collection model predicts that collector drops of the same size grow at the same rate if they fall through the same cloud of droplets. The *stochastic* (or *statistical*) *collection model* allows for the fact that collisions are individual events, statistically distributed in time and space. Consider, for example, 100 droplets, initially the same size as shown on line 1 in Fig. 6.24. After a certain interval of time, some of these droplets (let us say 10) will have collided with other droplets, so that the distribution will now be as depicted in line 2 of Fig. 6.24. Because of their larger size, these 10 larger droplets are now in a more favored position for making further collisions. The

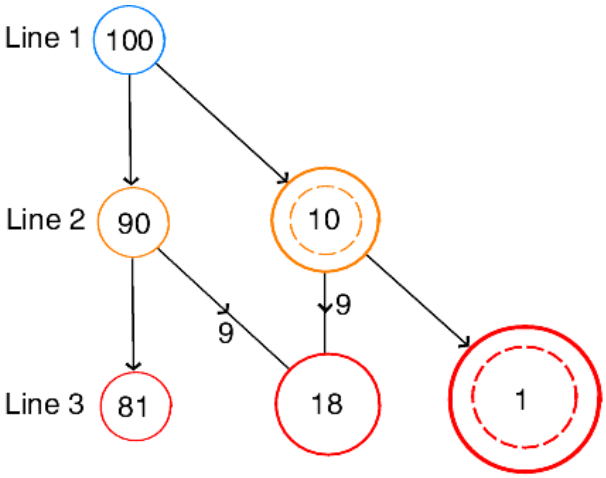

Figure 6.24. Schematic diagram to illustrate broadening of droplet sizes by statistical collisions. [Adapted from J. Atmos. Sci. 24, 689 (1967).]

second collisions are similarly statistically distributed, giving a further broadening of the droplet size spectrum, as shown in line 3 of Fig. 6.24 (where it has been assumed that in this time step, nine of the smaller droplets and one of the larger droplets on line 2 each had a collision). Hence, by allowing for a statistical distribution of collisions, three size categories of droplets have developed after just two time steps. This concept is important, since it not only provides a mechanism for developing broad droplet size spectra from the fairly uniform droplet sizes produced by condensation, but it also reveals how a small fraction of the droplets in a cloud can grow much faster than average by statistically distributed collisions.

The growth of drops by collection is also accelerated if they pass through pockets of higher than average LWC. Even if such pockets of high LWC exist for only a few minutes, and occupy only a few percent of the cloud volume, they can produce significant concentrations of large drops when averaged over the entire cloud volume. Measurements in clouds reveal such pockets of high LW (e.g., Fig. 6.10).

Much of what is presently known about both dynamical and microphysical cloud processes can be incorporated into computer models and numerical experiments can be carried out. For example, consider the growth of drops, by condensation and stochastic collisions, in warm cumulus clouds in typical marine and continental air masses. We have pointed out in Section 6.2 that the average droplet sizes

are significantly larger, and the droplet size spectra much broader, in marine than in continental cumulus clouds (Fig. 6.7). We have attributed these differences to the higher concentrations of CCN present in continental air (Fig. 6.5). Figure 6.25 illustrates the

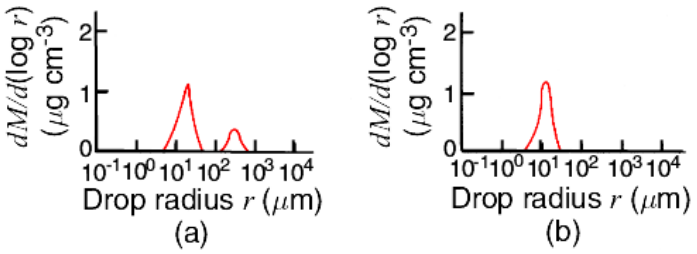

Figure 6.25. Numerical predictions of the mass spectrum of drops near the middle of a) a warm marine cumulus cloud, and b) a warm continental cloud after 67 minutes of growth. (B. C. Scott and P. V. Hobbs, unpublished.)

effects of these differences in cloud microstructures on the development of larger drops. The CCN spectra used as input data to the two clouds were based on measurements, with the continental air having much higher concentrations of CCN than the marine air (about 200 versus 45 cm^{-3} at 0.2% supersaturation). It can be seen that after 67 min the cumulus cloud in marine air develops some drops between 100 and 1000 μm in radius (that is, raindrops), whereas, the continental cloud does not contain any droplets greater than about 20 μm in radius. These markedly different developments are attributable to the fact that the marine cloud contains a small number of drops that are large enough to grow by collection, whereas the continental cloud does not. These model results support the observation that a marine cumulus cloud is more likely to rain than a continental cumulus cloud with similar updraft velocity, LWC and depth.

begin box

BOX 6.3: SHAPE, BREAKUP AND SIZE DISTRIBUTION OF RAINDROPS

Raindrops in free fall are often depicted as tear-shaped. In fact, as a drop increases in size above about 1 mm in radius it becomes flattened on its underside in free fall, and it gradually changes in shape from essentially spherical to increasingly parachute-(or jellyfish-)like. If the initial radius of the drop exceeds about 2.5 mm, the parachute

becomes a large inverted bag, with a toroidal ring of water around its lower rim. Laboratory and theoretical studies indicate that when the equivalent spherical diameter of the drop bag bursts to produce a fine spray of droplets and the toroidal ring breaks up into a number of large drops (Fig. 6.26). Interestingly, the largest raindrops ever observed at diameters of ∼0.8–1 cm, so they must have been on the verge of bag break-up.

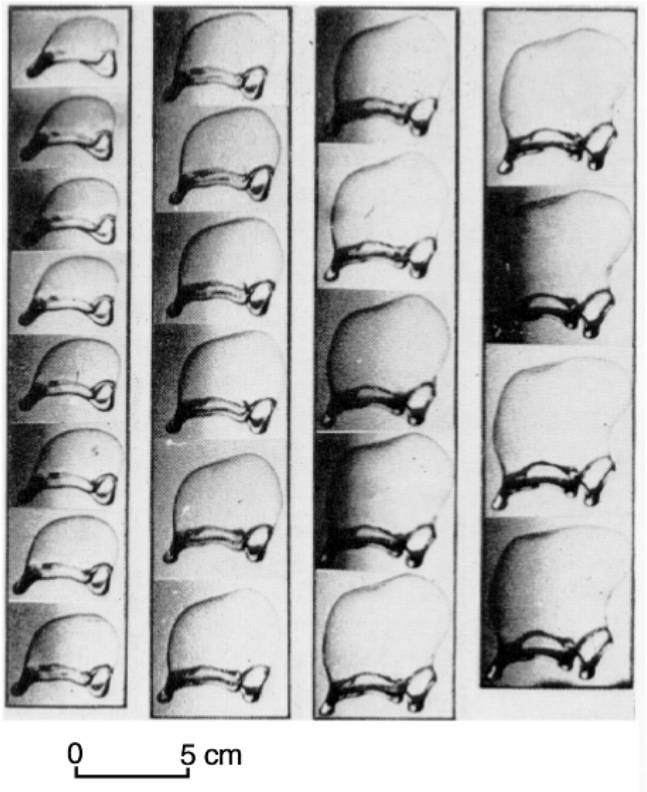

Figure 6.26. Sequence of high-speed photographs (starting at upper left and moving down and to the right) showing how a large drop in free fall forms a parachute-like shape with a toroidal ring of water around its lower rim. The toroidal ring becomes distorted and develops cusps separated by threads of water. The cusps eventually break away to form large drops and the thin film of water that forms the upper part of the parachute bursts to produce a spray of small droplets. Time interval between photographs = 1 ms. [From Quart. J. Roy. Met. Soc., 90, 275 (1964).]

Collisions between raindrops appears to be a more important path to break-up. The three main types of breakup following a collision are shown schematically in Fig. 6.27. The probabilities of the various types of breakup shown in Fig. 2.77 are: sheets 55%, necks 27% and disks 18%. Bag breakup may also occur following the collision of two drops, but it is very rare (<0.5%).

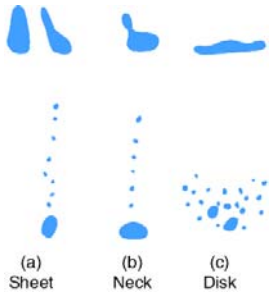

Figure 6.27. Schematic illustrations of three types of breakup following the collision of two drops. [Adapted from J. Atmos. Sci., 32, 1401 (1975).]

Theoretical predictions of the probability of breakup as a function of the sizes of two coalescing drops are shown in Fig. 6.28. For

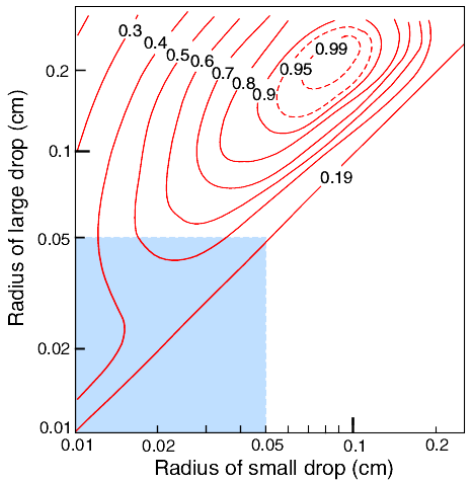

Figure 6.28. Empirical results for the probability of breakup (expressed as a fraction and shown on the contours) following the collision and initial coalescence of two drops. The shaded region is covered by Fig. 6.21, but note that Fig. 6.21 shows the probability of coalescence rather than breakup. [Adapted from K. C. Young, "Microphysical Processes in Clouds," Oxford University Press, New York, 1993, p. 192. Based on J. Atmos. Sci., 39, 1591 (1982).]

a fixed size of the larger drop, the probability of breakup initially increases as the size of the smaller drop increases, but as the smaller drop approaches the size of the larger the probability of breakup decreases due to the decrease in the kinetic energy of the impact.

The spectrum of raindrop sizes should reflect the combined influences of the drop growth processes discussed above, and the breakup of individual drops and of colliding drops. However, as we have seen, individual drops have to reach quite large sizes before they break up. Also, the frequency of collisions between raindrops is quite small, except in very heavy rain. For example, a drop with a radius of $\sim$1.7 mm in rain of 5 mm h^{-1}, would experience only one collision as it falls to the ground from a cloud base at 2 km above the ground. Consequently, it cannot be generally assumed that raindrops have had sufficient time to attain an equilibrium size distribution.

Measurements of the size distributions of raindrops that reach the ground can often be fitted to an expression, known as the *Marshall-Palmer* distribution, which is of the form

$$N(D) = N_o \exp(-\Lambda D) \tag{6.32}$$

where $N(D)dD$ is the number of drops per unit volume with diameters between D and $D + dD$, and N_o and Λ are empirical fitting parameters. The value of N_o tends to be constant, but Λ varies with the rainfall rate. end box

6.5 6.5 Microphysics of Cold Clouds

If a cloud extends above the 0°C level it is called a *cold cloud*. Even though the temperature may be below 0°C, water droplets can still exist in clouds, in which case they are referred to as *supercooled droplets*[27]. Cold clouds may also contain ice particles. If a cold cloud contains both ice particles and supercooled droplets it is said to be a *mixed cloud*; if it consists entirely of ice it is said to be *glaciated*.

[27] Saussure[28] observed, around 1783, that water could remain in the liquid state below 0°C. A spectacular confirmation of the existence of supercooled clouds was provided by a balloon flight made by Barrel[29] in 1850. He observed water droplets down to −10.5°C and ice crystals at lower temperatures.

[28] **Horace Bénédict de Saussure** (1740–1799) Swiss geologist, physicist, meteorologist, and naturalist. Traveled extensively, particularly in the Alps, and made the second ascent of Mont Blanc (1787).

[29] **Jean Augustine Barrel** (1819 –1884) French chemist and agriculturalist. First to extract nicotine from tobacco-leaf.

In this section we are concerned with the origins and concentrations of ice particles in clouds, the various ways in which ice particles can grow, and the formation of precipitation in cold clouds.

6.5.1 Nucleation of Ice Particles; Ice Nuclei

A supercooled droplet is in an unstable state. For freezing to occur, enough water molecules must come together within the droplet to form an embryo of ice large enough to survive and grow. The situation is analogous to the formation of a water droplet from the vapor phase discussed in Section 6.2.1. If an ice embryo within a droplet exceeds a certain critical size, its growth will produce a decrease in the energy of the system. On the other hand, any increase in the size of an ice embryo smaller than the critical size causes an increase in total energy. In the latter case, from an energetic point of view, it is preferable for the embryo to break up.

If a water droplet contains no foreign particles it can freeze only by *homogeneous nucleation*. Since the numbers and sizes of the ice embryos that form by chance aggregations increase with decreasing temperature, below a certain temperature (which depends on the volume of water considered) freezing by homogeneous nucleation becomes a virtual certainty. The results of laboratory experiments on the freezing of very pure water droplets, which were probably nucleated homogeneously, are shown by the blue symbols in Fig. 6.29. It appears from these results that homogeneous nucleation occurs at about $-41°$C for droplets about 1 μm in diameter, and at about $-35°$C for drops 100 μm in diameter. Hence, in the atmosphere, homogeneous nucleation of freezing generally occurs only in high clouds.

If a droplet contains a rather special type of particle, called a *freezing nucleus*, it may freeze by a process known as *heterogeneous nucleation*[30] in which water molecules in the droplet collect onto the surface of the particle to form an ice-like structure that may increase

[30] Studies of the heterogeneous nucleation of ice date back to 1724 when Fahrenheit[31] slipped on the stairs while carrying a flask of cold (supercooled) water and noticed that the water had become full of flakes of ice.

[31] **Gabriel Daniel Fahrenheit** (1686–1736) German instrument maker and experimental physicist. Lived in Holland from the age of 15 but traveled widely in Europe. Developed the thermometric scale that bears his name. Fahrenheit knew that the boiling point of water varies with atmospheric pressure [see Eq. (3.112)] and he constructed a thermometer from which the atmospheric pressure could be determined by noting the boiling point of water.

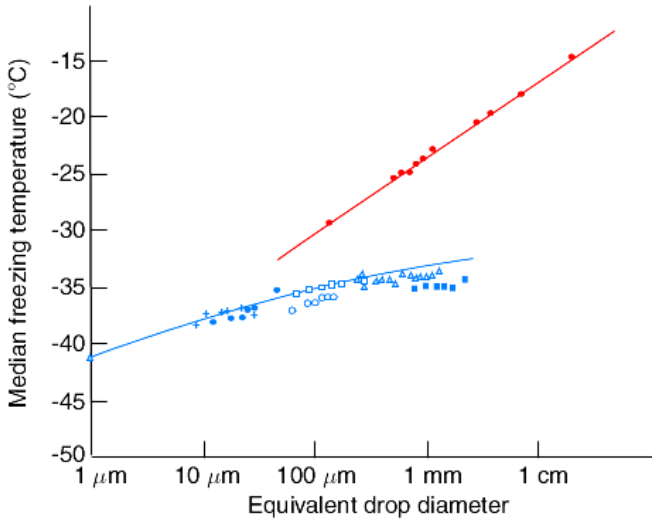

Figure 6.29. Median freezing temperatures of water samples as a function of their equivalent drop diameter. The different symbols are results from different workers. The red symbols and red line represent heterogeneous freezing and the blue symbols and line represent homogeneous freezing. [Adapted from B. J. Mason, "The Physics of Clouds," Oxford Univ. Press, Oxford, 1971, p. 160.]

in size and cause the droplet to freeze. Since the formation of the ice structure is aided by the freezing nucleus, and the ice embryo also starts off with the dimensions of the freezing nucleus, heterogeneous nucleation can occur at much higher temperatures than homogeneous nucleation. The red symbols in Fig. 6.29 show the results of laboratory experiments on the heterogeneous freezing of water droplets. The droplets consisted of distilled water from which most, but not all, of the foreign particles were removed. A large number of droplets of each of the sizes indicated in Fig. 6.28 were cooled, and the temperature at which half of the droplets had frozen was noted. It can be seen that this median freezing temperature increases as the size of the droplet increases. The size dependence reflects the fact that a larger drop is more likely to contain a freezing nucleus capable of causing heterogeneous nucleation at a given temperature.

We have assumed above that the particle that initiates the freezing is contained within the droplet. However, cloud droplets may also be frozen if a suitable particle in the air comes into contact with the droplet, in which case freezing is said to occur by *contact nucleation*, and the particle is referred to as a *contact nucleus*. Laboratory experiments suggest that some particles can cause a drop to freeze

by contact nucleation at temperatures several degrees higher than if they were embedded in the drop.

Certain particles in the air also serve as centers upon which ice can form directly from the vapor phase. These particles are referred to as *deposition nuclei*. Ice can form by deposition[32] provided that the air is supersaturated with respect to ice and the temperature is low enough. If the air is supersaturated with respect to water, a suitable particle may serve either as a freezing nucleus (in which case liquid water first condenses onto the particle and subsequently freezes) or as a deposition nucleus (in which case there is no intermediate liquid phase, at least on the macroscopic scale).

If we wish to refer to an ice nucleating particle in general, without specifying its mode of action, we will call it an *ice nucleus*. However, it should be kept in mind that the temperature at which a particle can cause ice to form depends, in general, upon the mechanism by which the particle nucleates the ice as well as upon the previous history of the particle.

Particles with molecular spacings and crystallographic arrangements similar to those of ice (which has a hexagonal structure) tend to be effective as ice nuclei, although this is neither a necessary or sufficient condition for a good ice nucleus. Most effective ice nuclei are virtually insoluble in water. Some inorganic soil particles (mainly clays) can nucleate ice at fairly high temperatures (i.e., above $-15°C$), and they probably play an important role in nucleating ice in clouds. For example, in one study 87% of the snow crystals collected on the ground had clay mineral particles at their centers and more than half of these were kaolinite. Many organic materials are effective ice nucleators. Decayed plant leaves contain copious ice nuclei, some active as high as $-4°C$. Ice nuclei active at $-4°C$ have also been found in sea water rich in plankton.

The results of laboratory measurements on condensation-freezing and deposition shown in Fig. 6.30 indicate that for a variety of materials the onset of ice nucleation occurs at higher temperatures under water supersaturated conditions (so that condensation-freezing is possible) than under water subsaturated conditions (when only ice deposition is possible). For example, kaolinite serves as an ice nucleus at $-10.5°C$ at water saturation, but at 17% supersaturation with respect to ice (but subsaturation with respect to water) the

[32] The transfer of water vapor to ice is sometimes referred to as *sublimation* by cloud physicists. However, since chemists use this term more appropriately to describe the evaporation of a solid, the term *deposition* is preferable and is used here.

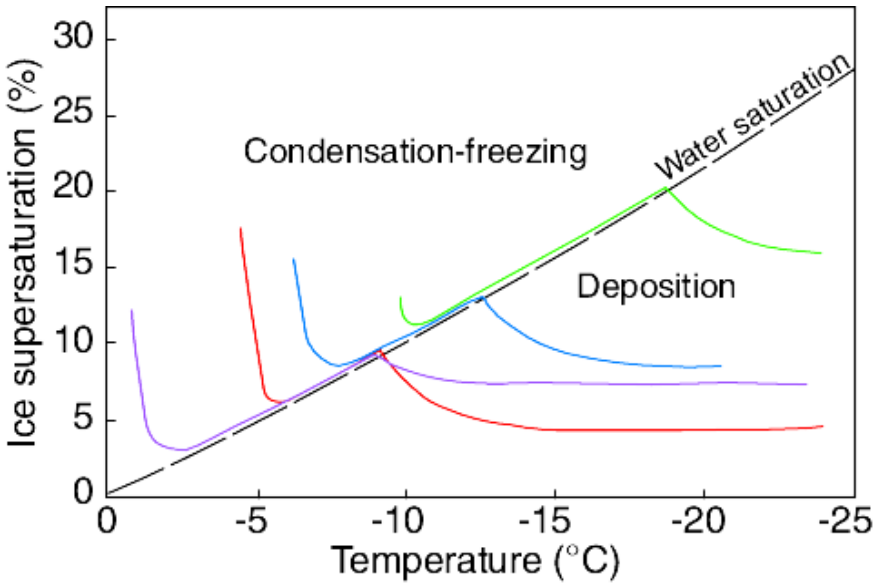

Figure 6.30. Onset of ice nucleation as a function of temperature and supersaturation for various compounds. Conditions for condensation-freezing and ice deposition are indicated. Ice nucleation starts above the indicated lines. The materials are silver iodide (red), lead iodide (blue), methaldehyde (violet), and kaolinite (green). [Adapted from J. Atmos. Sci., 36, 1788 (1979).]

temperature has to be about $-20°C$ for kaolinite to act as an ice nucleus.

In some cases, after a particle has served as an ice nucleus and all of the visible ice is then evaporated from it but the particle is not warmed above $-5°C$ or exposed to a relative humidity with respect to ice of less than 35%, it may subsequently serve as an ice nucleus at a temperature a few degrees higher than it did initially. This is referred to as *preactivation*. Thus, ice crystals from upper level clouds that evaporate before reaching the ground may leave behind preactivated ice nuclei.

Several techniques have been used for measuring the concentrations of particles in the air that are active as ice nuclei at a given temperature. A common method is to draw a known volume of air into a container and to cool it until a cloud is formed. The number of ice crystals forming at a particular temperature is then measured. In *expansion chambers* cooling is produced by compressing the air and

then suddenly expanding it; in *mixing chambers* cooling is produced by refrigeration. In these chambers particles may serve as freezing, contact, or deposition nuclei. The number of ice crystals that appear in the chamber may be determined by illuminating a certain volume of the chamber and estimating visually the number of crystals in the light beam, by letting the ice crystals fall into a dish of supercooled soap or sugar solution where they grow and can be counted, or by allowing the ice crystals to pass through a small capillary tube attached to the chamber where they produce audible clicks that can be counted electronically. In another technique for detecting ice nuclei, a measured volume of air is drawn through a Millipore filter that retains the particles in the air. The number of ice nuclei on the filter is then determined by placing it in a box held at a known supersaturation and temperature and counting the number of ice crystals that grow on the filter. More recently, ice nucleation has been studied using diffusion chambers in which temperature, supersaturation and pressure can be controlled independently.

World-wide measurements of ice nucleus concentrations as a function of temperature (Fig. 6.31) indicate that concentrations of ice

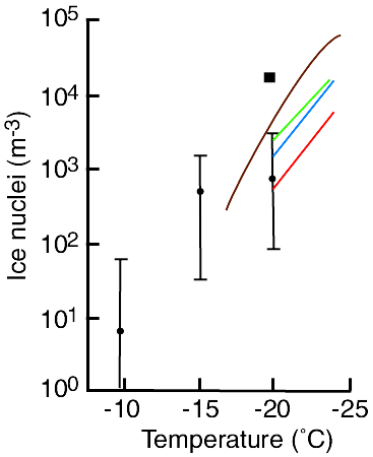

Figure 6.31. Measurements of average ice nucleus concentrations at close to water saturation in the northern and southern hemispheres. Southern hemisphere, expansion chamber (red); southern hemisphere, mixing chamber (blue); northern hemisphere, expansion chamber (green); northern hemisphere, mixing chamber (black square); Antarctica, mixing chamber (brown). The vertical lines show the range and mean values (dots) of ice nucleus concentrations based on Millipore filter measurements in many locations around the world.

nuclei tend to be higher in the northern than in the southern hemisphere. It should be noted however that ice nucleus concentrations can sometimes vary by several orders of magnitude over several hours. On the average, the number N of ice nuclei per liter of air active at temperature T tends to follow the empirical relationship

$$\ln N = a(T_1 - T) \tag{6.33}$$

where T_1 is the temperature at which one ice nucleus per liter is active (typically about -20°C) and a varies from about 0.3 to 0.8. For $a = 0.6$, (6.32) predicts that the concentration of ice nuclei increases by about a factor of 10 for every 4°C decrease in temperature. In urban air, the total concentration of aerosol is on the order of 10^8 liter^{-1} and only about one particle in 10^8 acts as an ice nucleus at -20°C.

PROBLEM 6.4 If the concentration of freezing nuclei in a drop that are active at temperature T is given by (6.33), show that the median freezing temperature of a number of drops should vary with their diameter as shown by the red line in Fig. 6.29. (If a drop contains n active freezing nuclei, assume that the probability p that it freezes in a given time interval is given by the Poisson distribution for random events, namely, $p = 1 - \exp(-n)$.) ◀

SOLUTION ▶ From (6.33) the number of active freezing nuclei at temperature T in 1 liter of a drop is

$$N = \exp[a(T_1 - T)]$$

where T_1 is the temperature at which $N = 1$ per liter. Therefore, the number of active freezing nuclei n at temperature T in a drop of diameter D (in meters) is equal to the volume of the drop (in m^3) multiplied by the number of active freezing nuclei per m^3 (i.e., 10^3 N). Therefore

$$n = \frac{4}{3}\pi\left(\frac{D}{2}\right)^3 10^3 \exp[a(T_1 - T)] \tag{6.34}$$

The probability p that a drop of diameter D, containing n freezing nuclei, is frozen is given by

$$p = 1 - \exp(-n)$$

When half of the drops are frozen (i.e., $p = 0.5$) n (and therefore $\ln n$) are constants. Hence, from (6.34)

$$\ln\ n = \text{constant} = \ln\left\{\frac{4}{3}\pi\left(\frac{D}{2}\right)^3 10^3 \exp[a(T_1 - T)]\right\}$$

or

$$3\ln D + a(T_1 - T) = \text{constant}$$

where (since $p = 0.5$) T is now the median freezing temperature. It follows from this last expression that

$$T = (\text{constant}) \ln D + (\text{constant})$$

Therefore, $\ln D$ plotted against the median freezing temperature T for drops of diameter D should be a straight line, as shown by the red line in Fig. 6.29. ◀

As we have seen, the activity of a particle as a freezing or a deposition nucleus depends not only on the temperature but also on the supersaturation of the ambient air. Supersaturation was not well controlled in many of the measurements shown in Fig. 6.31, on which (6.33) is based. The effect of supersaturation on measurements of ice nucleus concentrations is shown in Fig. 6.32, where it can be seen that at a constant temperature the greater the supersaturation with respect to ice the more particles serve as ice nuclei. The empirical equation to the best-fit line to these measurements (the red line in Fig. 6.32) is

$$N = \exp\{a + b[100(S_i - 1)]\} \tag{6.35}$$

where N is the concentration of ice nuclei per liter, S_i the supersaturation with respect to ice, $a = -0.639$ and $b = 0.1296$.

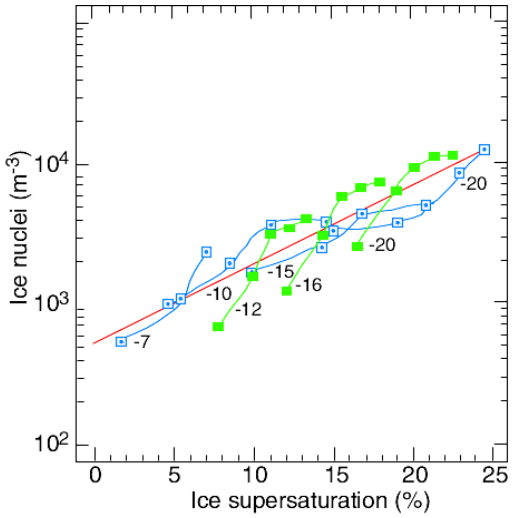

Figure 6.32. Ice nucleus concentration measurements versus ice supersaturation; temperatures are noted alongside each line. Data from Atmos. Res., 29, 209 (1993)—blue squares, and Atmos. Envir., 19, 1872 (1985)—green squares. The red line is eqn. (6.35).

6.5.2 Concentrations of Ice Particles in Clouds

The probability of ice particles being present in a cloud increases as the temperature decreases below 0°C, as illustrated in Fig. 6.33. The results shown in this figure indicate that the probability of ice being present is 100% for cloud top temperature below about −13°C. At higher temperatures the probability of ice being present falls off sharply, but it is greater if the cloud contains drizzle or raindrops. Clouds with top temperatures between about 0 and −8°C generally contain copious supercooled droplets. It is in clouds such as these that aircraft are most likely to encounter severe icing conditions, since supercooled droplets freeze when they collide with an aircraft.

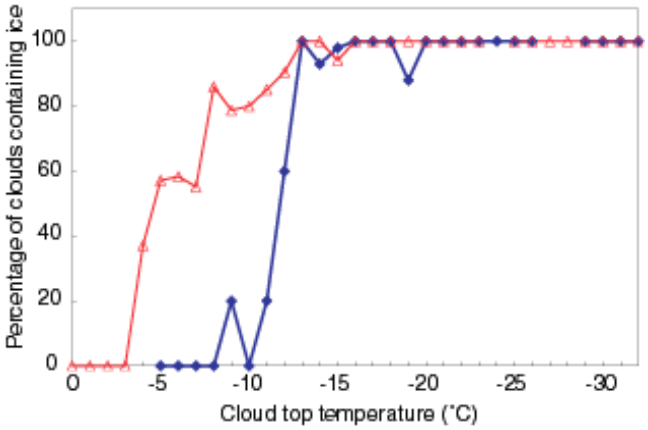

Figure 6.33. Percentage of clouds containing ice particle concentrations greater than about 1 per liter as a function of cloud top temperature. Note that on the abscissa temperatures decrease to the right. Blue curve: continental cumuliform clouds with base temperatures of 8 to −18°C containing no drizzle or raindrops prior to the formation of ice. [Data from Quart. J. Roy. Met. Soc., 120, 573 (1994).] Red curve: clean marine cumuliform clouds and clean arctic stratiform clouds with base temperatures from 25 to −3°C containing drizzle or raindrops prior to the formation of ice. [Data from Quart. J. Roy. Met. Soc., 11,7 207 (1991), Quart. J. Roy. Met. Soc., 124, 2035 (1998), J. Geophys. Res., 106, 15,065 (2001), and Cloud and Aerosol Research Group, University of Washington, unpublished data.]

Shown in Fig. 6.34 are measurements of the concentrations of ice particles in clouds. Also shown are the concentrations of ice nuclei

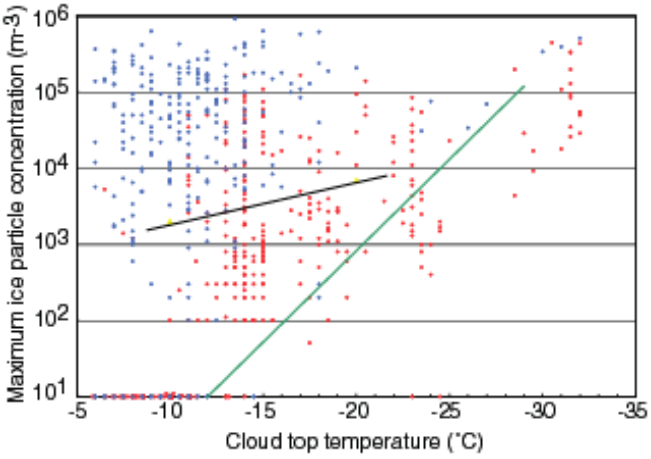

Figure 6.34. Maximum concentrations of ice particles versus cloud top temperature in mature and aging marine cumuliform clouds (blue dots) and in continental cumuliform clouds (red dots). Note that on the abscissa temperatures decrease to the right. The symbols along the abscissa indicate ice concentrations ≤ 1 liter^{-1}, which was the lower limit of detection. Shown by the green line are the ice nucleus concentrations predicted by Eq. (6.33) with $a = 0.6$ and $T_1 = 253$ K. The black line shows the ice nucleus concentrations from (6.35) assuming water saturated conditions. [Data from J. Atmos. Sci., 42, 2253 (1985), and Quart. J. Roy. Met. Soc., 117, 207 (1991) and 120, 573 (1994).]

given by (6.33) with $a = 0.6$ and $T_1 = 253°$K. It can be seen from these results that on some occasions ice particles are not detected, even when ice nucleus measurements indicate that they should be. On other occasions, ice particles are present in concentrations several orders of magnitude greater than ice nucleus measurements. At temperatures above about $-20°$C, marine clouds show a particular propensity for ice particle concentrations that are many orders of magnitude greater than ice nucleus measurements would suggest.

Several explanations have been proposed to account for the high ice particle concentrations observed in some clouds. First, it is possible that current techniques for measuring ice nuclei do not provide reliable estimates of the concentrations of ice nuclei active in natural clouds under certain conditions. It is also possible that ice particles in clouds increase in number without the action of ice nuclei, by what are termed *ice multiplication* (or *ice enhancement*) processes. For example, some ice crystals are quite fragile and may break up when they collide with other ice particles. However, the strongest

contender for an ice enhancement process in clouds is one that involves water droplets freezing. When a supercooled droplet freezes in isolation (e.g., in free fall), or after it collides with an ice particle (the freezing of droplets onto an ice particle is called *riming*), it does so in two distinct stages. In the first stage, which occurs almost instantaneously, a fine mesh of ice shoots through the droplet and freezes just enough water to raise the temperature of the droplet to 0°C. The second stage of freezing is much slower and involves the transfer of heat from the partially frozen droplet to the colder ambient air. During the second stage of freezing an ice shell forms over the surface of the droplet and then thickens progressively inward. As the ice shell advances inward, water is trapped in the interior of the droplet; as this water freezes it expands and sets up large stresses in the ice shell. These stresses may cause the ice shell to crack and even explode, throwing off numerous small ice splinters.

PROBLEM 6.5 Determine the fraction of the mass of a supercooled droplet that is frozen in the initial stage of freezing if the original temperature of the droplet is −20°C. What are the percentage increases in the volume of the droplet due to the first and to the second stages of freezing? (Latent heat of melting $= 3.3 \times 10^5$ J kg^{-1}; specific heat of liquid water $= 4218$ J K^{-1} kg^{-1}; specific heat of ice $= 2106$ J K^{-1} kg^{-1}; density of ice $= 0.917 \times 10^3$ kg m^{-3}.) ◀

SOLUTION ▶ Let m be the mass (in kg) of the droplet and dm the mass of ice that is frozen in the initial stage of freezing. Then the latent heat (in joules) released due to freezing is $3.3 \times 10^5\ dm$. This heat raises the temperature of the unfrozen water and the ice from −20 to 0°C (at which temperature the first stage of freezing ceases). Therefore,

$$3.3 \times 10^5\ dm = (2106 \times 20\ dm) + [4218 \times 20(m - dm)]$$

Hence

$$\frac{dm}{m} = \frac{4218}{(3.3 \times 10^5/20) - 2106 + 4218} = 0.23$$

Therefore, 23% of the mass of the droplet is frozen during the initial stage of freezing.

Since the density of water is 10^3 kg m^{-3}, when mass dm of water freezes the increase in volume is $[(1/0.917) - 1]\ dm/10^3$. The fractional increase in volume of the mixture is therefore $[(1/0.917) - 1]\, dm/\left(10^3 V\right)$, where V is the volume of mass m of water. But $m/V = 10^3$ kg m^{-3}. Therefore, the fractional increase in volume produced by the initial stage of freezing is

$$[(1/0.917) - 1]\ dm/m = [(1/0.917) - 1]0.23 = 0.021 \text{ or } 2.1\%$$

If the fraction of the mass of the droplet that is frozen in the initial stage of freezing is 0.23, the fraction that is frozen in the second stage of freezing is 0.77. Therefore, the fractional increase in volume produced by the second

stage of freezing is

$$[(1/0.917) - 1]\ dm/m = [(1/0.917) - 1]0.77 = 0.070 \text{ or } 7.0\%$$

◀

Since an ice particle falling through a supercooled cloud will be impacted by thousands of droplets, each of which might shed numerous ice splinters as it freezes onto the ice particle, ice splinter production by riming is potentially much more important than ice splinter production during the freezing of isolated droplets. Laboratory experiments indicate that ice splinters are ejected during riming provided the droplets involved have diameters $\geq$25 μm, temperatures are between -2.5 and -8.5°C (with peak ice splinter production from -4 to -5°C), and the impact speed (determined in a cloud by the fall speed of the ice particle undergoing riming) is between $\sim$0.2 and 5 m s^{-1} with peak splinter production at impact speeds of a few m s^{-1}. For example, laboratory measurements show that for a droplet spectrum characterized by 50 drops cm^{-3} with droplets ranging in diameter from $\sim$5 to 35 μm, a LWC of 0.2 g m^{-3}, a temperature of -4.5°C, and an impact speed of 3.6 m s^{-1}, $\sim$300 ice splinters are produced for every microgram of rime that is accumulated (for a spherical ice particle 1 mm in radius, 1 μg of accumulated rime corresponds to a layer of ice $\sim$0.1 μm thick).

The high concentrations of ice particles (100 liter^{-1} or more) observed in some clouds (see Fig. 6.34) are associated primarily with older clouds. Young cumulus towers generally consist entirely of water droplets, and generally require about 10 min before showing signs of plentiful ice particles. It also appears from measurements in clouds that high ice particle concentrations occur after the formation of drops with diameters $\gtrsim$25 μm and when rimed ice particles appear. These observations are consistent with the hypothesis that the high ice particle concentrations are due to the ejection of ice splinters during riming. However, calculations based on the results of laboratory experiments on ice splinter production during riming, suggest that this process is too slow to explain the explosive formation of extremely high concentrations of ice particles observed in some clouds. As indicated schematically in Fig. 6.35, an additional "super" ice enhancement mechanism may sometimes operate, but the exact nature of this mechanism remains a mystery.

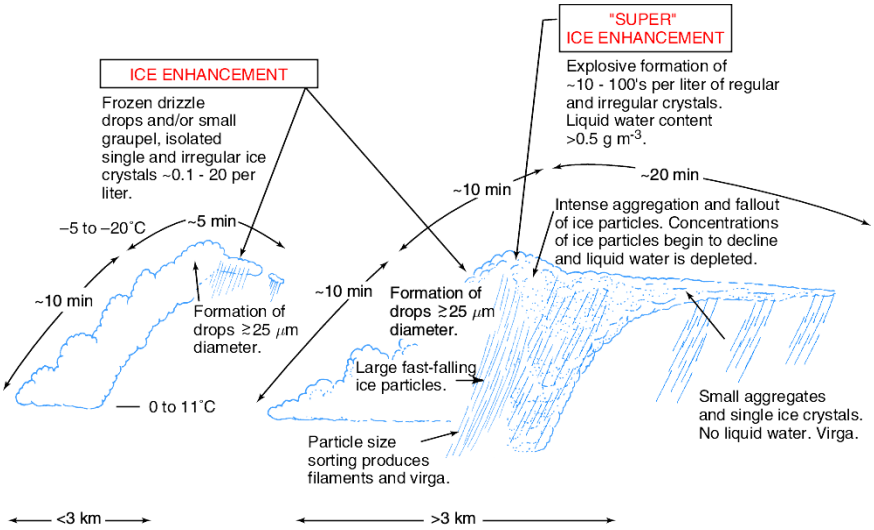

Figure 6.35. Schematic of ice development in small cumuliform clouds. [Adapted from Quart. J. Roy. Meteor. Soc., 117, 207 (1991).]

6.5.3 Growth of Ice Particles in Clouds

(a) *Growth from the vapor phase.* In a mixed cloud dominated by supercooled droplets, the air is close to saturated with respect to liquid water and is therefore supersaturated with respect to ice. For example, air saturated with respect to liquid water at $-10°C$ is supersaturated with respect to ice by 10%, and at $-20°C$ it is supersaturated by 21%. These values are much higher than the supersaturations of cloudy air with respect to liquid water, which rarely exceed 1%. Consequently, in mixed clouds dominated by supercooled water droplets, in which the cloudy air is close to water saturation, ice particles will grow from the vapor phase much more rapidly than droplets. In fact, if a growing ice particle lowers the vapor pressure in its vicinity below water saturation, adjacent droplets will evaporate (Fig. 6.36).

Cumulus turrets containing relatively large ice particles often have ill defined, fuzzy boundaries, whereas turrets containing only small droplets have well-defined, sharper boundaries, particularly if the cloud is growing (Fig. 6.37). Another factor that contributes to the difference in appearance of ice and water clouds is the lower equilibrium vapor pressure over ice than over water at the same temperature, which allows ice particles to migrate for greater distances

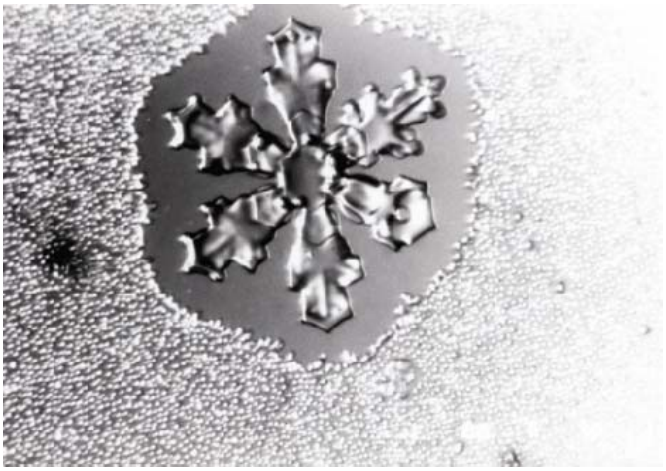

Figure 6.36. Laboratory demonstration of the growth of an ice crystal at the expense of surrounding supercooled water drops. [Photo: R. L. Pitter]

Figure 6.37. The growing cumulus clouds in the foreground with well defined boundaries contained primarily small droplets. The higher cloud behind with fuzzy boundaries was an older glaciated cloud full of ice crystals. [Photo: A. Rangno.]

than droplets into the non-saturated air surrounding a cloud before they evaporate. For the same reason, ice particles that are large enough to fall out of a cloud can survive great distances before evaporating completely, even if the ambient air is sub-saturated with respect to ice; ice particles will grow in air that is sub-saturated with respect to water, provided that it is supersaturated with respect to ice. The trails of ice crystals so produced are called *fallstreaks* or *virga* (Fig. 6.38).

Figure 6.38. Fallstreaks of ice crystals from cirrus clouds. The characteristic curved shape of the fallstreaks indicates that the wind speed was increasing (from left to right) with increasing altitude. [Photo: A. Rangno.]

The factors that control the mass growth rate of an ice crystal by deposition from the vapor phase are similar to those that control the growth of a droplet by condensation (see Section 6.4.1). However, the problem is more complicated because ice crystals are not spherical and therefore points of equal vapor density do not lie on a sphere centered on the crystal (as they do for a droplet). For the special case of a spherical ice particle of radius r we can write, by analogy with (6.19),

$$\frac{dM}{dt} = 4\pi r D \left[\rho_v(\infty) - \rho_{vc}\right]$$

where ρ_{vc} is the density of the vapor just adjacent to the surface of the crystal, and the other symbols have been defined in Section 6.4.1. We can derive an expression for the rate of increase in the mass of an ice crystal of arbitrary shape by exploiting the analogy between the vapor field around an ice crystal and the field of electrostatic potential around a charged conductor of the same size and shape.[33] The leakage of charge from the conductor (the analog of the flux of vapor to or from an ice crystal) is proportional to the electrostatic capacity C of the conductor, which is entirely determined by the size and shape of the conductor. For a sphere,

$$\frac{C}{\epsilon_0} = 4\pi r$$

where ϵ_0 is the permittivity of free space ($8.85 \times 10^{-12}\ C^2\ N^{-1}\ m^{-2}$). Combining the last two expressions, the mass growth rate of a spherical ice crystal is given by

$$\frac{dM}{dt} = \frac{DC}{\varepsilon_0}[\rho_v(\infty) - \rho_{vc}] \tag{6.36}$$

Equation (6.36) is quite general and can be applied to an arbitrarily shaped crystal of capacity C.

Provided that the vapor pressure corresponding to $\rho_v(\infty)$ is not too much greater than the saturation vapor pressure e_{si} over a plane surface of ice, and the ice crystal is not too small, (6.36) can be written as

$$\frac{dM}{dt} = \frac{C}{\varepsilon_0} G_i S_i \tag{6.37}$$

where S_i is the supersaturation (as a fraction) with respect to ice, $[e(\infty) - e_{si}]/e_{si}$, and

$$G_i = D\rho_v(\infty) \tag{6.38}$$

The variation of $G_i S_i$ with temperature for the case of an ice crystal growing in air saturated with water is shown in Fig. 6.39. The product $G_i S_i$ attains a maximum value at about $-14°$C, which is due mainly to the fact that the difference between the saturated vapor pressures over water and ice is a maximum near this temperature. Consequently, ice crystals growing by vapor deposition in mixed clouds increase in mass most rapidly at temperatures around $-14°$C.

[33] This analogy was suggested by Harold Jeffreys[34].

[34] **Harold Jeffreys** (1891–1989) English mathematician and geophysicist. First to suggest that the core of the Earth is liquid. Studied earthquakes and the circulation of the atmosphere. Proposed models for the structure of the outer planets and the origin of the solar system.

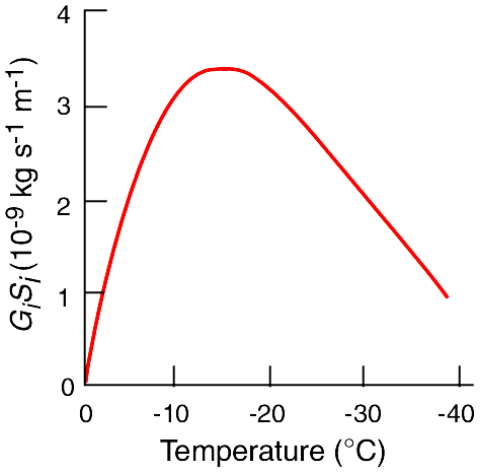

Figure 6.39. Variation of $G_i S_i$ (see eqn. (6.37)) with temperature for an ice crystal growing in a water saturated environment at a total pressure of 1000 hPa.

The majority of ice particles in clouds are irregular in shape (sometimes referred to as "junk" ice). This may be due, in part, to ice enhancement. However, laboratory studies show that under appropriate conditions ice crystals that grow from the vapor phase can assume a variety of regular shapes (or *habits*) that are either *platelike* or *columnlike*. The simplest platelike crystals are plane hexagonal plates (Fig. 6.40a), and the simplest columnlike crystals are solid columns that are hexagonal in cross section (Fig. 6.40b).

Studies of the growth of ice crystals from the vapor phase under controlled conditions in the laboratory, and observations in natural clouds, have shown that the basic habit of an ice crystal is determined by the temperature at which it grows (Table 6.1). In the temperature range between 0 and −60°C the basic habit changes three times. These changes occur near −3, −8, and −40°C. When the air is saturated or supersaturated with respect to water the basic habits become embellished. For example, at close to or in excess of water saturation, columnlike crystals take the form of long thin needles between −4 and −6°C, from −12 to −16°C platelike crystals appear like ferns, called dendrites (Fig. 6.40c), from −9 to −12°C and −16 to −20°C sector plates grow (Fig. 6.40d), and below −40°C the columnlike crystals take the form of column (often called bullet) rosettes (Fig. 6.40e). Since ice crystals are generally exposed to continually changing temperatures and supersaturations as they fall

through clouds and to the ground, crystals can assume quite complex shapes.

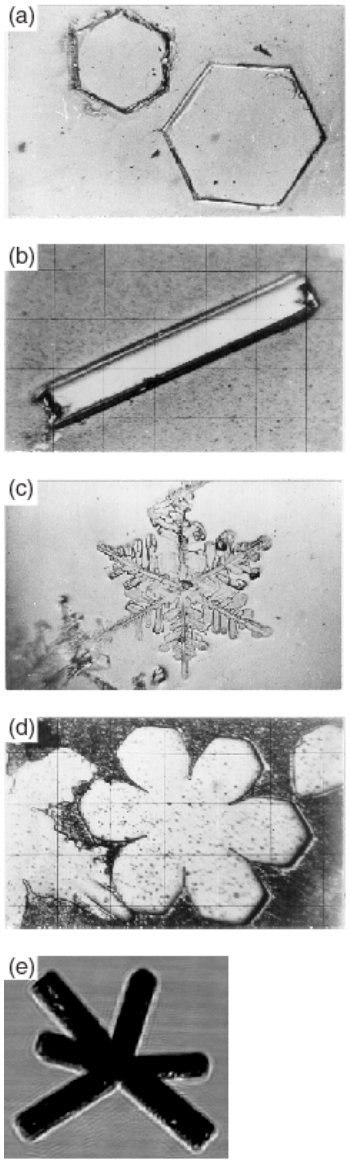

Figure 6.40. Ice crystals grown from the vapor phase: a) hexagonal plates, b) column, c) dendrite and d) sector plate [Cloud and Aerosol Research Group, University of Washington], and (e) bullet rosette [Photo: A. Heymsfield].

Table 6.1
Variations in the basic habits of ice crystals with temperature. (From information provided by J. Hallet and M. Bailey.)

Temperature (°C)	Basic habit	Supersaturation[a, b]	
		Between ice and water saturation	Near to or greater than water saturation
0 to −2.5	Platelike	Hexagonal plates	Dendrites −1 to −2°C
−3	Transition	Equiaxed	Equiaxed
−3.5 to −7.5	Columnlike	Columns	Needles −4 to −6°C Hollow columns −6 to −8°C
−8.5	Transition	Equiaxed	Equiaxed
−9 to −40	Platelike	Plates and multiple habits[c]	Scrolls and sector plates −9 to −12°C Dendrites −12 to −16°C Sector plates −16 to −20°C
−40 to −60	Columnlike	Solid column rosettes below −41°C	Hollow column rosettes below −41°C

[a] If the ice crystals are sufficiently large to have significant fall speeds, they will be ventilated by the airflow. Ventilation of an ice crystal has a similar effect on embellishing the crystal habit as increasing the supersaturation.

[b] At low supersaturations, crystal growth depends on the presence of molecular defects. As water saturation is approached, surface nucleation occurs near the crystal edges, and layers of ice spread toward the crystal interior. Growth at the edges of a crystal is limited by vapor and/or heat transfer, and in the interior of a crystal by kinetic processes at the ice-vapor interface.

[c] At lower supersaturations different crystal habits grow under identical ambient conditions depending on the defect structure inherited at nucleation.

(b) *Growth by riming; hailstones.* In a mixed cloud, ice particles can increase in mass by colliding with supercooled droplets which then freeze onto them. This process, referred to as growth by riming, leads to the formation of various rimed structures, some examples of which are shown in Fig. 6.41. Figure 6.41a shows a needle that collected a few droplets on its leading edge as it fell through the air; Fig. 6.41b a uniformly, densely rimed column; Fig. 6.41c a rimed plate, and Fig. 6.41d a rimed stellar crystal. When riming proceeds beyond a certain stage it becomes difficult to discern the original shape of the ice crystal. The rimed particle is then referred to as *graupel*. Examples of spherical and conical graupel are shown in Fig. 6.41e and f, respectively.

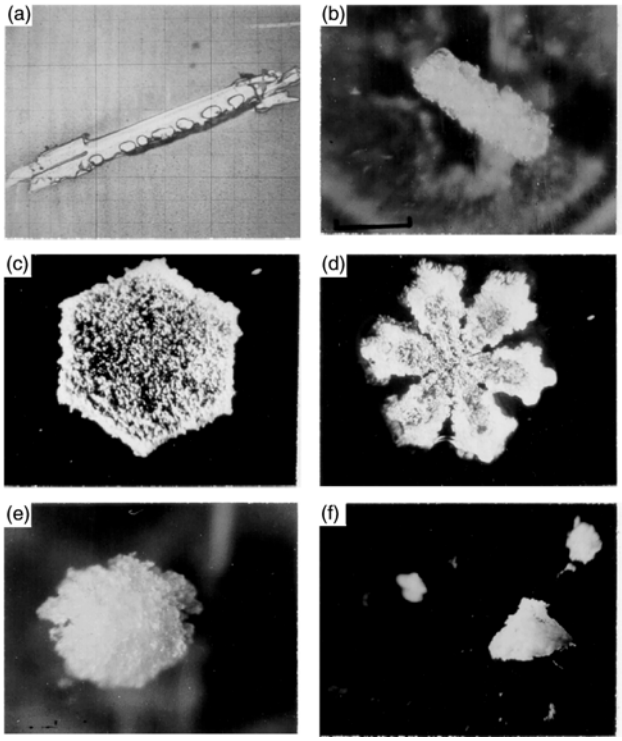

Figure 6.41. (a) Lightly rimed needle; (b) rimed column; (c) rimed plate; (d) rimed stellar; (e) spherical graupel; (f) conical graupel. [Cloud and Aerosol Research Group, University of Washington.]

Hailstones represent an extreme case of the growth of ice particles by riming. They form in vigorous convective clouds that have high liquid water contents. The largest hailstone reported in the United States (Nebraska) was 13.8 cm in diameter and weighed about 0.7 kg. However, hailstones about 1 cm in diameter are much more common. If a hailstone collects supercooled droplets at a very high rate, its surface temperature rises to 0°C and some of the water it collects remains unfrozen. The surface of the hailstone then becomes covered with a layer of water and the hailstone is said to grow *wet*. Under these conditions some of the water may be shed in the wake of the hailstone, but some of the water may be incorporated into a water-ice mesh to form what is known as *spongy hail*.

If a thin section is cut from a hailstone and viewed in transmitted light, it is often seen to consist of alternate dark and light layers (Fig. 6.42). The dark layers are opaque ice containing numerous small air bubbles, and the light layers are clear (bubble-free) ice. Clear ice is more likely to form when the hailstone is growing wet. Detailed examination of the orientation of the individual crystals within a hailstone (which can be seen when the hailstone is viewed between crossed polarizing filters-see inset to Fig. 6.42) can also reveal whether wet growth has occurred. It can be seen from Figs. 6.42

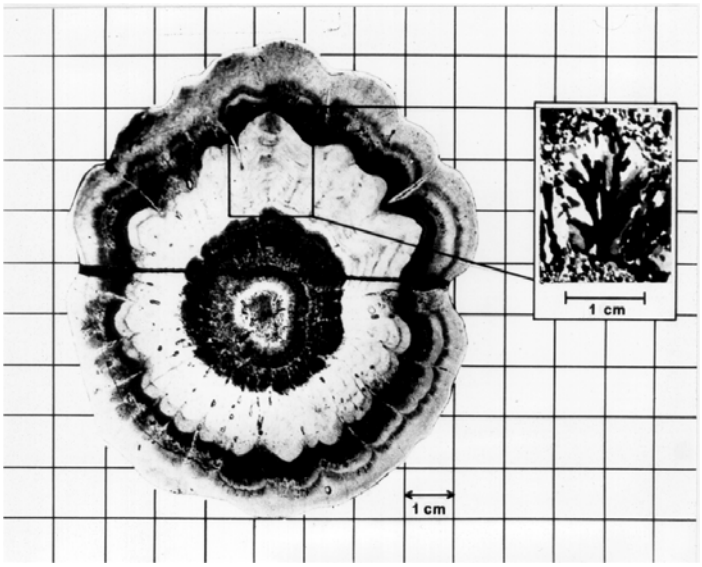

Figure 6.42. Thin section through the center of a hailstone. [From Quart. J. Roy. Met. Soc., 92, 10 (1966).]

and 6.43 that the surface of a hailstone can contain fairly large lobes. Lobelike growth appears to be more pronounced when the accreted droplets are small and growth is near the wet limit. The development of lobes may be due to the fact that any small bumps on a hailstone will be areas of enhanced collection efficiencies for droplets.

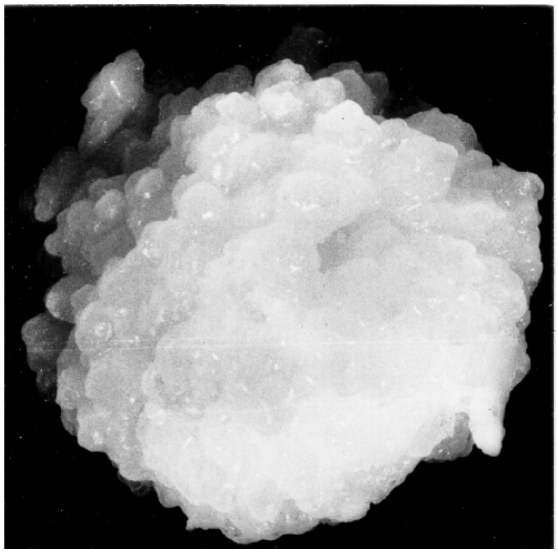

Figure 6.43. Artificial hailstone (i.e., grown in the laboratory) showing a lobe structure. Growth was initially dry but tended toward wet growth as the stone grew. [From Quart. J. Roy. Met. Soc. 94, 10 (1968).]

(c) *Growth by aggregation.* The third mechanism by which ice particles grow in clouds is by colliding and aggregating with one another. Ice particles can collide with each other provided their terminal fall speeds are different. The terminal fall speed of an unrimed column-like ice crystal increases as the length of the crystal increases; for example, the fall speeds of needles 1 and 2 mm in length are about 0.5 and 0.7 m s^{-1}, respectively. In contrast, unrimed platelike ice crystals have terminal fall speeds that are virtually independent of their diameter for the following reason. The thickness of a platelike crystal is essentially independent of its diameter, therefore, its mass varies linearly with its cross-sectional area. Since the drag force acting on a platelike crystal also varies as the cross-sectional area of the crystal, the terminal fall speed, which is determined by a balance between the drag and the gravitational forces acting on a crystal, is independent of the diameter of a plate. Since unrimed platelike crys-

tals all have similar terminal fall speeds, they are unlikely to collide with each other (unless they come close enough to be influenced by wake effects). The terminal fall speeds of rimed crystals and graupel are strongly dependent upon their degrees of riming and their dimensions. For example, graupel particles 1 and 4 mm in diameter have terminal fall speeds of about 1 and 2.5 m s^{-1}, respectively. Consequently, the frequency of collisions of ice particles in clouds is greatly enhanced if some riming has taken place.

The second factor that influences growth by aggregation is whether or not two ice particles adhere when they collide. The probability of adhesion is determined primarily by two factors: the types of ice particles and the temperature. Intricate crystals, such as dendrites, tend to adhere to one another because they become entwined on collision, whereas two solid plates will tend to rebound. Apart from this dependence upon habit, the probability of two colliding crystals adhering increases with increasing temperature, adhesion being particularly likely above about $-5°C$ at which temperatures ice surfaces become quite "sticky." Some examples of ice particle aggregates are shown in Fig. 6.44.

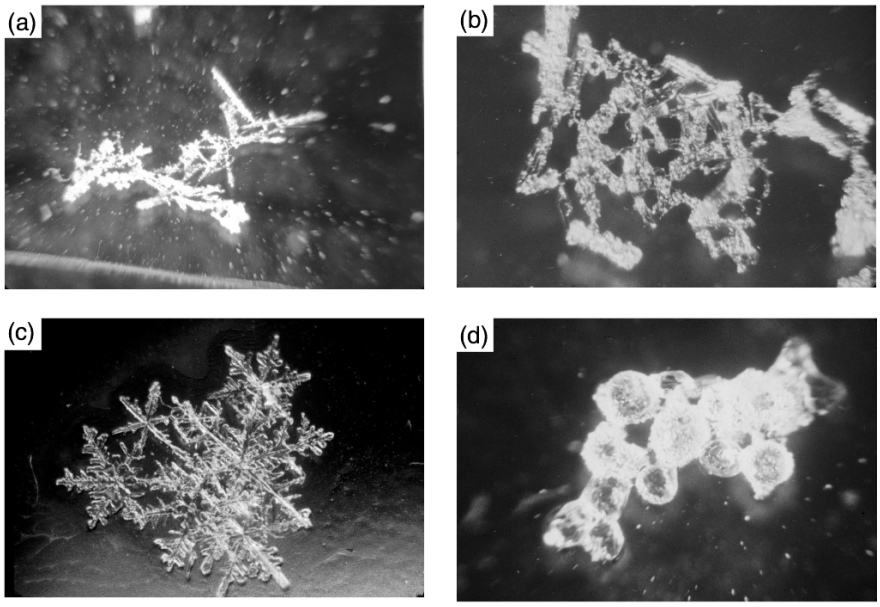

Figure 6.44. Aggregates of a) rimed needles; b) rimed columns; c) dendrites; d) rimed frozen drops. [Cloud and Aerosol Research Group, University of Washington.]

6.5.4 Formation of precipitation in cold clouds

As early as 1784 Franklin[35] suggested that "much of what is rain, when it arrives at the surface of the Earth, might have been snow, when it began its descent..." This idea was not developed until the early part of the last century when Wegener, in 1911, stated that ice particles would grow preferentially by deposition from the vapor phase in a mixed cloud. Subsequently, Bergeron, in 1933, and Findeisen[36], in 1938, developed this idea in a more quantitative manner and indicated the importance of ice nuclei in the formation of crystals. Since Findeisen carried out his field studies in northwestern Europe, he was led to believe that all rain originates as ice. However, as we have seen in Section 6.4.2, rain can also form in warm clouds by the collision–coalescence mechanism.

We will now consider the growth of ice particles to precipitation size in a little more detail. Application of (6.36) to the case of a hexagonal plate growing by deposition from the vapor phase in air saturated with respect to water at $-5°$C shows that the plate can obtain a mass of ~ 7 μg (that is, a radius of ~ 0.5 mm) in half an hour (see Exercise 6.27). Thereafter, its mass growth rate decreases significantly. On melting, a 7 μg ice crystal would form a small drizzle drop about 130 μm in radius, which could reach the ground, provided that the updraft velocity of the air were less than the terminal fall speed of the crystal (about 0.3 m s^{-1}) and the drop survived evaporation as it descended through the sub-cloud layer. Calculations such as this indicate that the growth of ice crystals by deposition of vapor is not sufficiently fast to produce large raindrops.

Unlike growth by deposition, the growth rates of an ice particle by riming and aggregation increase as the ice particle increases in size. A simple calculation shows that a platelike ice crystal, 1 mm in diameter, falling through a cloud with a liquid content of 0.5 g m^{-3},

[35] **Benjamin Franklin** (1706–1790) American scientist, inventor, statesman, and philosopher. Largely self-taught, and originally a printer and publisher by trade. First American to win international fame in science. Carried out fundamental work on the nature of electricity (introduced the terms "positive charge," "negative charge" and "battery"). Showed lightning to be an electrical phenomenon (1752). Attempted to deduce paths of storms over North America. Invented the lightning conductor, daylight savings time, bifocals, Franklin stove, and the rocking chair! First to study the Gulf Stream.

[36] **Theodor Robert Walter Findeisen** (1909–1945) German meteorologist. Director of Cloud Research, German Weather Bureau, Prague, Czechoslovakia, from 1940. Laid much of the foundation of modern cloud physics and foresaw the possibility of stimulating rain by introducing artificial ice nuclei. Disappeared in Czechoslovakia at the end of World War II.

could develop into a spherical graupel particle about 0.5 mm in radius in a few minutes (see Exercise 6.28). A graupel particle of this size, with a density of 100 kg m^{-3}, has a terminal fall speed of about 1 m s^{-1} and would melt into a drop about 230 μm in radius. The radius of a snowflake can increase from 0.5 mm to 0.5 cm in ∼30 min due to aggregation with ice crystals, provided that the ice content of the cloud is about 1 g m^{-3} (see Exercise 6.29). An aggregated snow crystal with a radius of 0.5 cm has a mass of about 3 mg and a terminal fall speed of about 1 m s^{-1}. Upon melting, a snow crystal of this mass would form a drop about 1 mm in radius. We conclude from these calculations that the growth of ice crystals, first by deposition from the vapor phase in mixed clouds and then by riming and/or aggregation, can produce precipitation-sized particles in reasonable time periods (say about 40 min).

The role of the ice phase in producing precipitation in cold clouds is demonstrated by radar observations. For example, Fig. 6.45 shows a radar screen (on which the intensity of radar echoes reflected from atmospheric targets are displayed) while the radar antenna was pointing vertically upward and clouds drifted over the radar. The horizontal band (in brown) just above a height of 2 km was produced by the melting of ice particles. This is referred to as the "*bright band*." The radar reflectivity is high around the melting level because, while melting, ice particles become coated with a film of water that greatly increases their radar reflectivity. When the crystals

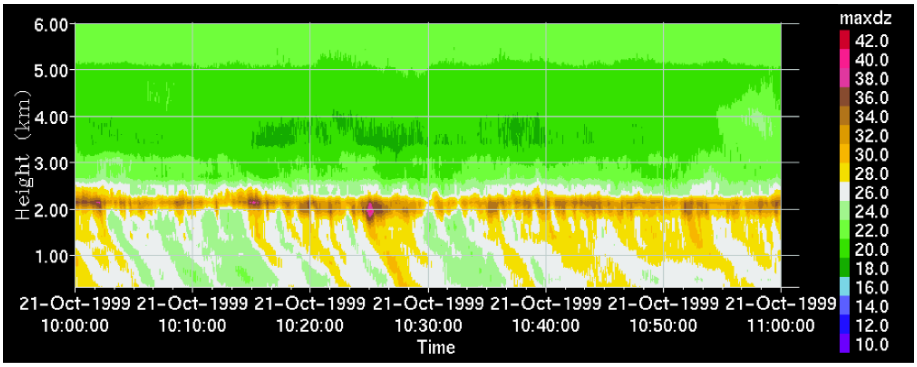

Figure 6.45. Reflectivity (or "echo") from a vertically-pointing radar. The horizontal band of high reflectivity values (in brown), located just above a height of 2 km, is the melting band. The curved trails of relatively high reflectivity (in yellow) emanating from the bright band are fallstreaks of precipitation, some of which reach the ground. [Quart. J. Roy. Met. Soc., 129, 455 (2003).]

have melted completely they collapse into droplets, and their terminal fall speeds increase so that the concentration of particles is reduced. These changes result in a sharp decrease in radar reflectivity below the melting band.

The sharp increase in particle fall speeds produced by melting is illustrated in Fig. 6.46, which shows the spectrum of fall speeds of precipitation particles measured at various heights with a vertically pointing Doppler radar.[37] At heights above 2.2 km the particles are ice with fall speeds centered around 2 m s^{-1}. At 2.2 km the particles are partially melted, and below 2.2 km there are raindrops with fall speeds centered around 7 m s^{-1}.

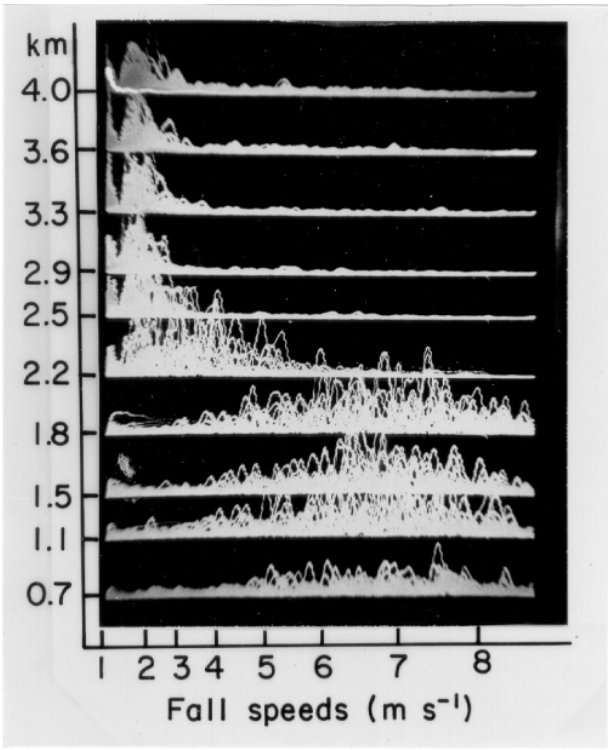

Figure 6.46. Spectra of Doppler fall speeds for precipitation particles at ten heights in the atmosphere. The melting level is at about 2.2 km. (Cloud and Aerosol Research Group, University of Washington.)

[37] Doppler radars, unlike conventional meteorological radars, transmit coherent electromagnetic waves. From measurements of the difference in frequencies between the returned and transmitted waves, the velocity of the target (for example, precipitation particles) along the line of sight of the radar can be deduced. The radars used by the police for measuring the speeds of motor vehicles are based on the same principle.

6.5.5 Classification of Solid Precipitation

The growth of ice particles by deposition from the vapor phase, riming, and aggregation leads to a very wide variety of solid precipitation particles. A relatively simple classification into ten main classes is shown in Table 6.2.

Table 6.2–TWO-PAGE TABLE SAME AS TABLE 4.3 IN 1ST ED
[PRINTER: ELECTRONIC FILE PROVIDED OF "TYPICAL FORMS", "SYMBOL" & "GRAPHIC SYMBOL" COLUMNS OF FIRST PAGE OF TABLE, DOUBLE-COLUMN WIDE PAGE]

Table 6.2
A classification of solid precipitation[a,b,c]

Typical forms	Symbol	Graphic symbol
[SAME GRAPHICS	F1	[SAME GRAPHICS
AS TABLE 4.3	F2	AS TABLE 4.3
IN 1ST ED]	F3	IN 1ST ED]
[ELECTRONIC	F4	[ELECTRONIC
FILE FROM	F5	FILE
SCANNED PHOTO	F6	PROVIDED]
PROVIDED]	F7	
	F8	
	F9	
	F10	

[a)] Suggested by the International Association of Hydrology's commission of snow and ice in 1951. (Photo: V. Schaefer.)

[b)] Additional characteristics: p, broken crystals; r, rime-coated particles not sufficiently coated to be classed as graupel; f, clusters, such as compound snowflakes, composed of several individual snow crystals; w, wet or partly melted particles.

start 2nd page of Table 6.2

Description

A plate is a thin, platelike snow crystal the form of which more or less resembles a hexagon or, in rare cases, a triangle. Generally all edges or alternative edges of the plate are similar in pattern and length.

A stellar crystal is a thin, flat snow crystal in the form of a conventional star. It generally has six arms but stellar crystals with three or twelve arms occur occasionally. The arms may lie in a single plane or in closely spaced parallel planes in which case the arms are interconnected by a very short column.

A column is a relatively short prismatic crystal, either solid or hollow, with plane, pyramidal, truncated, or hollow ends. Pyramids, which may be regarded as a particular case, and combinations of columns are included in this class.

A needle is a very slender, needlelike snow particle of approximately cylindrical form. This class includes hollow bundles of parallel needles, which are very common, and combinations of needles arranged in any of a wide variety of fashions.

A spatial dendrite is a complex snow crystal with fernlike arms which do not lie in a plane or in parallel planes but extend in many directions from a central nucleus. Its general form is roughly spherical.

A capped column is a column with plates of hexagonal or stellar form at its ends and, in many cases, with additional plates at intermediate positions. The plates are arranged normal to the principal axis of the column. Occasionally only one end of the column is capped in this manner.

An irregular crystal is a snow particle made up of a number of small crystals grown together in a random fashion. Generally the component crystals are so small that the crystalline form of the particle can only be seen with the aid of a magnifying glass or microscope.

Graupel, which includes soft hail, small hail, and snow pellets, is a snow crystal or particle coated with a heavy deposit of rime. It may retain some evidence of the outline of the original crystal although the most common type has a form which is approximately spherical.

Ice pellets (frequently called sleet in North America) are transparent spheroids of ice and are usually fairly small. Some ice pellets do not have a frozen center which indicates that, at least in some cases, freezing takes place from the surface inwards.

A hailstone[d] is a grain of ice, generally having a laminar structure and characterized by its smooth glazed surface and its translucent or milky-white center. Hail is usually associated with those atmospheric conditions which accompany thunderstorms. Hailstones are sometimes quite large.

---

[c] Size of particle is indicated by the general symbol D. The size of a crystal or particle is its greatest extension measured in millimeters. When many particles are involved (for example, a compound snowflake) it refers to the average size of the individual particles.

[d] Hail, like rain, refers to a number of particles, while hailstone, like raindrop, refers to an individual particle.

End 2-page table

6.6 6.6 Artificial Modification of Clouds and Precipitation

We have seen in Sections 6.2–6.5 that the microstructures of clouds are influenced by the concentrations of CCN and ice nuclei, and that the growth of precipitation particles is a result of instabilities that exist in the microstructures of clouds. These instabilities are of two main types. First, in warm clouds the larger drops increase in size at the expense of the smaller droplets due to growth by the collision–coalescence mechanism. Second, if ice particles exist in a certain optimum range of concentrations in a mixed cloud they grow by deposition at the expense of the droplets (and subsequently by riming and aggregation). In light of these ideas, the following techniques have been suggested whereby clouds and precipitation might be artificially modified by so-called *cloud seeding*:

- Introducing large hygroscopic particles or water drops into warm clouds to stimulate the growth of raindrops by the collision–coalescence mechanism.

- Introducing artificial ice nuclei into cold clouds (which may be deficient in ice particles) to stimulate the production of precipitation by the ice crystal mechanism.

- Introducing comparatively high concentrations of artificial ice nuclei into cold clouds to reduce drastically the concentrations of supercooled droplets and thereby inhibit the growth of ice particles by deposition and riming, thereby dissipating the clouds and suppressing the growth of precipitable particles.

6.6.1 Modification of Warm Clouds

Even in principle, the introduction of water drops into the tops of clouds is not a very efficient method for producing rain, since large quantities of water are required. A more efficient technique might be to introduce small water droplets (radius $\simeq$30 μm) or hygroscopic particles (e.g., NaCl) into the base of a cloud; these particles might then grow by condensation, and then by collision-coalescence, as they are carried up and subsequently fall through a cloud.

In the second half of the last century, a number of cloud seeding experiments on warm clouds were carried out, using water drops and hygroscopic particles. In some cases rain appeared to be initiated by the seeding, but since neither extensive physical nor rigorous statistical evaluations were carried out the results were inconclusive. Recently, there has been somewhat of a revival of interest in seeding warm clouds with hygroscopic nuclei to increase precipitation but, as yet, the efficacy of this technique has not been proven.

Seeding with hygroscopic particles has been used in attempts to improve visibility in warm fogs. Since the visibility in a fog is inversely proportional to the number concentration of droplets and to their total surface area, visibility can be improved by decreasing either the concentration or the size of the droplets. When hygroscopic particles are dispersed into a warm fog they grow by condensation (causing partial evaporation of some of the fog droplets) and the droplets so formed slowly fall out of the fog. Fog clearing by this method has not been widely used due to its expense and lack of dependability. At the present time, the most effective methods for

dissipating warm fogs are "brute force" approaches, involving evaporating the fog droplets by ground-based heating.

6.6.2 Modification of Cold Clouds

We have seen in Section 6.5.3 that when supercooled droplets and ice particles coexist in a cloud the ice particles may increase to precipitation size rather rapidly. We also saw in Section 6.5.1 that in some situations the concentrations of ice nuclei may be less than that required for the efficient initiation of the ice crystal mechanism for the formation of precipitation. Under these conditions, it is argued, clouds might be induced to rain by seeding them with artificial ice nuclei or some other material that might increase the concentration of ice particles. This idea was the basis for most of the cloud seeding experiments carried out in the second half of the twentieth century.

A material suitable for seeding cold clouds was first discovered in July 1946 in Project Cirrus, which was carried out under the direction of Irving Langmuir.[38] One of Langmuir's assistants, Vincent Schaefer,[39] observed in laboratory experiments that when a small piece of Dry Ice (i.e., solid carbon dioxide) is dropped into a cloud of supercooled droplets, numerous small ice crystals are produced and the cloud is quickly glaciated. In this transformation Dry Ice does not serve as an ice nucleus in the usual sense of this term, but rather, because it is so cold ($-78°$C), it causes numerous ice crystals to form in its wake by homogeneous nucleation. For example, a pellet of Dry Ice 1 cm in diameter falling through air at $-10°$C produces about 10^{11} ice crystals.

The first field trials using Dry Ice were made in Project Cirrus on 13 November 1946, when about 1.5 kg of crushed Dry Ice were dropped along a line about 5 km long into a layer of supercooled altocumulus cloud. Snow was observed to fall from the base of the

[38] **Irving Langmuir** (1881–1957) American physicist and chemist. Spent most of his working career as an industrial chemist in the GE Research Laboratories in Schenectady, New York. Made major contributions to several areas of physics and chemistry and won the Nobel Prize in chemistry in 1932 for work on surface chemistry. His major preoccupation in later years was cloud seeding. His outspoken advocacy of large-scale effects of cloud seeding involved him in much controversy.

[39] **Vincent Schaefer** (1906–1993) American naturalist and experimentalist. Left school at age 16 to help support the family income. Initially worked as a toolmaker at the GE Research Laboratory, but subsequently became Langmuir's research assistant. Schaefer helped to create the Long Path of New York (a hiking trail from New York City to Whiteface Mt. in the Adirondacks); also an expert on Dutch barns.

seeded cloud for a distance of about 0.5 km before it evaporated in the dry air.

Because of the large numbers of ice crystals that a small amount of Dry Ice can produce, it is most suitable for *overseeding* cold clouds, rather than producing ice crystals in the optimal concentrations ($\sim$1 liter^{-1}) for enhancing precipitation. When a cloud is overseeded it is converted completely into ice crystals (i.e., it is glaciated). The ice crystals in a glaciated cloud are generally quite small and, since there are no supercooled droplets present, supersaturation with respect to ice is either low or non-existent. Therefore, instead of the ice crystals growing (as they would in a mixed cloud at water saturation) they tend to evaporate. Consequently, seeding with Dry Ice can dissipate large areas of supercooled cloud or fog (Fig. 6.47). This technique is used for clearing supercooled fogs at several international airports.

Figure 6.47. A γ-shaped path cut in a layer of supercooled cloud by seeding with Dry Ice. (Photo by courtesy of the General Electric Company, Schenectady, New York.)

Following the demonstration that supercooled clouds can be modified by Dry Ice, Bernard Vonnegut,[40] who was also working with

[40] **Bernard Vonnegut** (1914–1997) American physical chemist. In addition to his research on cloud seeding, Vonnegut had a lifelong interest in thunderstorms and lightning. His brother, Kurt Vonnegut the novelist, wrote "My longest experience with common decency, surely, has been with my older brother, my only brother, Bernard...We were given very different sorts of minds at birth. Bernard could never be a writer and I could never be a scientist." Interestingly, following Project Cirrus, neither Vonnegut nor Schaefer became deeply involved in the quest to increase precipitation by artificial seeding.

Langmuir, began searching for artificial ice nuclei. In this search he was guided by the expectation that an effective ice nucleus should have a crystallographic structure similar to that of ice. Examination of crystallographic tables revealed that silver iodide fulfilled this requirement. Subsequent laboratory tests showed that silver iodide could act as an ice nucleus at temperatures as high as $-4°C$.

The seeding of natural clouds with silver iodide was first tried as part of Project Cirrus on 21 December 1948. Pieces of burning charcoal impregnated with silver iodide were dropped from an aircraft into about 16 km^2 of supercooled stratus cloud 0.3 km thick, at a temperature of $-10°C$. The cloud was converted into ice crystals by less than 30 g of silver iodide!

Many artificial ice nucleating materials are now known (e.g., lead iodide, cupric sulfide) and some organic materials (e.g., phloroglucinol, metaldehyde) are more effective as ice nuclei than silver iodide. However, silver iodide has been used in most cloud seeding experiments.

Since the first cloud seeding experiments in the 1940s, many more experiments have been carried out all over the world. It is now well established that the concentrations of ice crystals in clouds can be increased by seeding with artificial ice nuclei and that, under certain conditions, precipitation can be artificially initiated in some clouds. However, the important question is: under what conditions (if any) can seeding with artificial ice nuclei be employed to produce significant increases in precipitation on the ground in a predictable manner and over a large area? This question remains unanswered.

So far we have discussed the role of artificial ice nuclei in modifying the microstructures of cold clouds. However, when large volumes of a cloud are glaciated by overseeding, the resulting release of latent heat provides added buoyancy to the cloudy air. If, prior to seeding, the height of a cloud were restricted by a stable layer, the release of the latent heat of fusion caused by artificial seeding might provide enough buoyancy to push the cloud through the inversion and up to its level of free convection. The cloud top might then rise to much greater heights than it would have done naturally. Figure 6.48 shows the explosive growth of a cumulus cloud which may have been produced by overseeding.

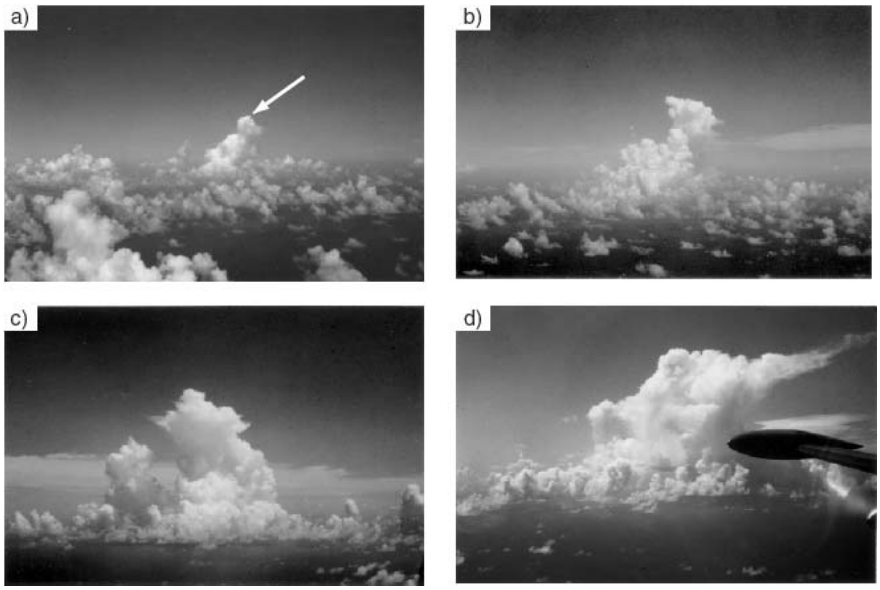

Figure 6.48. The "explosive" growth of a cumulus cloud (indicated by the arrow) following seeding with silver iodide. (a) About 10 min after seeding; (b) 19 min after seeding; (c) 29 min after seeding; (d) 48 min after seeding. Note that the neighboring unseeded clouds have not grown significantly. (Photo: J. Simpson.)

Seeding experiments have been carried out in attempts to reduce the damage produced by hailstones. Seeding with artificial nuclei should tend to increase the number of small ice particles competing for the available supercooled droplets. Therefore, seeding should result in a reduction in the average size of the hailstones. It is also possible that, if a hailstorm is overseeded with extremely large numbers of ice nuclei, the majority of the supercooled droplets in the cloud will be nucleated, and the growth of hailstones by riming will be significantly reduced. Although these hypotheses are plausible, the results of experiments on hail suppression have not been encouraging.

Exploratory experiments have been carried out to investigate if orographic snowfall might be redistributed by overseeding. Rimed ice particles have relatively large terminal fall speeds ($\sim$1 m s^{-1}), therefore they follow fairly steep trajectories as they fall to the ground. If clouds on the windward side of a mountain are artificially overseeded, supercooled droplets can be virtually eliminated and growth

by riming significantly reduced (Fig. 6.49). In the absence of riming, the ice particles grow by deposition from the vapor phase and their fall speeds are reduced by roughly a factor of 2. Winds aloft can then carry these crystals farther before they reach the ground. In this way, it is argued, it might be possible to divert snowfall from the windward slopes of mountain ranges (where precipitation is often heavy) to the drier leeward slopes.

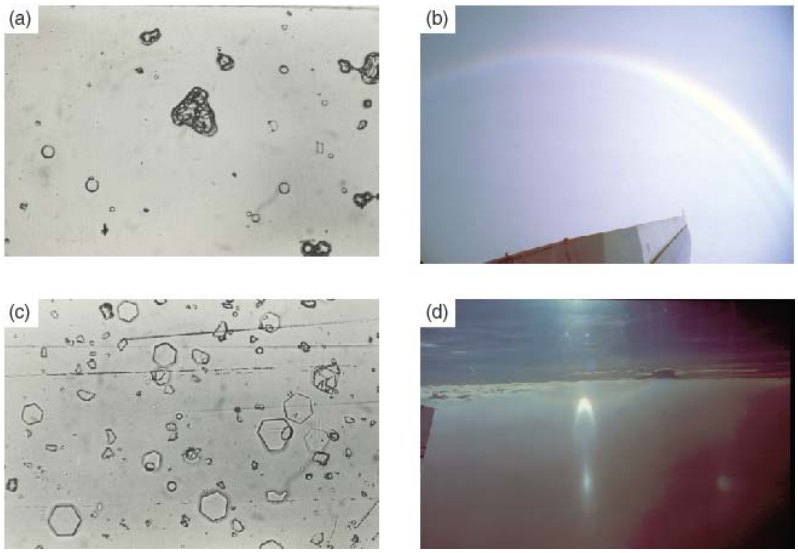

Figure 6.49. (a) Large rimed irregular particles and small water droplets collected in unseeded clouds over the Cascade Mountains. (b) Cloud bow produced by the refraction of light in small water droplets. Following heavy seeding with artificial ice nuclei, the particles in the cloud were converted into small unrimed plates (c) which markedly changed the appearance of the clouds. In (d) the uniform cloud in the foreground is the seeded cloud and the more undulating cloud in the background is the unseeded cloud. In the seeded cloud, optical effects due to ice particles (portion of the 22° halo, lower tangent arc to 22° halo, and subsun) can be seen. (Cloud and Aerosol Research Group, University of Washington.)

6.6.3 Inadvertent Modification

Some industries release large quantities of heat, water vapor, and cloud-active aerosol (CCN and ice nuclei) into the atmosphere. Consequently, these effluents might modify the formation and structure of clouds and affect precipitation. For example, the effluents from

a single paper mill can profoundly affect the surrounding area out to about 30 km (Fig. 6.50). Paper mills, the burning of agricultural wastes, and forest fires, emit large numbers of CCN ($\sim 10^{17}$ s^{-1} active at 1% supersaturation), which can change droplet concentrations in clouds downwind. High concentrations of ice nuclei have been observed in the plumes from steel mills.

Figure 6.50. The cloud in the valley in the background formed due to effluents from a paper mill. In the foreground, the cloud is spilling through a gap in the ridge into an adjacent valley. (Photo: C. L. Hosler.)

Large cities can affect the weather in their vicinities. Here the possible interactions are extremely complex since, in addition to being areal sources of aerosol, trace gases, heat, and water vapor, large cities modify the radiative properties of the Earth's surface, the moisture content of the soil, and the surface roughness. The existence of urban "heat islands," several degrees warmer than adjacent less populated regions, is well documented. In the summer months increases in precipitation of 5–25% over background values occur 50–75 km downwind of some cities (e.g., St. Louis, Missouri). Thunderstorms and hailstorms may be more frequent, with the areal extent and magnitude of the perturbations related to the size of the city. Model simulations indicate that enhanced upward air velocities, associated with variations in surface roughness and the heat island effect, are most likely responsible for these anomalies.

6.7 6.7 Thunderstorm Electrification

The dynamical structure of thunderstorms is described in Chapter 10. Here we are concerned with the microphysical mechanisms that are thought to be responsible for the electrification of thunderstorms, and with the nature of lightning flashes and thunder.

6.7.1 Charge Generation

All clouds are electrified to some degree.[41] However, in vigorous convective clouds sufficient electrical charges are separated to produce electric fields that exceed the dielectric breakdown of cloudy air

[41] Benjamin Franklin, in July 1750, was the first to propose an experiment to determine whether thunderstorms are electrified. He suggested that a sentry box, large enough to contain a man and an insulated stand, be placed at a high elevation and that an iron rod 20–30 ft in length be placed vertically on the stand, passing out through the top of the box. He then proposed that if a man stood on the stand and held the rod he would "be electrified and afford sparks" when an electrified cloud passed overhead. Alternatively, he suggested that the man stand on the floor of the box and bring near to the rod one end of a piece of wire, held by an insulating handle, while the other end of the wire was connected to the ground. In this case, an electric spark jumping from the rod to the wire would be proof of cloud electrification. (Franklin did not realize the danger of these experiments: they can kill a person—and have done so—if there is a direct lightning discharge to the rod.) The proposed experiment was set up in Marly-la-Ville in France by d'Alibard[42], and on 10 May 1752 an old soldier, called Coiffier, brought an earthed wire near to the iron rod while a thunderstorm was overhead and saw a stream of sparks. This was the first direct proof that thunderstorms are electrified. Joseph Priestley described it as "the greatest discovery that has been made in the whole compass of philosophy since the time of Sir Isaac Newton." (Since Franklin proposed the use of the lightning conductor in 1749, it is clear that by that date he had already decided in his own mind that thunderstorms were electrified.) Later in the summer of 1752 (the exact date is uncertain), and before hearing of d'Alibard's success, Franklin carried out his famous kite experiment in Philadelphia and observed sparks to jump from a key attached to a kite string to the knuckles of his hand. By September 1752 Franklin had erected an iron rod on the chimney of his home, and on 12 April 1753, by identifying the sign of the charge collected on the lower end of the rod when a storm passed over, he had concluded that "clouds of a thundergust are most commonly in a negative state of electricity, but sometimes in a positive state—the latter, I believe, is rare." No more definitive statement as to the electrical state of thunderstorms was made until the second decade of the 20th century when C. T. R. Wilson[43] showed that the lower regions of thunderstorms are generally negatively charge while the upper regions are positively charged.

[42] **Thomas Francois d'Alibard** (1703–1779) French naturalist. Translated into French Franklin's "Experiments and Observations on Electricity," Durand, Paris, 1756, and carried out many of Franklin's proposed experiments.

[43] **C. T. R. Wilson** (1869–1959) Scottish physicist. Invented the cloud chamber named after him for studying ionizing radiation (e.g., cosmic rays) and charged particles. Carried out important studies on condensation nuclei and atmospheric electricity. Awarded the Nobel Prize in physics in 1927.

($\sim$1 MV m^{-1}), resulting in an initial *intracloud* (i.e., between two points in the same cloud) lightning discharge.

The distribution of charges in thunderstorms has been investigated with special radiosondes (called altielectrographs), by measuring the changes in the electric field at the ground that accompany lightning flashes, and with instrumented aircraft. A summary of the results of such studies, for a relatively simple cloud, is shown in Fig. 6.51. The magnitudes of the lower negative charge and the upper positive charge are $\sim$10–100 coulombs (hereafter symbol "C"), or a few nC m^{-3}. The location of the negative charge (called the *main charging zone*) is rather well defined between the -10°C and about -20°C temperature levels. The positive charge is distributed in a more diffuse region above the negative charge. Although there have been a few reports of lightning from warm clouds, the vast majority of thunderstorms occur in cold clouds.

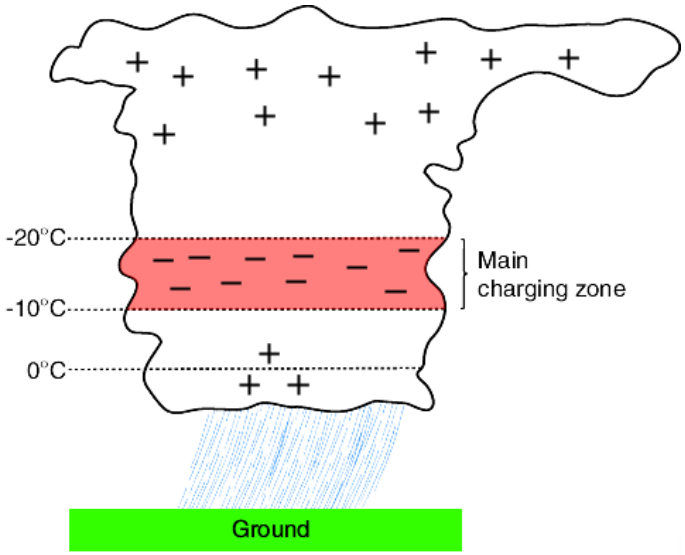

Figure 6.51. Schematic showing the distribution of electric charges in a typical and relatively simple thunderstorm. The lower and smaller positive charge is not always present.

An important observational result, which provides the basis for most theories of thunderstorm electrification, is that the onset of strong electrification follows the occurrence (detected by radar) of heavy precipitation within the cloud in the form of graupel or hailstones. Most theories assume that as a graupel particle or hailstone

(hereafter called the *rimer*) falls through a cloud it is charged negatively due to collisions with small cloud particles (droplets or ice), giving rise to the negative charge in the main charging zone. The corresponding positive charge is imparted to cloud particles as they rebound from the rimer, and these small particles are then carried by updrafts to the upper regions of the cloud. The exact conditions and mechanism by which a rimer might be charged negatively, and smaller cloud particles charged positively, has been a matter of debate for some hundred years. Many potentially promising mechanisms have been proposed but subsequently found to be unable to explain the observed rate of charge generation in thunderstorms or, for other reasons, found to be untenable.

PROBLEM 6.6 The rate of charge generation in a thunderstorm is ∼1 C km^{-3} min^{-1}. Determine the electric charge that would have to be separated for each collision of an ice crystal with a rimer (e.g., a graupel particle) to explain this rate of charge generation. Assume that the concentration of ice crystals is 10^5 m^{-3}, their fall speed is negligible compared to that of the rimer, the ice crystals are uncharged prior to colliding with the rimer, their collision efficiency with the rimer is unity, and all of the ice crystals rebound from the rimer. Assume also that the rimers are spheres of radius 2 mm, the density of a rimer is 500 kg m^{-3}, and the precipitation rate due to the rimers is 5 cm per hour of water equivalent. ◀

SOLUTION ▶ If $\frac{dN}{dt}$ is the number of collisions of ice crystals with rimers in a unit volume of air in 1 s, and each collision separates q coulombs (C) of electric charge, the rate of charge separation per unit volume of air per unit time in the cloud by this mechanism is

$$\frac{dQ}{dt} = \frac{dN}{dt} q \tag{6.39}$$

If the fall speed of the ice crystals is negligible, and the ice crystals collide with and separate from a rimer with unit efficiency,

$$\begin{aligned} \frac{dN}{dt} &= (\text{volume swept out by one rimer in 1 s}) \\ &\quad (\text{number of rimers per unit volume of air}) \\ &\quad (\text{number of ice crystals per unit volume of air}) \\ &= \left(\pi r_H^2 v_H\right)(n_H)(n_I) \end{aligned} \tag{6.40}$$

where, r_H, v_H and n_H are the radius, fall speed, and number concentration of rimers and n_I the number concentration of ice crystals.

Now consider a rain gauge with cross-sectional area A. Since all of the rimers within a distance v_H of the top of the rain gauge will enter the rain gauge in 1 s, the number of rimers that enter the rain gauge in 1 s is equal to the number of rimers in a cylinder of cross-sectional area A and height v_H; that is, in a cylinder of volume $v_H A$. The number of rimers in this volume is

$v_H A n_H$. Therefore, if each rimers has mass m_H, the mass of rimers that enter the rain gauge in 1 s is $v_H A n_H m_H$, where $m_H = (4/3)\pi r_H^3 \rho_H$ and ρ_H is the density of a rimer. When this mass of rimers melt in the rain gauge, the height h of water of density ρ_l that it will produce in 1 s is given by

$$hA\rho_l = v_H A n_H \left(\tfrac{4}{3}\pi r_H^3 \rho_H\right)$$

or

$$v_H n_H = \frac{3h}{4\pi}\frac{\rho_l}{\rho_H}\frac{1}{r_H^3} \tag{6.41}$$

From (6.39)–(6.41)

$$q = \frac{4\rho_H r_H}{3h\rho_l n_I}\frac{dQ}{dt}$$

Substituting, $\dfrac{dQ}{dt} = \dfrac{1}{60 \times 60}$ C km^{-3} s^{-1}, $h = \dfrac{5 \times 10^{-2}}{60 \times 60}$ m s^{-1}, $\rho_l = 10^3$ kg m^{-3}, $n_I = 10^5$ m^{-3}, $\rho_H = 500$ kg m^{-3} and $r_H = 2 \times 10^{-3}$ m, we obtain $q = 16 \times 10^{-15}$ C per collision or 16 fC per collision. ◀

We will now describe briefly a proposed mechanism for charge transfer between a rimer and a colliding ice crystal that appears promising, although it remains to be seen whether it can withstand the test of time.

Laboratory experiments show that electric charge is separated when ice particles collide and rebound. The magnitude of the charge is typically about 10 fC per collision which, as we have seen in Exercise 6.6, would be sufficient to explain the rate of charge generation in thunderstorms. The sign of the charge received by the rimer depends on temperature, the liquid water content of the cloud, and on the relative rates of growth from the vapor phase of the rimer and the ice crystals. If the rimer grows more slowly by vapor deposition than the ice crystals, the rimer receives negative charge and the ice crystals receive the corresponding positive charge. Since the latent heat released by the freezing of supercooled droplets on a rimer as it falls through a cloud will raise the surface temperature of the rimer above ambient temperatures, the rate of growth of the rimer by vapor deposition will be less than that of ice crystals in the cloud. Consequently, when an ice crystal rebounds from a rimer, the rimer should receive a negative charge and the ice crystal a positive charge, as required to explain the main distribution of charges in a thunderstorm.

The charge transfer appears to be due to the fact that positive ions move through ice much faster than negative ions. As new ice surface is created by vapor deposition, the positive ions migrate rapidly into the interior of the ice, leaving the surface negatively charged.

During a collision material from each of the particles is mixed, but negative charge is transferred to the particle with the slower growth rate.

In some thunderstorms, a relatively weak positive charge is observed just below the main charging zone (Fig. 6.51). This may be associated with the charging of solid precipitation during melting or to mixed-phase processes.

6.7.2 Lightning and Thunder

As electrical charges are separated in a cloud, the electric field intensity increases and eventually exceeds that which the air can sustain. The resulting dielectric breakdown assumes the form of a lightning flash that can be either 1) within the cloud itself, between clouds, or from the cloud to the air (which we will call *cloud flashes*), or 2) between the cloud and the ground (a *ground flash*).

Ground flashes that charge the ground negatively originate from the lower main negative charge center in the form of a discharge, called the *stepped leader*, which moves downward toward the Earth in discrete steps. Each step lasts for about 1 μs, during which time the stepped leader advances about 50 m; the time interval between steps is about 50 μs. It is believed that the stepped leader is initiated by a local discharge between the small pocket of positive charge at the base of a thundercloud and the lower part of the negatively charged region (Fig. 6.52b). This discharge releases electrons that were previously attached to precipitation particles in the negatively charged region. These free electrons neutralize the small pocket of positive charge that may be present below the main charging zone (Fig. 6.52c) and then move toward the ground (Fig. 6.52c–e). As the negatively charged stepped leader approaches the ground it induces positive charges on the ground, especially on protruding objects, and when it is 10–100 m from the ground a discharge moves up from the ground to meet it (Fig. 6.52f). After contact is made between the stepped leader and the upward connecting discharge, large numbers of electrons flow to the ground and a highly luminous and visible *lightning stroke* propagates upward in a continuous fashion from the ground to the cloud along the path followed by the stepped leader (Fig. 6.52g and h). This flow of electrons (called the *return stroke*) is responsible for the bright channel of light that is observed as a lightning stroke. Since the stroke moves upward so quickly (in

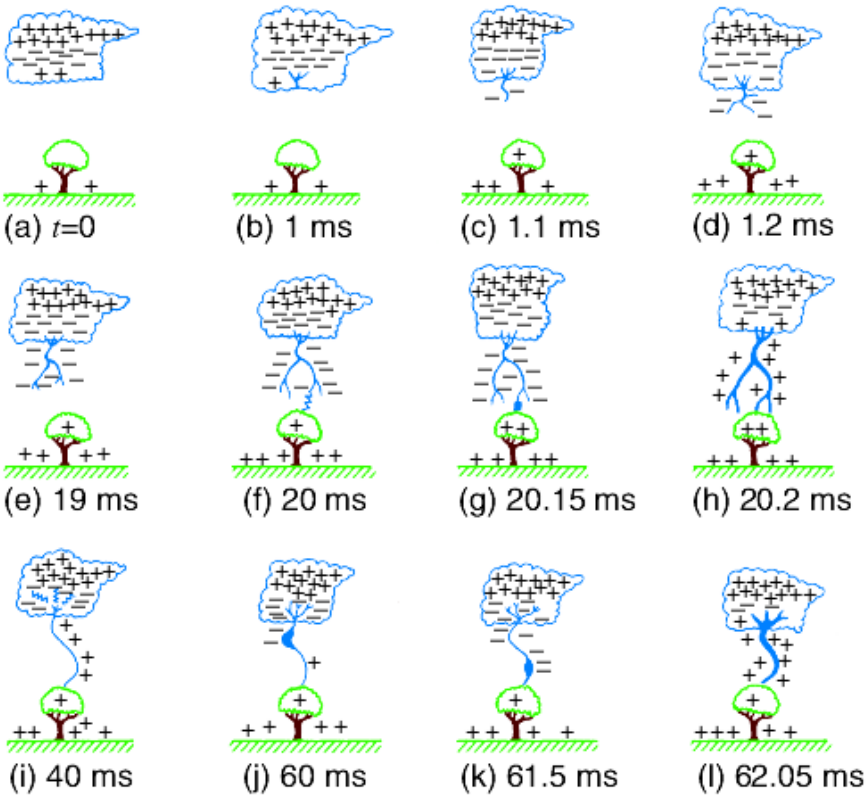

Figure 6.52. Schematics (not drawn to scale) to illustrate some of the processes leading to a ground flash that charges the ground negatively. (a) cloud charge distribution, (b) preliminary breakdown, (c)–(e) stepped leader, (f) attachment process, (g)–(h) first return stroke, (i) K and J processes, (j)–(k) the dart leader, and (l) the second return stroke. [Adapted from M. Uman, "The Lightning Discharge," Academic Press, Inc., New York, 1987, p. 12.]

about 100 μs), the whole return stroke channel appears to the eye to brighten simultaneously. After the downward flow of electrons, both the return stroke and the ground, to which it is linked, remain positively charged in response to the remainder of the negative charge in the main charging zone.

Following the first stroke, which typically carries the largest current (average 30,000 A), subsequent strokes can occur along the same main channel, provided that additional electrons are supplied to the top of the previous stroke within about 0.1 s of the cessation of

current. The additional electrons are supplied to the channel by so-called K or J *streamers*, which connect the top of the previous stroke to progressively more distant regions of the negatively charged area of the cloud (Fig. 6.52i). A negatively charged leader, called the *dart leader*, then moves continuously downward to the Earth along the main path of the first-stroke channel and deposits further electrons on the ground (Fig. 6.52j and k). The dart leader is followed by another visible return stroke to the cloud (Fig. 6.52l). The first stroke of a flash generally has many downward-directed branches (Fig. 6.53a) because the stepped leader is strongly branched; subsequent strokes usually show no branching since they follow only the main channel of the first stroke.

(a)

(b)

Figure 6.53. a) A time exposure of a ground lightning flash that was initiated by a stepped leader that propagated from the cloud to the ground. Note the downward-directed branches that were produced by the multibranched stepped leader. (Courtesy: NOAA/NSSL.) b) A time exposure of a lightning flash from a tower on a mountain to a cloud above the tower. This flash was initiated by a stepped leader that started from the tower and propagated upward to the cloud. In contrast to (a), note the upward-directed branching in (b). (Photo: R. E. Orville.)

Most lightning flashes contain three or four strokes, separated in time by about 50 ms, which can remove 20 C or more of charge from the lower region of a thundercloud. The charge-generating mechanisms within the cloud must then refurbish the charge before another stroke can occur. This they can do in as little as 10 s.

In contrast to the lightning flashes described above, most flashes to mountain tops and tall buildings are initiated by stepped leaders that start near the top of the building, move upward, and branch toward the base of a cloud (Fig. 6.53b). Lightning rods[44] protect tall structures from damage by routing the strokes to the ground through the rod and down conductors rather than through the structure itself.

A lightning discharges within a cloud generally neutralizes the main positive and negative charge centers. Instead of consisting of several discrete strokes, such a discharge generally consists of a single, slowly moving spark or leader that travels between the positively and negatively charged regions in a few tenths of a second. This current produces a low but continuous luminosity in the cloud upon which may be superimposed several brighter pulses, each lasting about 1 ms. Tropical thunderstorms produce about ten cloud discharges for every ground discharge, but in temperate latitudes the frequencies of the two types of discharge are similar.

The return stroke of a lightning flash raises the temperature of the channel of air through which it passes to above 30,000 K in such a short time that the air has no time to expand. Therefore, the pressure in the channel increases almost instantaneously to 10–100 atm. The high-pressure channel then expands rapidly into the surrounding air and creates a very powerful shock wave (which travels faster than the speed of sound) and, farther out, a sound wave that is heard as *thunder*.[45] Thunder is also produced by stepped and dart leaders, but it is much weaker than that from return strokes. Thunder generally cannot be heard more than 25 km from a lightning discharge. At greater distances the thunder passes over an observer's head because

[44] The use of lightning rods was first suggested by Benjamin Franklin in 1749, who declined to patent the idea or otherwise profit from their use. Lightning rods were first used in France and the United States in 1752. The chance of houses roofed with tiles or slate being struck by lightning is reduced by a factor of about 7 if the building has a lightning rod.

[45] This explanation for thunder was first given by Hirn[46] in 1888.

[46] **Gustave Adolfe Hirn** (1815 –1890) French physicist. One of the first to study the theory of heat engines. Established a small network of meteorological stations in Alsace that reported observations to him.

it is generally refracted upwards due to the decrease of temperature with height.

Although most ground lightning flashes carry negative charge to the ground, about 10% of the lightning flashes in midlatitude thunderstorms carry positive charge to the ground. Moreover, these flashes carry the largest peak currents and charge transfers. Such flashes may originate from the horizontal displacement by wind shear of positive charge in the upper regions of a thunderstorm (as depicted in Fig. 6.51) or, in some cases, from the main charge centers in a thunderstorm being inverted from normal.

6.7.3 The Global Electrical Circuit

Below an altitude of a few tens of kilometers there is a downward-directed electric field in the atmosphere during fair weather. Above this layer of relatively strong electric field is a layer, called the *electrosphere*, extending upward to the top of the ionosphere in which the electrical conductivity is so high that it is essentially at a constant electric potential. Since the electrosphere is a good electrical conductor, it serves as an almost perfect electrostatic shield. Consequently, charged particles from outside the electrosphere (e.g., those associated with auroral displays) rarely penetrate below the electrosphere and the effects of thunderstorms in the lower atmosphere do not extend above the electrosphere.

The magnitude of the fair weather electric field near the surface of the Earth averaged over the ocean $\sim$130 V m^{-1}, and in industrial regions it can be as high as 360 V m^{-1}. The high value in the latter case is due to the fact that industrial pollutants decrease the electrical conductivity of the air because large, slow-moving particles tend to capture ions of higher mobility. Since the vertical current density (which is equal to the product of the electric field and electrical conductivity) must be the same at all levels, the electric field must increase if the conductivity decreases. At heights above about 100 m, the conductivity of the air increases with height and therefore the fair weather electric field decreases with height. The increase in electrical conductivity with height is due to the greater ionization by cosmic rays and diminishing concentrations of large particles. Thus, at 10 km above the Earth's surface the fair weather electric field is only 3% of its value just above the surface. The average potential of

the electrosphere with respect to the Earth is ∼250 kV, but most of the voltage drop is in the troposphere.

The presence of the downward-directed fair weather electric field implies that the electrosphere carries a net positive charge and the Earth's surface a net negative charge. Lord Kelvin, who in 1860 first suggested the existence of a conducting layer in the upper atmosphere, also suggested that the Earth and the electrosphere act as a gigantic spherical capacitor, the inner conductor of which is the Earth, the other conductor the electrosphere, and the (leaky) dielectric the air. The electric field is nearly constant despite the fact that the current flowing in the air (which averages about 2 to 4×10^{-12} A m^{-2}) would be large enough to discharge the capacitor in a matter of minutes. Thus, there must be an electrical generator in the system. In 1920, C.T.R. Wilson proposed that the principal generators are thunderstorms, and this idea is now almost universally accepted. As we have seen, thunderstorms separate electric charges in such a way that their upper regions become positively charged and their bases negatively charged. The upper positive charges are leaked to the base of the electrosphere through the relatively highly conducting atmosphere at these levels. This produces a diffuse positive charge on the electrosphere, which decreases with height (as does the fair weather electric field). Below a thunderstorm the electrical conductivity of the air is low. However, under the influence of the very large electric fields, a current of positive charges, the *point discharge current*,[47] flows upwards from the Earth (through trees and other pointed obstacles). Precipitation particles are polarized by the fair weather electric field, and the field beneath thunderstorms, in such a way that they tend to preferentially collect positive ions as they fall to the ground. A positive charge equivalent to about 30% of that from point discharges is returned to the Earth in this way. Finally, ground lightning flashes transport negative charges from the bases of thunderstorms to the ground.

A schematic of the main global electrical circuit is shown in Fig. 6.54. A rough electrical budget for the Earth (in units of C km^{-2} yr^{-1}) is 90 units of positive charge gained from the fair weather conductivity and 30 units gained from precipitation, and 100 units of positive charge lost through point discharges and 20 units lost due to the transfer of negative charges to the Earth by ground lightning flashes.

[47] Point discharges at mastheads, etc., are know as *St. Elmo's fire*.

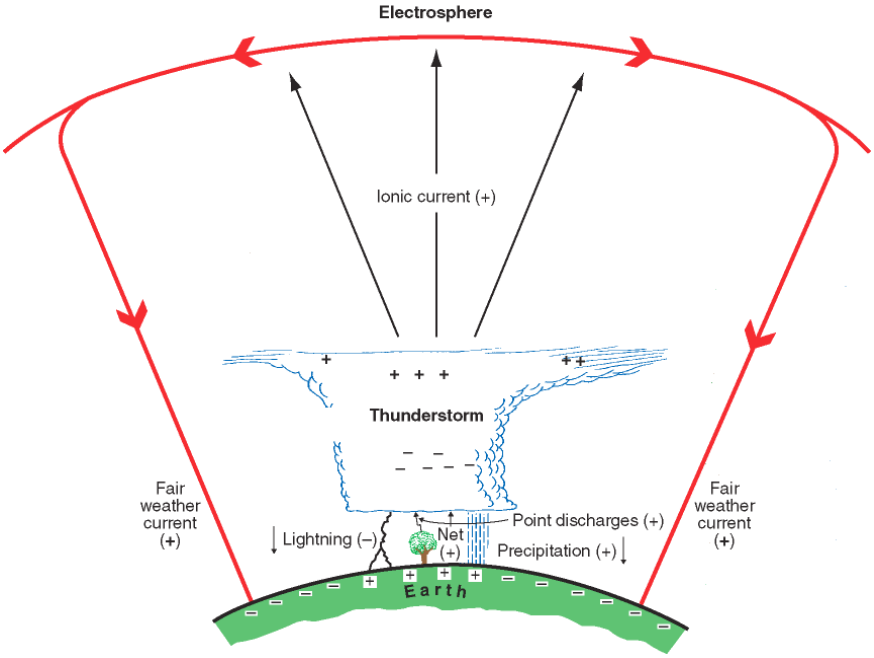

Figure 6.54. Schematic (not drawn to scale) of the main global electrical circuit. The positive and negative signs in parentheses indicate the signs of the charges transported in the direction of the arrows. The system can be viewed as an electrical circuit (red arrows) in which electrified clouds are the generators (or batteries). In this circuit positive charge flows from the tops of electrified clouds to the electrosphere. The so-called fair-weather current continuously leaks positive charge to the Earth's surface. The circuit is completed by the transfer of net positive charge to the bases of electrified clouds due to the net effect of point discharges, precipitation and lightning. In keeping with the normal convention, the current is shown in terms of the direction of movement of positive charge, but in fact it is negative charge in the form of electrons that flows in the opposite direction. See text for further details.

Monitoring of lightning flashes from satellites (Fig. 6.55) shows that the global average rate of ground flashes is ∼12–16 s^{-1}, with a maximum rate of ∼55 s^{-1} over land in summer in the northern hemisphere. The global average rate of total lightning flashes (cloud and ground flashes) is 44±5 s^{-1}, with a maximum of 55 s^{-1} in the northern hemisphere summer, and a minimum of 35 s^{-1} in the northern hemisphere winter. About 70% of all lightning occurs between

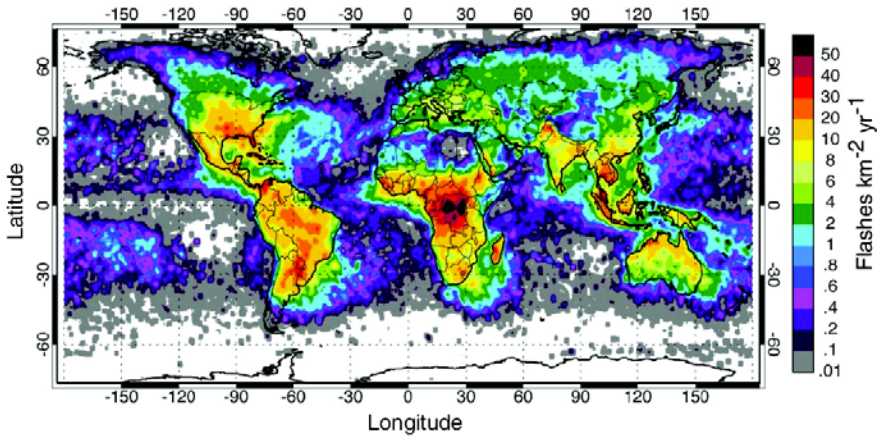

Figure 6.55. Global frequency and distribution of total lightning flashes observed from satellite. [From J. Geophys. Res., 108(D1), 4005, doi:10.1029/2002JD002347 (2003).]

30°S and 30°N, which reflects the high incidence of deep, convective clouds in this region. Over the North American continent ground flashes occur about 30 million times per year!

Over the United States there is a ground network that detects ground flashes. By combining counts of ground flashes from this network with counts of total flashes from satellite observations, the ratio of cloud flashes to ground cloud can be derived. This ratio varies greatly over the United States, from a maximum of ∼10 over Kansas and Nebraska, most of Oregon and parts of northwest California to a ratio of ∼1 over the Appalachian Mountains, the Rockies and the Sierra Nevada Mountains.

begin box **BOX 6.3: UPWARD ELECTRICAL DISCHARGES**

In 1973 a NASA pilot, in a surveillance aircraft flying at 20 km, recorded the following: *"I approached a vigorous, convective turret close to my altitude that was illuminated from within by frequent lightning. The cloud had not yet formed an anvil. I was surprised to see a bright lightning discharge, white-yellow in color, that came directly out of the center of the cloud at its apex and extended vertically upwards far above my altitude. The discharge was very nearly straight, like a beam of light, showing no tortuosity or branching. Its duration was greater than an ordinary lightning flash, perhaps as much as five seconds."*

Since then numerous types of lightning-related, transient luminous phenomena in the stratosphere and mesosphere have been documented, which go under the names of *sprites*, *elves*, and *blue jets* (Fig. 6.56).

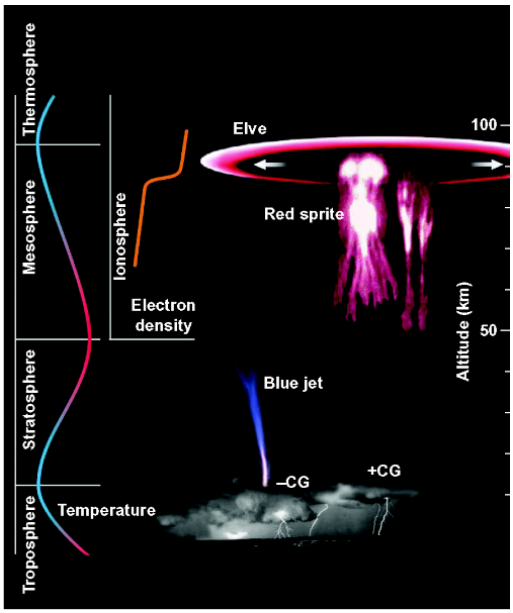

Figure 6.56. Transient luminous emissions in the stratosphere and mesosphere. [From Science, 300, 747 (2003).]

Sprites are luminous flashes that last from a few to a few hundred milliseconds. Sprites may extend from ∼90 km altitude almost down to cloud tops and more than 40 km horizontally. They are primarily red, with blue highlights on their lower regions; they can sometimes be seen by eye. Sprites are believed to be generated by an electric field pulse when particularly large amounts of positive charge are transferred from a thunderstorm to the ground by a lightning stroke, often from the stratiform regions of large mesoscale convective systems discussed in **Section 10.??**. In contrast to the fully ionized channels of a normal lightning stroke, sprites are only weakly ionized.

Elves are microsecond-long luminous rings located at ∼90 km altitude, and centered over a lightning stroke. They expand outward horizontally at the speed of light, and are caused by atmospheric heating produced by the electromagnetic pulse generated by a lightning stroke. They are not visible by eye.

Blue jets are partially ionized, luminous cones that propagate upward from the tops of thunderstorms at speeds of ∼100 km s^{-1} and reach altitudes of ∼40 km. On occasions, blue jets trigger sprites, thereby creating a direct, high-conductivity electrical connection from a thunderstorm to the ionosphere. These rare events do not appear to be directly associated with cloud-to-ground lightning flashes. They last only ∼100–200 ms, and are difficult to see by eye even at night.

Other less well documented upward propagating discharges have been reported. Figure 6.57 shows an upward-extending column of white light, about 1 km in length, from the top of a thunderstorm.

These various phenomena likely play a role in the global electrical circuit, and perhaps also in the chemistry of the stratosphere and mesosphere, in ways yet to be elucidated.

Figure 6.57. Upward discharge from a thunderstorm near Darwin, Australia. There is a blue "flame" at the top of the white channel that extends upward another kilometer or so. [From Bull. Amer. Meteor. Soc., 84, 445 (2003).]

end box

6.8 6.8 Cloud and Precipitation Chemistry[48]

In Chapter 6 we discussed trace gases and aerosols in the atmosphere. This section is concerned with the roles of clouds and precipitation in atmospheric chemistry. We will see that clouds serve as both sinks and sources of gases and particles, and they redistribute chemical species in the atmosphere. Precipitation scavenges particles and gases from the atmosphere, and deposits them on the surface of the Earth, the most notable example being *acid precipitation* or *acid rain*.

6.8.1 Overview

Some important processes that play a role in cloud and precipitation chemistry are shown schematically in Fig. 6.58. They include the

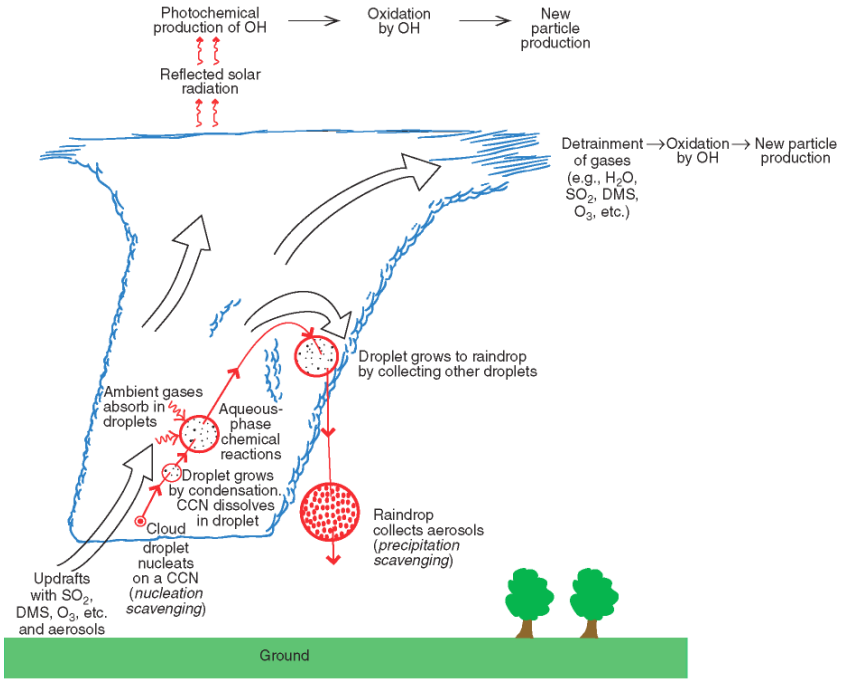

Figure 6.58. Schematic of cloud and precipitation processes that affect the distribution and nature of chemicals in the atmosphere and the chemical compositions of cloud water and precipitation. The large arrows indicate airflow. Not drawn to scale.

[48] See footnote 1 in Chapter 5.

transport of gases and particles, nucleation scavenging, dissolution of gases into cloud droplets, aqueous-phase chemical reactions, and precipitation scavenging. These processes, and their effects on the chemical composition of cloud water and precipitation, are discussed in turn below.

6.8.2 Transport of Particles and Gases

As depicted on the left side of Fig. 6.58, gases and particles are carried upward on the updrafts that feed clouds. Some of these gases and particles are transported to the upper regions of the clouds and ejected into the ambient air at these levels. In this way, pollutants from near the surface of the Earth (e.g., SO_2, O_3, particles) are distributed aloft. Solar radiation above the tops of clouds is enhanced by reflection from cloud particles, thereby enhancing photochemical reactions in these regions, particularly those involving OH. In addition, the evaporation of cloud water humidifies the air for a considerable distance beyond the boundaries of a cloud. Consequently, the oxidation of SO_2 and DMS by OH, and the subsequent production of new aerosol in the presence of water vapor (see Section 5.4.1.d), is enhanced near clouds.

6.8.3 Nucleation Scavenging

As we have seen in Section 6.1.2, a subset of the particles that enter the base of a cloud serves as cloud condensation nuclei (CCN) onto which water vapor condenses to form cloud droplets. Thus, each cloud droplet contains at least one particle from the moment of its birth. The incorporation of particles into cloud droplets in this way is called *nucleation scavenging*. If a CCN is partially or completely soluble in water, it will dissolve in the droplet that forms on it to produce a solution droplet.

6.8.4 Dissolution of Gases in Cloud Droplets

As soon as water condenses to form cloud droplets (or haze or fog droplets), gases in the ambient air begin to dissolve in the droplets. At equilibrium, the number of moles per liter of any particular gas that is dissolved in a droplet (called the *solubility*, C_g, of the gas) is given by Henry's law (see Exercise 5.3). Since the liquid phase is increasingly favored over the gas phase as the temperature is lowered,

greater quantities of a gas become dissolved in water droplets at lower temperatures.

PROBLEM 6.7 Determine the value of the Henry's law constant for a gas that is equally distributed (in terms of mass) between air and cloud water if the liquid water content (LWC) of the cloud is 1 g m^{-3} and the temperature is 5°C. (Assume that 1 mole of the gas occupies a volume of 22.8 liters at 1 atm and 5°C.) ◄

SOLUTION ► Let the gas be X, and its solubility in the cloud water C_g. Then

Amount of X (in moles) in the cloud water contained in 1 m^3 of air

$$= C_g \text{ (number of liters of cloud water in 1 } m^3 \text{ of air)}$$

$$= C_g \frac{LWC}{\rho_l} \tag{6.42}$$

where LWC is in kg m^{-3} and ρ_w is the density of water in kg $liter^{-1}$. From (5.3) and (6.42)

Amount of X (in moles) in the cloud water contained in 1 m^3 of air

$$= k_H p_g \frac{LWC}{\rho_l} \tag{6.43}$$

where, p_g is the partial pressure of X in atm and k_H the Henry's law constant for gas X. Since 1 mole of the gas at 1 atm and 5°C occupies a volume of 22.8 liters (or 0.0228 m^3), $(0.0228)^{-1}$ moles of the gas occupies a volume of 1 m^3 at 1 atm and 5°C. Therefore, for a partial pressure p_g of X,

$$1 \text{ } m^3 \text{ of air contains } \frac{p_g}{0.0228} \text{ moles of } X \text{ at } 5°C \tag{6.44}$$

For the same number of moles of X (and therefore mass of X) in the air and in the water, we have from (6.42) and (6.40)

$$k_H \; p_g \frac{LWC}{\rho_l} = \frac{p_g}{0.0228}$$

or

$$k_H = \frac{\rho_l}{0.0228\,(LWC)}$$

Since, $\rho_l = 10^3$ kg $m^{-3} = 1$ kg per liter, and for a $LWC = 1$ g $m^{-3} = 10^{-3}$ kg m^{-3},

$$k_H = \frac{1}{0.0228\,(10^{-3})} = 4.38 \times 10^4 \text{ mole liter}^{-1} \text{ atm}^{-1}$$

This value of k_H corresponds to a very soluble gas, such as hydrogen peroxide (H_2O_2). ◄

6.8.5 Aqueous-Phase Chemical Reactions

The relatively high concentrations of chemical species within cloud droplets, particularly in polluted air masses, lead to fast aqueous phase chemical reactions. To illustrate the basic principles involved, we will consider the important case of the conversion of SO_2 to H_2SO_4 in cloud water.

The first step in this process is the dissolution of SO_2 gas in cloud water, which forms the bisulfite ion ($HSO_3^-(aq)$) and the sulfite ion ($SO_3^{2-}(aq)$)

$$SO_2(g) + H_2O(\ell) \rightleftarrows SO_2 \cdot H_2O(aq) \tag{6.45a}$$

$$SO_2 \cdot H_2O(aq) + H_2O(\ell) \rightleftarrows HSO_3^-(aq) + H_3O^+(aq) \tag{6.45b}$$

$$HSO_3^-(aq) + H_2O(\ell) \rightleftarrows SO_3^{2-}(aq) + H_3O^-(aq) \tag{6.45c}$$

As a result of these reactions, much more SO_2 can be dissolved in cloud water than is predicted by Henry's law, which does not allow for any aqueous-phase chemical reactions of the dissolved gas.

After $SO_2 \cdot H_2O(aq)$, $HSO_3^-(aq)$ and $SO_3^{2-}(aq)$ are formed within a cloud droplet, they are oxidized very quickly to sulfate. The oxidation rate depends on the oxidant and, in general, on the pH of the droplet.[49] The fastest oxidant in the atmosphere, over a wide range of pH values, is hydrogen peroxide (H_2O_2). Ozone (O_3) also serves as a fast oxidant for pHs in excess of about 5.5.

6.8.6 Precipitation Scavenging

Precipitation scavenging refers to the removal of gases and particles by cloud and precipitation elements (i.e., *hydrometeors*). Precipitation scavenging is crucially important for cleansing the atmosphere of pollutants, but it can also lead to acid rain on the ground.

In Section 6.8.3 we discussed how aerosol particles are incorporated into cloud droplets through nucleation scavenging. Additional ways by which particles may be captured by hydrometeors are *diffusional* and *inertial collection*. Diffusional collection refers to the diffusional migration of particles through the air to hydrometeors.

[49] The pH of a liquid is defined as

$$pH = -\log[H_3O^+(aq)]$$

where $[H_3O^+(aq)]$ is the concentration (in mole per liter) of H_3O^+ ions in the liquid. Note that a change of unity in the pH corresponds to a change of a factor of ten in $[H_3O^+(aq)]$. *Acid* solutions have pH <7 and *basic* solutions pH >7.

Diffusional collection is most important for sub-micrometeor particles, since they diffuse through the air more readily than larger particles. Inertial collection refers to the collision of particles with hydrometeors as a consequence of their differential fall speeds. Consequently, inertial collection is similar to the collision and coalescence of droplets discussed in Section 6.4.2. Since very small particles follow closely the streamlines around a falling hydrometeor, they will tend to avoid capture. Consequently, inertial collection is important only for particles greater than a few micrometers in radius.

6.8.7 Sources of Sulfate in Precipitation

The relative contributions of nucleation scavenging, aqueous-phase chemical reactions, and precipitation scavenging to the amount of any chemical that is in hydrometeors that reach the ground depends on the ambient air conditions and the nature of the cloud. For illustration we will consider results of model calculations on the incorporation of sulfate (an important contributor to acid rain) into hydrometeors that originate in warm clouds.

For a warm cloud situated in heavily polluted urban air, the approximate contributions to the sulfate content of rain reaching the ground are: nucleation scavenging (37%), aqueous-phase chemical reactions (61%), and below cloud base precipitation scavenging (2%). The corresponding approximate percentages for a warm cloud situated in clean marine air are 75, 14 and 11. Why do the percentages for polluted and clean clouds differ so much? The principal reason is that polluted air contains much greater concentrations of SO_2 than clean air. Therefore, the production of sulfate by the aqueous-phase chemical reactions discussed in Section 6.8.5 is much greater in polluted air than in clean air.

6.8.8 Chemical Composition of Rain

The pH of pure water in contact only with its own vapor is 7. The pH of rainwater in contact with very clean air is 5.6. The lowering of the pH by clean air is due to the absorption of CO_2 into the rainwater and the formation of carbonic acid.

The pH of rainwater in polluted air can be significantly lower than 5.6, which gives rise to acid rain. The high acidity is due to the incorporation of gaseous and particulate pollutants into the rain by the mechanisms discussed in Sections 6.8.3–6.8.7. In addition to

sulfate (discussed in Sections 6.8.5 and 6.8.7), many other chemical species contribute to the acidity of rain. For example, in Pasadena, California, there is more nitrate than sulfate in rain, due primarily to emissions of NO_x from cars. In the eastern United States, where much of the acidity of rain is due to the long-range transport of emissions from electric power plants, sulfuric acid and nitric acid contribute ∼60% and ∼30%, respectively, to the acidity.

6.8.9 Production of Aerosol by Clouds

We have seen in Section 6.8.5 that due to aqueous-phase chemical reactions in cloud droplets, particles released from evaporating clouds may be larger and more soluble than the original CCN on which the cloud droplets formed. Hence, cloud-processed particles can serve as CCN at lower supersaturations than the original CCN involved in cloud formation. We will now describe another way in which clouds can affect atmospheric aerosol.

In the same way as small water droplets can form by the combination of water molecules in air that is highly supersaturated, that is, by homogeneous nucleation (see Section 6.1.1), under appropriate conditions the molecules of two gases can combine to form aerosol particles; a process referred to as *homogeneous-bimolecular nucleation*. The conditions that favor the formation of new particles by homogeneous-bimolecular nucleation are high concentrations of the two gases, low ambient concentrations of preexisting particles (which would otherwise provide a large surface area onto which the gases could condense, rather than condensing as new particles), and low temperatures (which favor the condensed phase). These conditions can be satisfied in the outflow regions of clouds for the following reasons.

As shown in Fig. 6.58, and discussed above, some of the particles carried upward in a cloud are removed by cloud and precipitation processes. Therefore, the air detrained from a cloud particle will contain relatively low concentrations of particles, but the relative humidity of the detrained air will be elevated (due to the evaporation of cloud droplets) as will the concentrations of gases, such as SO_2, DMS and O_3. Also, in the case of deep convective clouds, the air detrained near cloud tops will be at low temperatures. All of these conditions are conducive to the production of new particles in the detrained air. For example, O_3 can be photolyzed to form the OH radical, which

can then oxidize SO_2 to form H_2SO_4(g). The H_2SO_4(g) can then combine with H_2O(g) through homogeneous-bimolecular nucleation to form solution droplets of H_2SO_4.

As shown schematically in Fig. 6.59, the formation of particles in the outflow regions of convective clouds may act on a large scale to supply large numbers of particles to the upper troposphere in the tropics and subtropics and also, perhaps, to the subtropical marine boundary layer. In this scenario, air containing DMS and SO_2 from the tropical boundary layer is transported upward by large convective clouds into the upper troposphere. Particle production occurs in the outflow regions of these clouds. These particles are then transported away from the tropics in the upper branch of the Hadley cell circulation (see **Section ???**), and then subside in the subtropics. During this transport some of the particles may grow sufficiently (by further condensation, coagulation and cloud processing) to provide particles that are efficient enough as CCN to nucleate droplets even at the low supersaturations typical of stratiform clouds in the subtropical marine boundary layer.

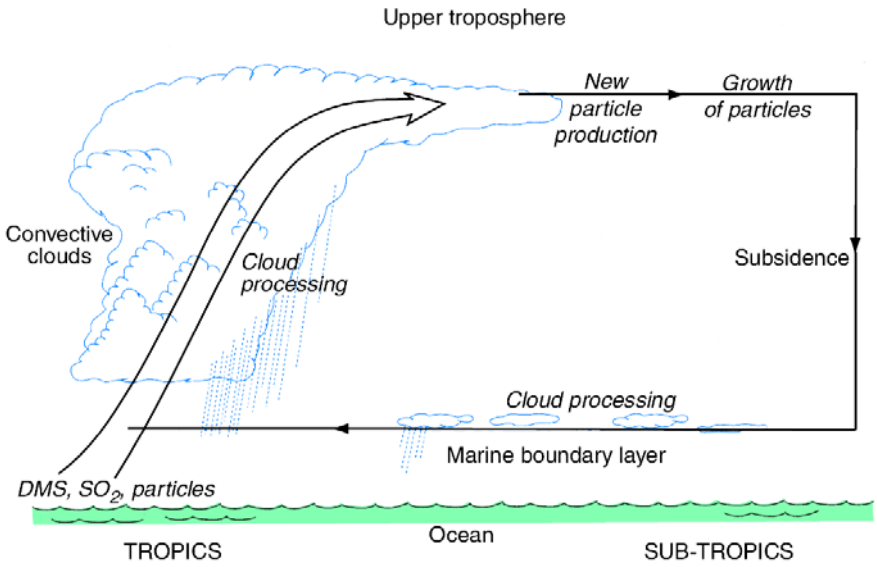

Figure 6.59. Transport of aerosol between the tropics and subtropics by means of the Hadley cell circulation. [Adapted from Dimethylsulfide: Oceans, Atmospheres and Climate, Kluwer Academic Publishers, p. 317 (1993).]

6.9 EXERCISES[50]

ACADEMIC PRESS: DELETE SECTION NUMBERING ("6.9") FROM "EXERCISES" SECTION TAG AND FROM PAGE HEADER

6.8 Answer or explain the following in light of the principles discussed in Chapter 6.

(a) Small droplets of pure water evaporate in air, even when the relative humidity is 100%.

(b) A cupboard may be kept dry by placing a tray of salt in it.

(c) The air must be supersaturated for a cloud to form.

(d) Cloud condensation nucleus concentrations do not always vary in the same way as Aitken nucleus concentrations.

(e) CCN tend to be much more numerous in continental air than in marine air.

(f) Growth by condensation in warm clouds is too slow to account for the production of raindrops.

(g) Measurements of cloud microstructures are more difficult from fast-flying than from slow-flying aircraft.

(h) If the liquid water content of a cloud is to be determined from measurements of the droplet spectrum, particular attention should be paid to accurate measurements of the larger drops.

(i) The tops of towering cumulus clouds often change from a cauliflower appearance to a more diffuse appearance as the clouds grow.

(j) Why are actual LWC in clouds usually less than the adiabatic values? Can you suggest circumstances that might produce cloud LWC that are greater than adiabatic values?

(k) Patches of unsaturated air are observed in the interior of convective clouds.

(l) Cloud droplets growing by condensation near the base of a cloud affect each other primarily by their combined influence on the ambient air rather than by direct interactions. [Hint: consider the average separation between small cloud droplets.]

[50] More difficult exercises are indicated by an asterisk after the number of the exercise. Solutions to the more difficult exercises are given in **Section ???**.

(m) After landing on a puddle, raindrops sometime skid across the surface for a short distance before disappearing.

(n) The presence of an electric field tends to raise the coalescence efficiency between colliding drops.

(o) Raindrops are more likely to form in marine clouds than in continental clouds of comparable size.

(p) Collision efficiencies may be greater than unity, but coalescence efficiencies may not.

(q) In some parts of convective clouds the liquid water content may be much higher than the water vapor mixing ratio at cloud base.

(r) In the absence of coalescence, cloud droplet spectra in warm clouds would tend to become monodispersed.

(s) Raindrops reaching the ground do not exceed a certain critical size.

(t) Ice crystals can be produced in a deep-freeze container by shooting the cork out of a toy pop-gun.

(u) Large supersaturations with respect to water are rare in the atmosphere but large supercoolings of droplets are common.

(v) Large volumes of water rarely supercool by more than a few degrees.

(w) The Millipore filter technique may be used to distinguish deposition from freezing nuclei.

(x) Aircraft icing may sometimes be reduced if the aircraft climbs to a higher altitude.

(y) Present techniques for measuring ice nucleus concentrations may not simulate atmospheric conditions very well.

(z) Ice particles are sometimes much more numerous than measurements of the concentrations of ice nuclei would suggest they should be.

(aa) The length of a needle crystal increases relatively rapidly when it is growing by the deposition of water vapor.

(bb) Natural snow crystals are often comprised of more than one basic ice crystal habit.

(cc) No two snowflakes are entirely identical.

(dd) Riming tends to be greatest at the edges of ice crystals (see, for example, Fig. 6.40c and d).

(ee) Riming significantly increases the fall speeds of ice crystals.

(ff) Graupel pellets tend to be opaque, rather than transparent.

(gg) Strong updrafts are required to produce large hailstones.

(hh) Aggregated ice crystals have relatively low fall speeds for their masses.

(ii) When snow is just about to change to rain, the snowflakes often become very large.

(jj) The melting level is a prominent feature in radar imagery.

(kk) Cold fogs are easier to disperse by artificial means than are warm fogs.

(ll) The charging mechanism responsible for the small pocket of positive charge that exists below the melting level in some thunderstorms must be more powerful than the mechanism responsible for the generation of the main charge centers.

(mm) When the atmospheric electric field between cloud base and the ground is directed downward, precipitation particles reaching the Earth generally carry a negative charge, and when the electric field is in the upward direction the precipitation is generally positively charged.

(nn) The presence of water drops in the air reduces the potential gradient required for dielectric breakdown.

(oo) The ratio of cloud-to-ground to intercloud lightning flashes is $\sim$10 over Kansas and Nebraska but only $\sim$1 over the Rocky Mountains.

(pp) Lightning is rarely observed in warm clouds.

(qq) Lightning occurs much more frequently over the continents than over the oceans (Fig. 6.56).

(rr) Visibility often improves after a thunderstorm.

(ss) The concentrations of aerosols between cloud droplets (called *interstitial aerosol*) are generally less than they are in the ambient air.

(tt) The residence time for particles in the atmosphere is short ($\sim$1 min) for particles $\sim 10^{-3}$ μm in diameter, large ($\sim$ months) for particles $\sim$1 μm in diameter, and short ($\sim$1 min) for particles in excess of $\sim$100 μm in diameter.

(uu) Feed lots for cattle contribute to the amount of nitrate in rain.

6.9 Figure 6.60 indicates a film of liquid (for example, a soap film) on a wire frame. The area of the film can be changed by moving a frictionless wire that forms one side of the frame. The surface tension of the liquid is defined as the force per unit length that the liquid exerts on the movable wire (as indicated by the broad black arrow in Fig. 6.60). If the surface energy of the liquid is defined as the work required to create a unit area of new liquid, show that the numerical values of the surface tension and surface energy of the liquid are the same.

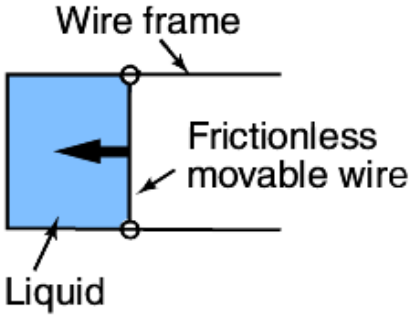

Figure 6.60.

6.10 Calculate the relative humidity of the air adjacent to a pure water droplet 0.2 μm in radius if the temperature is 0°C. (The surface energy of water at 0°C is 0.076 J m^{-2} and the number density of molecules in water at 0°C is 3.3×10^{28} m^{-3}.)

Answer 100.6%

6.11 Use the Köhler curves shown in Fig. 6.3 to estimate:

(a) The radius of the droplet that will form on a sodium chloride particle of mass 10^{-18} kg in air that is 0.1% supersaturated.

(b) The relative humidity of the air adjacent to a droplet of radius 0.04 μm that contains 10^{-19} kg of dissolved ammonium sulfate.

(c) The critical supersaturation required for an ammonium sulfate particle of mass 10^{-19} kg to grow beyond the haze state.

Answer (a) $\simeq 0.45$ μm; (b) $\simeq 90\%$; (c) $\simeq 0.47\%$

6.12* Show that for a very weak solution droplet ($m \ll \frac{4}{3}\pi r^3 \rho' M_s$), (6.8) can be written as

$$\frac{e'}{e_s} \simeq 1 + \frac{a}{r} - \frac{b}{r^3}$$

where $a = 2\sigma'/n'kT$ and $b = imM_w/\frac{4}{3}\pi\rho' M_s$. What is your interpretation of the second and third terms on the right-hand side of this expression? Show that in this case the peak in the Köhler curve occurs at

$$r \simeq \left(\frac{3b}{a}\right)^{1/2} \text{ and } \frac{e'}{e_s} \simeq 1 + \left(\frac{4a^3}{27b}\right)^{1/2}$$

6.13 Assuming that cloud condensation nuclei (CCN) are removed from the atmosphere by first serving as the centers on which cloud droplets form, and the droplets subsequently grow to form precipitation particles, estimate the residence time of a CCN in a column extending from the surface of the Earth to an altitude of 5 km. Assume that the annual rainfall is 100 cm and the cloud liquid water content is 0.30 g m^{-3}.

Answer 15 hours

6.14 A thermal diffusion chamber, used for measuring the concentration of CCN active at a given supersaturation, consists of a large shallow box of height 5 cm. The top of the box is maintained at 30°C, the base of the box at 20°C, and the temperature in the box varies linearly with height above the base of the box. The inside surfaces of the top and base of the box are covered with water (Fig. 6.61). (a) What is the maximum supersaturation (in %), with respect to a plain surface of water, inside the box? (b) What distance above the base of the box does this maximum supersa

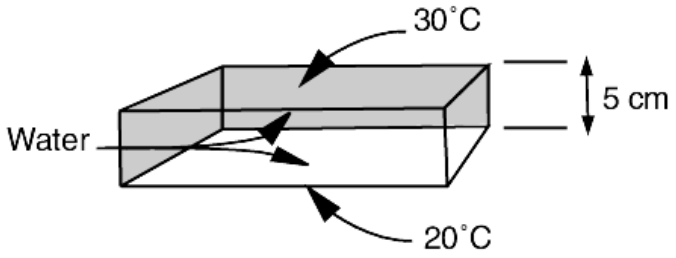

Figure 6.61.

To answer this question, use the values given below to plot on a large sheet of graph paper e_s, the saturation vapor pressure over a plain surface of water, as a function of temperature T from the bottom to the top of the box. Plot the actual vapor pressure e in the box as a function of T on the same graph.

T (°C)	e_s (hPa)	T (°C)	e_s (hPa)
20	23.4	26	33.6
21	24.9	27	35.6
22	26.4	28	37.8
23	28.1	29	40.1
24	29.8	30	42.4
25	31.7		

Answer (a) 3.5% (b) 2.75 cm

6.15* The air at the 500 hPa level in a cumulonimbus cloud has a temperature of 0°C and a liquid water content of 3 g m^{-3}. (a) Assuming the cloud drops are falling at their terminal fall speeds, calculate the downward frictional drag that the cloud drops exert on a unit mass of air. (b) Express this downward force in terms of a (negative) virtual temperature correction. (In other words, find the decrease in temperature the air would have to undergo if it contained no liquid water in order to be as dense as the air in question.) [Hint: At temperatures around 0°C the virtual temperature correction due to the presence of water vapor in the air can be neglected.]
Answer (a) 0.461 N kg^{-1}. (b) 1.28°C.

6.16 For droplets much larger than the wavelength of visible light, and for a droplet spectrum sufficiently narrow that the effective droplet radius r_e is approximately equal to the mean droplet radius, the optical depth τ_c of a cloud is given approximately by

$$\tau_c = 2\pi\ h\ r_e^2\ N$$

where h is the cloud depth and N the number concentration (m^{-3}) of cloud droplets. Derive approximate expressions for (a) the cloud liquid water content (LWC in kg m^{-3}) in terms of r_e, N and the density of water ρ_l, (b) the LWC in terms of r_e and

τ_c, and (c) an expression for the liquid water path (LWP in kg m^{-2}) in terms of r_e, τ_c and ρ_l.

Answer (a) LWC $= 4\pi\rho_l r_e^3 N/3$
(b) LWC $= 2\rho_l r_e \tau_c / 3h$
(c) LWP $= \frac{2}{3}\rho_l r_e \tau_c$

6.17 Air with a relative humidity of 20% at 500 hPa and -20°C is entrained into a cloud. It remains at 500 hPa while cloud droplets are evaporated into it. To what temperature can it be cooled by this process? Suppose the same parcel of air is carried down to 1000 hPa in a downdraft. What will be the temperature of the air parcel if it remains saturated? What will be its temperature if its relative humidity is 50% when it reaches the ground? [Use a skew $T - \ln p$ chart to solve this exercise.]
Answer −22.5°C, 12°C and 25°C

6.18 (a) For the case of no condensation and no entrainment, that is the dry adiabatic case, show that Eqn. (6.18) reduces to $d\theta' = 0$. (b) For the case of condensation but no entrainment, show that Eqn. (6.18) reduces to the equivalent of Eqn. (3.98). (c) Show from Eqn. (6.18) that when entrainment is present the temperature of a rising parcel of cloudy air decreases faster than when entrainment is absent.

6.19 Assuming that the radius of a rising parcel of warm air (i.e., a *thermal*), considered as a sphere, is proportional to its height above the ground, show that the *entrainment rate* (defined as dm/mdt, where m is the mass of the thermal at time t) is inversely proportional to the radius of the thermal and directly proportional to the upward speed of the thermal.

6.20* Consider a saturated parcel of air that is lifted adiabatically. The rate of change in the supersaturation ratio S ($S = e/e_s$ where e is the vapor pressure of the air and e_s the saturated vapor pressure) of the air parcel may be written as

$$\frac{dS}{dt} = Q_1 \frac{dz}{dt} - Q_2 \frac{d(LWC)}{dt}$$

where dz/dt and LWC are the vertical velocity and the liquid water content of the air parcel, respectively.
a) Assuming that S is close to unity, and neglecting the difference

between the actual temperature and the virtual temperature of the air, show that

$$Q_1 \simeq \frac{g}{TR_d}\left(\frac{\varepsilon L_v}{Tc_p} - 1\right)$$

where, T is the temperature of the parcel (in degrees kelvin), L_v the latent heat of condensation, g the acceleration due to gravity, R_d and R_v are the gas constants for 1 kg of dry air and 1 kg of water vapor, respectively, $\varepsilon = R_d/R_v$, and c_p the specific heat at constant pressure of the saturated air. [Hint: Consider ascent with no condensation. Introduce the mixing ratio of the air, which is related to e by Eqn. (3.62).]
b) Derive a corresponding approximate expression for Q_2 in terms of R_d, T, e, e_s, L_v, p, c_p and the density of the moist air (ρ). Assume that $e/e_s \simeq 1$, $T \simeq T_v$ and $\varepsilon >> w$ (the mixing ratio of the air). [Hint: Consider condensation and associated cooling in the absence of any vertical air motion, and proceed in a similar manner to (a).]

Answer $Q_2 = \rho\left[\frac{R_d T}{\varepsilon e_s} + \frac{\epsilon L_v^2}{pTc_p}\right]$

6.21 Derive an expression for the height h above cloud base of a droplet at time t that is growing by condensation only in a cloud with a steady updraft velocity w and supersaturation S. [Hint: Use (6.24) for the terminal fall speed of a droplet together with (6.21).]

Answer $h = wt - 2g\rho_l SG_l t^2/9\eta$

6.22 An isolated parcel of air is lifted from cloud base at 800 hPa, where the temperature is 5°C, up to 700 hPa. Use the skew $T - \ln p$ chart (back endpapers) to determine the amount of liquid water (in grams per kilogram of air) that is condensed during this ascent (i.e., the adiabatic liquid water content (LWC)).

Answer 1.8 g kg^{-1}

6.23 A drop with an initial radius of 100 μm falls through a cloud containing 100 droplets per cubic centimeter that it collects in a continuous manner with a collection efficiency of 0.800. If all the cloud droplets have a radius of 10 μm, how long will it take

for the drop to reach a radius of 1 mm? You may assume that for the drops of the size considered in this problem the terminal fall speed v (in m s^{-1}) of a drop of radius r (in meters) is given by $v = 6 \times 10^3 r$. Assume that the cloud droplets are stationary and that the updraft velocity in the cloud is negligible.

Answer 76.3 min

6.24* If a raindrop has a radius of 1 mm at cloud base, which is located 5 km above the ground, what will be its radius at the ground and how long will it take to reach the ground if the relative humidity between cloud base and ground is constant at 60%? [Hint: Use (6.21) and the relationship between v and r given in Exercise 6.23. If r is in micrometers, the value of G_l in (6.21) is 100 for cloud droplets, but for the large drop sizes considered in this problem the value of G_l should be taken as 700 to allow for ventilation effects.

Answer 0.67 mm and 16.4 min

6.25* A large number of drops, each of volume V, are cooled simultaneously at a steady rate $\beta(= dT/dt)$. Let $p(V, t)$ be the probability of ice nucleation taking place in a volume V of water during a time interval t. (a) Derive a relationship between $p(V, t)$ and $\int_0^{T_t} J_{LS}\, dT$, where J_{LS} is the ice nucleation rate (per unit volume per unit time) and T_t the temperature of the drops at time t. (b) Show that a n-fold increase in the cooling rate produces the same depression in the freezing temperature as an n-fold decrease in drop volume. [Hint: For (b) you will need to use some of the expressions derived in Exercise (6.4).]

Answer $\ln[1 - p(V, t)] = -\dfrac{V}{\beta} \int_0^{T_t} J_{LS}\, dT$

6.26 A cloud cylindrical in shape and has a cross-sectional area of 10 km^2 and a height of 3 km. All of the cloud is initially supercooled and the liquid water content is 2 g m^{-3}. If all of the water in the cloud is transferred onto ice nuclei present in a uniform concentration of 1 $liter^{-1}$, determine the total number of ice crystals in the cloud and the mass of each ice crystal produced. If all the ice crystals precipitate and melt before they reach the ground, what will be the total rainfall produced?

Answer 3×10^{13}, 2 mg and 6 mm

6.27 Calculate the radius and the mass of an ice crystal after it has grown by deposition from the vapor phase for half an hour in a water-saturated environment at $-5°$C. Assume that the crystal is a thin circular disk with a constant thickness of 10 μm. [Hint: Use Eqn. (6.37) and Fig. 6.39 to estimate the magnitude of $G_i S_i$. The electrostatic capacity C of a circular disk of radius r is given by $C = 8r\varepsilon_0$, where ε_0 is the permittivity of free space.]

Answer 0.5 mm and 7.2 μg

6.28 Calculate the time required for an ice crystal, which starts off as a plane plate with an effective circular radius of 0.5 mm and a mass of 0.010 mg, to grow by riming into a spherical graupel particle 0.5 mm in radius if it falls through a cloud containing 0.50 g m^{-3} of small water droplets that it collects with an efficiency of 0.60. Assume that the density of the final graupel particle is 100 kg m^{-3} and that the terminal fall speed v (in m s^{-1}) of the crystal is given by $v = 2.4M^{0.24}$, where M is the mass of the crystal in milligrams.

Answer 2.8 mins

6.29 Calculate the time required for the radius of a spherical snowflake to increase from 0.5 mm to 0.5 cm if it grows by aggregation as it falls through a cloud of small ice crystals present in an amount 1 g m^{-3}. Assume the collection efficiency is unity, the density of the snowflake is 100 kg m^{-3}, and that the difference in the fall speeds of the snowflake and the ice crystals is constant and equal to 1 m s^{-1}.

Answer 30 min

6.30 Determine the minimum quantity of heat that would have to be supplied to each cubic meter of air to evaporate a fog containing 0.3 g m^{-3} of liquid water at 10°C and 1000 hPa. [Hint: You will need to inspect the saturation vapor pressure of air as a function of temperature, shown on the back endpapers of this book.]

Answer 1558 J

6.31 If 40 liters of water in the form of drops 0.5 mm in diameter were poured into the top of a cumulus cloud and all of the drops grew

to a diameter of 5 mm before they emerged from the base of the cloud, which had an area of 10 km^2, what would be the amount of rainfall induced? Can you suggest any physical mechanisms by which the amount of rain produced in this way might be greater than this exercise suggests?

Answer 4×10^{-3} mm

6.32 Compare the increase in the mass of a drop in the previous exercise with that of a droplet 20 μm in radius which is introduced at cloud base, travels upward, then downwards, and finally emerges from cloud base with a diameter of 5 mm.

Answer Factors of 10^3 and 2×10^6, respectively

6.33 If hailstones of radius 5 mm are present in concentrations of 10 m^{-3} in a region of a hailstorm where the hailstones are competing for the available cloud water, determine the size of the hailstones that would be produced if the concentrations of hailstone embryos were increased to 10^4 m^{-3}.

Answer 0.5 mm

6.34 A supercooled cloud is completely glaciated at a particular level by artificial seeding. Derive an approximate expression for the increase in the temperature ΔT at this level in terms of the original liquid water content w_l (in g kg^{-1}), the specific heat of the air c, the latent heats of fusion L_f and deposition L_d of the water substance, the original saturation mixing ratio with respect to water w_s (in g kg^{-1}), and the final saturation mixing ratio with respect to ice w_i (in g kg^{-1}).

Answer $c\ \Delta T = w_l(10^{-3}L_f) + (w_s - w_i)(10^{-3}L_d)$

6.35 Ignoring the second term on the right-hand side of the answer given in the previous exercise, calculate the increase in temperature produced by glaciating a cloud containing 2 g kg^{-1} of water.

Answer 0.7°C

6.36 On a certain day, towering cumulus clouds are unable to penetrate above the 500 hPa level, where the temperature is −20°C, because of the presence of a weak stable layer in the vicinity of

that level where the environmental lapse rate is 5°C km^{-1}. If these clouds are seeded with silver iodide so that all of the liquid water in them (1 g m^{-3}) is frozen, by how much will the tops of the cumulus clouds rise? Under what conditions might such seeding be expected to result in a significant increase in precipitation? [Hint: From the skew $T - \ln p$ chart, the saturated adiabatic lapse rate at 500 hP is about 6°C km^{-1}.]

Answer ~480 m

6.37* If the velocities of sound in two adjacent thin layers of air are v_1, and v_2, a sound wave will be refracted at the interface between the layers and $\dfrac{\sin i}{\sin r} = \dfrac{v_1}{v_2}$ (see Fig. 6.62)

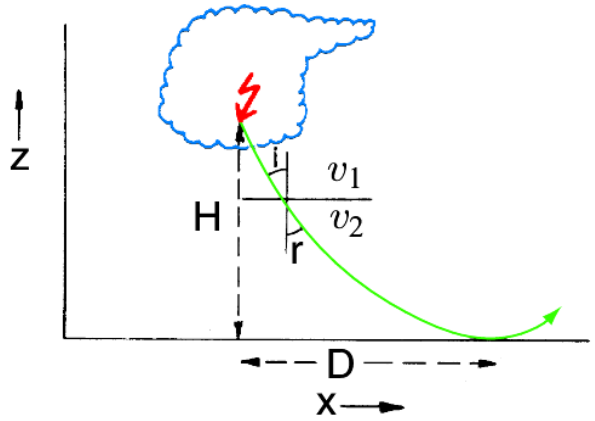

Figure 6.62.

Use this relationship, and the fact that $v \propto \sqrt{T}$, where T is the air temperature (in degrees kelvin), to show that the equation for the path of a sound wave produced by thunder that is heard at the maximum horizontal distance from the origin of the thunder is

$$dx = -\left(T/\Gamma z\right)^{1/2}\ dz$$

where x and z are the coordinates indicated in Fig. 6.62, Γ the temperature lapse rate in the vertical (assumed constant), and T the temperature at height z.

6.38* Use the expression derived in Exercise (6.37) to show that the maximum distance D at which a sound wave produced by thun-

der can be heard is given approximately by (see Fig. E6.37)

$$D = 2\,(T_0 H/\Gamma)^{1/2}$$

where T_0 is the temperature at the ground. Calculate the value of D given that $\Gamma = 7.50\ ^\circ\text{C km}^{-1}$, $T_0 = 300$ K, and $H = 4$ km.

Answer 25.3 km

6.39 An observer at the ground hears thunder 10 s after he sees a lightning flash, and the thunder lasts for 8 s. How far is the observer from the closest point of the lightning flash and what is the minimum length of the flash? Under what conditions would the length of the flash you have calculated be equal to the true length? (Speed of sound is 0.34 km s^{-1}.)

Answer 3.4 km and 2.72 km

6.40 (a) What is the change in the oxidation number of sulfur when $HSO_3^-(aq)$ is oxidized to $H_2SO_4(aq)$? (b) What are the changes in the oxidation numbers of sulfur in $SO_2{\cdot}H_2O(aq)$ and $SO_3^{2-}(aq)$ when they are converted to H_2SO_4?

Answer (a) An increase from 4 to 6. (b) Both increase from 4 to 6.